TOPOLOGY OPTIMIZATION OF MICRO FLUIDIC COOLING SYSTEMS

Midtermproject

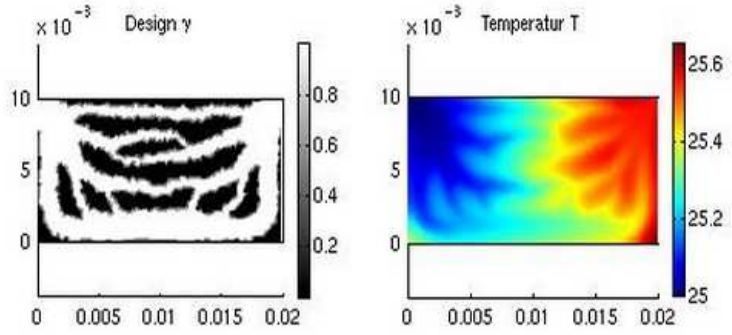

Signe Sarah Shim s021977
Pernille Voss Larsen s022005

Supervisors:
Fridolin Okkels and Henrik Bruus

MIC - Department of Micro- and Nanotechnology
DTU - Technical University of Denmark

4 July 2005

Abstract

I this project topology optimizations are performed for micro fluidic cooling systems. The average temperature of a well-defined design area has to be as low as possible, when a pressure difference is determined over the area. Optimizations are performed with MatLab and FEMLab.
To examine whether the optimized cooling systems are optimal in practice too, they are fabricated in PMMA using a CO_2 laser. First several measurements are performed for parts of the experimental set-up to obtain as exact measurements as possible for the micro fluidic cooling systems.

Resume

I dette projekt topologi optimeres designet af mikrofluide kølesystemer, således at gennemsnitstemperaturen over et veldefineret designområde bliver mindst mulig, når et givet trykfald er fastsat over dette. Optimeringerne udføres ved hjælp af MatLab og FEMLab.
For at undersøge om de optimerede kølesystemer også er optimale i praksis, fremstilles disse i PMMA med en CO_2-laser. Indledende udføres en række målinger på dele af systemet ved hjælp af forsøgsopstillingen for at kunne opnå så præcise målinger som muligt for de mikrofluide kølesystemer.

Preface

This project concerns with topology optimizations of micro fluidic cooling systems. The background for choosing the project was a significant interest of physics involving micro technology and a wish of getting more knowledge within this interesting and essential field. Furthermore, it was a condition for us that we could perform a project including both an theoretical and a practical part, to obtain a connection between theory and practice.
The project report is split up into three part. In the first part the theory necessary for the simulations, for instance the Navier-Stokes equation and the heat equation, and the methods of the simulations, for instance the topology optimization method, are described. The computer simulations are described in the second part of the report, while the practical experiments are carefully treated i the third section of the report. The simulations and the experiments are described in a continuous order and sub-conclusions are given for each obtained result. At the end of the report an appendix with further theory and data sheets is included, while the simulation programmes and experimental results are attached on a CD-ROM.
It is our opinion that it has been a very exciting project implementation process. We have learnt at lot about computer simulations performed by use of MatLab and FEMLab, and we have learnt a lot of fluid fluid mechanics, which was almost a totally new field for us. While performing the experiments we have had free hand to try out our ideas in practice and give the project a personal mark, which have been very positive.
In connection to the project we would like to thank some persons for kind help and guidance through the project implementation process. First and foremost we would like to thank our supervisors Fridolin Okkels and Henrik Bruus for many useful inputs and for a good and open collaboration. Furthermore, we would like to thank Detlef Snakenborg and Anders Brask for helping us with the experimental set-up and for answer to many practical questions.

Table of contents

Chapter 1

Introduction

The main purpose of this project is to perform topology optimizations of micro fluidic cooling systems. The optimization program calculates the solution to the problem numerically. The program is initiated through MatLab. The geometry of the micro fluid cooling systems is defined using FEMLab. Furthermore, the systems are fabricated in PMMA with a CO_2 laser. This is done in order to determine whether the systems are optimized compared to a system optimized to a different pressure.
Topology optimizations of micro fluid cooling systems are interesting because they can be used in, for instance, the computer industry to cool the CPU of a computer. Today water cooling can be used to cool the CPU. This is a more efficient way of cooling a CPU than the traditional method using a metal rib which is cooled by a fan. This way of cooling a CPU is quite noisy, because it contains moving parts.
If the topology optimized cooling system was used to cool a CPU the most efficient cooling at a given pressure difference over the inlet and outlet would always be obtained.
To preform the topology optimization of the micro fluidic cooling system, a pressure difference is defined over the inlet and outlet of a well-defined design area, at which the geometry is optimized, so that the average temperature of the design area is minimized.
When the optimization is performed, a pressure difference between the inlet and outlet is defined and the structure of the design area is optimized. This is done for a series of different pressures to determine the changes of the optimal structure as a function of the pressure difference.
When an optimal temperature corresponding to a particular pressure is found for each system, the pressure is changed and a new temperature is calculated for the same system. The temperature is plotted as function of the pressure to determine whether the obtained structure is optimal compared to a system optimized at a different pressure.
During the project the geometry and the dimensions of the inlet and outlet are changed until a final geometry is chosen. Micro fluidic cooling systems based on this geometry are fabricated in PMMA with a CO_2 laser.
Before carrying out experiments with the final micro fluidic system, several experiments have been performed to estimate the errors occurring during the measurements. The first measurement performed is heat transportation through a PMMA plate to estimated whether it is necessary to isolated the cooling system from the surroundings.
Also investigated is the resistance of a tube having well-defined dimensions and the result is compared to the theoretically calculated resistance of the tube. The result is used to estimate the precision that can be determined for the hydraulic resistance of the inlet and outlet of the micro fluidic cooling system. The determined resistance of the inlet and outlet is used to determine the pressure difference over the area containing the cooling system.

An experiment is carried out to establish the time needed to obtain reasonable results for the average temperature.
Finally, experiments are performed with micro fluidic cooling systems optimized at different pressures to examine whether it is possible to distinguish between the two systems based on the average temperatures obtained. This is done in order to determine the agreement between the experiments and the simulations.

Chapter 2

Theory

2.1 Fluids

Normally three states of matter are recognised: Solid, liquid and gas. However, both liquids and gasses are fluids, and their nature is very different to that of solids.
A molecule is always surrounded by a number of other molecules within atomic distances. The difference between fluids and solids is primary the density and the distance between the molecules, which for gasses is about 3 nm and for liquids about 0.3 nm. Thereby the densities and intermolecular interactions between constitution molecules differ for the two groups. Because of the big intermolecular distance between gas particles it is possible to compress them. For liquids on the other hand, compression cannot be performed in the same way, because the molecules are very close together. Therefore liquids can be very well assumed as being incompressible, and thereby the density of liquids is comparable to that of solids having molecules packed as close as possible.
I this project the calculations are performed on water, which is assumed as being an incompressible liquid.
But in contrast to solids liquids do not have a preferred shape and so only individual elements within it cannot be considered. Different parts a liquid may be rearranged, that is the ordering is not fixed in time and space but fluctuates at short time intervals and up to a few molecular diameters. In contrast to solids liquids cannot resist deformation, causing them to move or flow under action of external forces, which are able to change the shape continuously as long as they are applied. Therefore liquids can be assumed as continuous steams without a beginning or an end. When no shearing forces are acting, a liquid will be at rest.

2.2 The continuum hypothesis

Fluids are considered as being continuous media. This is, after all, not the case, because fluids are containing a number of molecules which mass is not continuous distributed in space.
The continuum hypothesis is valid when treating fluids under normal conditions. It only breaks down when treating very small characteristic dimensions having the same size as the mean free path of the problem, for instance when treating rarefied gas flows. Then since, in this project, the fluid particles of water are presented on a macroscopic length scale, not on nanoscale, the continuum hypothesis is assumed to be valid.
Each property of a fluid, such as density, temperature and velocity, is assumed to have a define value at every point in space, as a consequence of the continuum hypothesis.

Therefore these properties of a fluid are considered to be continuous functions of position and time.
Now, the density at a point of a fluid is treated as an example. A point, $C = (x_0, y_0, z_0)$, is considered, and the average density in a volume, $\overline{V}$, around it is

$$\rho = \frac{m}{\overline{V}}. \tag{2.1}$$

A figure showing the defined region of the fluid is shown in figure 2.1.

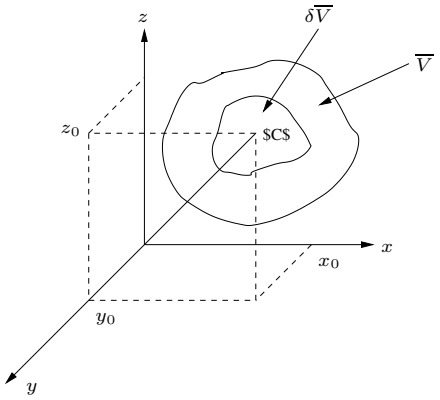

Figure 2.1: *Figure showing a region of a fluid used to derive the density, ρ, at a point.* [1]

This density is not equal to the density at the point C, because the fluid may not be uniform. To determine the density at C, it is necessary to consider an even smaller volume, $\delta\overline{V}$ surrounding it and then determine the density. The volume, $\delta\overline{V}$, must be large enough to yield a meaningful, reproducible value for the density at the location, but yet small enough to be called a point. The average density for the volume, $\delta\overline{V}$, then tend to enclose only homogeneous fluid in the immediate neighbourhood of C, as the volume is decreased. The size of the volume has a lower limit, $\delta\overline{V'}$, where it become so small that it is impossible to fix a define value for the density, because molecules constant move in and out of the volume. Thus the density at the point C becomes

$$\rho = \lim_{\delta\overline{V} \to \delta\overline{V'}} \frac{\delta m}{\delta\overline{V}} \tag{2.2}$$

C is an arbitrary point, and so the density at any other point could be determined in the same manner. Therefore the density distribution becomes

$$\rho = (x, y, z, t), \tag{2.3}$$

where the time, t, is represented because the density at a point also is dependent on time. [9]
Therefore, the continuum hypothesis states that for quantities bigger than the molecular scale, the macroscopic properties of a fluid are the same as if the fluid were perfectly continuous in structure instead of, as in reality, consisting of molecules, and so physical quantities associated with a small volume have to be taken as the sum over a large number of molecules within a small volume. The size of the volume is not known exact wherefore calculations are performed for physical properties per volume, where the volume is taken to be the limit of a small, but finite fluid particle volume. [1] [5]

2.3 Flow and Reynold's number

The Navier-Stokes equation is a very important differential equation in fluid dynamics when describing the flow of continuous media. But before derivation of the Navier-Stokes equation, the phenomenon turbulence has to be described.
When forces are acting on a fluid, it begins to move. A force could for instance be caused by a pressure difference or a pressure gradient at the two ends of a pipe or a micro fluidic device like in this project. If the pressure gradient is constant, the flow becomes stationary and will not change with time. The movement of a fluid is either laminar (stratified) or turbulent (with eddys). The condition for a steady-state flow is that the velocity everywhere is independent of time. Therefore it shas to be laminar. If the fluid then were split up into infinite decimal layers, these layers will flow parallel to each other, not being mixed. Otherwise the flow will become turbulent. A sketch of respectively laminar and turbulent flow is shown in figure 2.2.

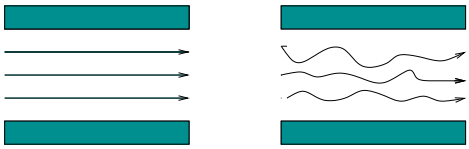

Figure 2.2: *A sketch of respectively laminar and turbulent flow.*

Turbulence has to be avoid in this project, because otherwise the flow of the fluid will become unpredictable because eddys come into existence, so that the Naviers-Stokes equation becomes difficult to solve.
The magnitude of Reynold's number, Re, describes whether a stationary flow is laminar or turbulent. Reynold's number is a dimensionless quantity that gives the relation between inertial and viscous forces,

$$Re = \frac{\rho u_0 h}{\eta}, \tag{2.4}$$

where u_0 determines a characteristic velocity or a mean velocity, h determines a height of a two dimensional channel with parallel planes, ρ is the density of the fluid and η is the viscosity of it. For more information about stress-fiels and viscosity, see appendix 10.
If Reynold's number is bigger than a critical value, $Re_{\text{cr}} = 2300$, the flow is turbulent.[7] [1]

2.4 The continuity equation

Two fundamental equations describe the flow of continuous fluids. The Navier-Stokes equation states that the momentum is kept constant and has already been mentioned, but it will first be derived a little later. The other equation is the continuity equation. It states that the mass is kept constant, so that the net mass flux into a small volume within a fluid is equal to the energy stored in the system,

$$\frac{\partial \rho}{\partial t} = -(\vec{\nabla} \cdot \rho \vec{u}), \tag{2.5}$$

where ρ is the density and $\vec{u} = [u_x(x,y,z), u_y(x,y,z), u_z(x,y,z)]$ is the velocity field of the fluid in Cartesian coordinates.
If the density of the fluid is assumed to be constant in time and space, which means

that $\frac{\partial \rho}{\partial t} = 0$ and $\vec{\nabla}\rho = 0$, then

$$\begin{aligned} & 0 = -(\vec{\nabla} \cdot \rho\vec{u}) \\ \Updownarrow \quad & \\ & 0 = (\vec{\nabla} \cdot \rho\vec{u}) \\ \Updownarrow \quad & \\ & 0 = (\vec{\nabla}\rho \cdot \vec{u}) + \rho(\vec{\nabla} \cdot \vec{u}) \\ \Updownarrow \quad & \\ & 0 = \vec{\nabla}\vec{u} \end{aligned} \tag{2.6}$$

This very important equation is the continuity equation valid for incompressible fluids. [7]

2.5 Navier-Stokes equation for incompressible fluids

As described in section 2.1, the liquid in this project can be assumed as being incompressible:Therefores the Navier-Stokes equation for compressible fluids will not be derivated here.
The Navier-Stokes equation for incompressible fluids is Newton's second law for fluid particles, and it is compatible with continuous fluids.
From classical mechanics Newton's second law for an ordinary particle with mass m influenced by external forces $\sum_j \vec{F}_j$ has the form

$$m\vec{a} = m\frac{d\vec{u}}{dt} = \sum_j \vec{F}_j. \tag{2.7}$$

In fluid mechanics it is easier to work with the density, ρ, instead of the mass, m, wherefore the equation is divided by the volume, V. Thus

$$\begin{aligned} & \tfrac{m}{V}\tfrac{d\vec{u}}{dt} = \textstyle\sum_j \tfrac{\vec{F}_j}{V} \\ \Updownarrow \quad & \\ & \rho\tfrac{d\vec{u}}{dt} = \textstyle\sum_j \vec{f}_j, \end{aligned} \tag{2.8}$$

where $\vec{f}_j$ is the volume specific force or force density.
The velocity in a microscopic space somewhere in the fluid is called the Euler velocity. It means that the velocity for a single fluid particle is a function of time, t, and space, $\vec{r}$, and so the volume specific velocity is written $\vec{u}(\vec{r}, t)$.
Differentiation with regard to time and summation over all directions in space, represented by i, gives

$$\frac{d\vec{u}}{dt} = \frac{\partial \vec{u}}{\partial t} + \left(\frac{\partial}{\partial t} r_i\right) \partial_i \vec{u} = \frac{\partial \vec{u}}{\partial t} + v_i \partial_i \vec{u}. \tag{2.9}$$

Thus

$$\frac{d\vec{u}}{dt} = \frac{\partial \vec{u}}{\partial t} + (\vec{u} \cdot \vec{\nabla})\vec{u}. \tag{2.10}$$

Now Newton's Second law reads

$$\sum_j \vec{f}_j = \rho\frac{d\vec{u}}{dt} = \rho\left(\frac{\partial \vec{u}}{dt} + (\vec{u} \cdot \vec{\nabla})\vec{u}\right), \tag{2.11}$$

The external forces acting on a fluid are the so-called body-forces that has to be determined.
The force density of the gravitation force, $\vec{g}$, acting on a fluid can be derived from the expression from classical mechanics, when divided by the volume, V,

$$\begin{aligned} & \vec{F}_{\text{grav}} = m\vec{g} \\ \Updownarrow \quad & \\ & \tfrac{\vec{F}_{\text{grav}}}{V} = \tfrac{m}{V}\vec{g} \\ \Updownarrow \quad & \\ & \vec{f}_{\text{grav}} = \rho\vec{g}. \end{aligned} \tag{2.12}$$

The force density of an electrical force acting on a polarized fluid is found in the same way as the gravity force. Thus

$$\vec{f}_{\text{el}} = \rho_{\text{el}}\vec{E}, \tag{2.13}$$

where ρ_{el} is the charge density and $\vec{E}$ is an external electrical field.
The force density caused by a pressure is derived by considering a region, Ω, in a fluid and the corresponding surface $\delta\Omega$ with a surface normal vector $\vec{n}$ pointing outwards perpendicular to it.
Using Gauss's theorem the external force, $\vec{f}_{\text{pres}}$, acting on this region due to the pressure p is given by the surface integral over $-\vec{n}p$, beeing the outward force per area from the region acting on the surroundings,

$$\vec{F}_{\text{pres}} = \int_{\delta\Omega}(-\vec{n}p)da = \int_{\Omega}(\vec{\nabla}p)dr. \tag{2.14}$$

Now the force density of the pressure acting on the fluid becomes [1]

$$\vec{f}_{\text{pres}} = -\vec{\nabla}p. \tag{2.15}$$

The last force derived here is the viscous force.
From an expression for conservation of the monentum, Navier-Stokes equation can be written as

$$\rho(\partial_t\vec{u} + (\vec{u}\cdot\vec{\nabla})\vec{u}) = (\vec{\nabla}\cdot\vec{\tau}) + \rho\vec{g} + \rho_{\text{el}}\vec{E}, \tag{2.16}$$

where τ is a stress-tensor defined as

$$\tau = -pI_{ij} + \eta(\vec{\nabla}\vec{u} + (\vec{\nabla}\vec{u})^{\dagger}) - (\frac{2}{3}\eta - k)(\vec{\nabla}\cdot\vec{u})\vec{\partial_{ij}} \tag{2.17}$$

$(\vec{\nabla}\vec{u})^{\dagger}$ is the transposed of $(\vec{\nabla}\vec{u})$, I_{ij} is the identity matrix, p is the pressure and k is the thermal conductivity. For incompressible fluids $\vec{\nabla}\vec{u} = 0$ in accordance with the continuity equation and so the last term can be neglected. The stress-tensor can then be written on the form

$$\begin{aligned} &\tau = -pI_{ij} + \eta(\vec{\nabla}(\vec{u}) + (\vec{\nabla}v)^{\dagger}) \\ \Updownarrow\ &\\ &\tau = -pI_{ij} - \eta\dot{\gamma} \end{aligned} \tag{2.18}$$

where $\dot{\gamma} = \vec{\nabla}\vec{u} + (\vec{\nabla}\vec{u})^{\dagger}$ is a shear rate-tensor. The first part of the stress-tensor, $p\vec{\partial}$, is equivalent to the pressure contribution to an inviscosit fluid, and the second part, $\eta\dot{\gamma}$, is the contribution from viscous forces in the fluid.
Now an expression for the term $(\vec{\nabla}\nabla\tau)$ in the Navier-Stokes can be derived,

$$\begin{aligned} &(\vec{\nabla}\cdot\vec{\tau}) = \vec{\nabla}\cdot(-pI_{ij} + \eta\dot{\vec{\gamma}}) \\ \Updownarrow\ &\\ &(\vec{\nabla}\cdot\vec{\tau}) = -\vec{\nabla}\cdot(pI_{ij}) + \vec{\nabla}\cdot(\eta\dot{\vec{\gamma}}) \\ \Updownarrow\ &\\ &(\vec{\nabla}\cdot\vec{\tau}) = -\vec{\nabla}p + \vec{\nabla}\cdot(\eta(\vec{\nabla}\vec{u} + (\vec{\nabla}\vec{u})^{\dagger})) \\ \Updownarrow\ &\\ &(\vec{\nabla}\cdot\vec{\tau}) = -\vec{\nabla}p + \vec{\nabla}\cdot(\eta\vec{\nabla}\vec{u}) + \vec{\nabla}\cdot(\eta(\vec{\nabla}\vec{u})^{\dagger}) \\ \Updownarrow\ &\\ &(\vec{\nabla}\cdot\vec{\tau}) = -\vec{\nabla}p + \eta\vec{\nabla}^2\vec{u} + \vec{\nabla}\cdot(\eta(\vec{\nabla}\vec{u})^{\dagger}) \\ \Updownarrow\ &\\ &(\vec{\nabla}\cdot\vec{\tau}) = -\vec{\nabla}p + \eta\vec{\nabla}^2\vec{u} + \eta\vec{\nabla}\cdot(\vec{\nabla}\vec{u}) \\ \Updownarrow\ &\\ &(\vec{\nabla}\cdot\vec{\tau}) = -\vec{\nabla}p + \eta\vec{\nabla}^2\vec{u}. \end{aligned} \tag{2.19}$$

In the derivation it is used that the identity matrix states that $I = 1$ when $i = j$, or otherwise $I_{ij} = 0$. For derivation of the last part of the equation is it used that the fluid is incompressible and steady-state and so $\vec{\nabla}\cdot\vec{u} = 0$.

In the expression derived, the force density of the pressure force and the force density of the viscous force is included. The force density and the pressure force is known from equation 2.15. Then the force density of the viscous force becomes [7]

$$\vec{f_{\text{visc}}} = \eta\vec{\nabla}^2\vec{u} \tag{2.20}$$

The sum of all the body-forced is the resulting force written on the right side of the Navier-Stokes equation for a compressible fluid. Therefore the Navier-Stokes equation reads [1]

$$\begin{aligned} &\rho(\tfrac{\partial\vec{u}}{\partial t} + (\vec{u}\cdot\vec{\nabla})\vec{u}) = \textstyle\sum_j \vec{f_j} \\ \Updownarrow \quad &\\ &\rho(\tfrac{\partial\vec{u}}{\partial t}\vec{u} + (\vec{u}\cdot\vec{\nabla})\vec{u}) = \rho\vec{g} + \rho_{\text{el}}\vec{E} - \vec{\nabla}p + \eta\vec{\nabla}^2\vec{u}. \end{aligned} \tag{2.21}$$

The continuity equation states, that for a steady-state flow $\vec{\nabla}\cdot\vec{u} = 0$. This expression enter into the Navier-Stokes that now becomes

$$0 = \rho\vec{g} + \rho_{\text{el}}\vec{E} - \vec{\nabla}p + \eta\vec{\nabla}^2\vec{u}. \tag{2.22}$$

In this project only the pressure force dencity and the viscous force density have to be considered. There is no electrical force acting on the fluid, and the gravitation force and the hydrostatic pressure will cancel each other out. Therefore the first two terms in the Navier-Stokes equation do not have to be considered. Then, finally, the Navier-Stokes equation that is solved in this project becomes

$$0 = -\vec{\nabla}p + \eta\vec{\nabla}^2\vec{u}. \tag{2.23}$$

2.6 Poiseuille flow

The Navier-Stokes equation is a nonlinear differential equation. It is difficult to solve analytically, but in a few cases analytical solutions can be found. One of the cases for which it is possible to solve the Navier-Stokes equation analytical is for a pressure induced steady-state flow in an infinity long and translational invariant channel. This flow problem is called a Poiseuille flow problem and is very important for this project. On the microscopic level, a no-slip boundary condition is obtained for complete momentum relaxation between the molecules in the fluid and the molecules in the wall,

$$u(r) = 0, \qquad \text{for } r \in \delta\Omega. \tag{2.24}$$

In general the no-slip boundary condition for the velocity field is valid for micro fluidic systems.In a Poiseuille flow problem the fluid is driven through a long straight rigid channel by imposing a pressure difference between the two ends of the channel.
When a fluid is flowing through a channel parallel to the x axis, the channel is assumed to be translation invariant in that direction. The constant cross section in the yz direction is denoted C, while the boundary is denoted δC. A constant pressure difference, Δp, over a segment, L, of the channel is maintained, see figur 2.3. Then the boundary conditions for the pressure field becomes

$$p(0) = p_0 + \Delta p, \tag{2.25}$$

$$p(L) = p_0. \tag{2.26}$$

The gravitational force is eliminated by the hydrostatic pressure gradient in the vertical direction and thus it is left out of the analyze.
The translation invariance of the channel in the z direction combined with the vanishing forces in the yz plane implies that the velocity field is not dependent on x, while the only non zero velocity component is in the x direction. This implies that the nonlinear term $(v\cdot\Delta)v$ in the Navier-Stokes equation is zero. Thus the Navier-Stokes equation becomes

$$0 = \eta\vec{\nabla}^2 u_x(y,z) - \vec{\nabla}p. \tag{2.27}$$

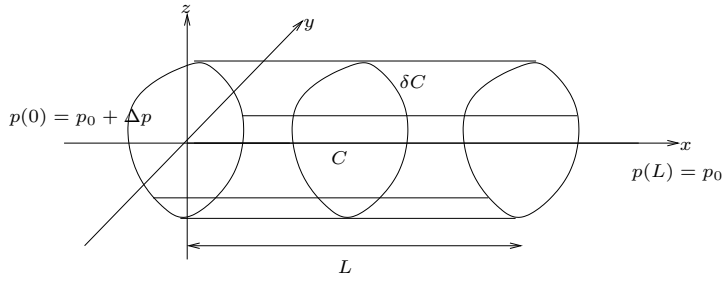

Figure 2.3: *Pouiseuille flow problem in a channel.* [1]

As stated earlier the velocity field in the y and z directions are zero. Therefore, the terms $\delta_y p$ and $\delta_z p$ are zero. Consequently the pressure field is only dependent on x. Then the Navier-Stokes equation becomes

$$\eta[\delta_y^2 + \delta_z^2]u_x(y,z) = \delta_x p(x). \tag{2.28}$$

As seen from the equation, the left hand side is a function of y and z while the right hand side is only a function of x. The only solution to this equation is obtained when both sides are equal to the same constant.
The solution to the right hand side is simple because the constant pressure gradient implies that the pressure field is a linear function of x, when the boundary conditions is used to obtain the pressure,

$$p(r) = \frac{\Delta p}{L}(L - x) + p_0. \tag{2.29}$$

The obtained result is used in the Navier-Stokes equation to obtain

$$\eta[\delta_y^2 + \delta_z^2]u_x(y,z) = -\frac{\Delta p}{L}, \quad \text{for (y, z)} \in \text{C} \tag{2.30}$$

$$u(y,z) = 0, \quad \text{for (y, z)} \in \delta\text{C} \tag{2.31}$$

When the velocity field is determined, it is possible to determinate the fluid volume discharge per time, which is also called the flow rate, Q

$$Q = \int_c v_x(y,z)dydz. \tag{2.32}$$

Now, having obtained an expression for the flow rate, Q, the is how far it is possible to get without specifying the actual shape of the channel.

2.6.1 Cross-sections

In the following sections the flow rate will be calculated for some specific cross-sections of the channels.
The calculations are important for the experiments, when the flow rate through a device containing a micro fluidic cooling systems is estimated.

2.6.1.1 Circular cross-section

The first cross-section for which the flow rate, Q, now will be derived, is a circular cross-section because all tubes in experimental set-up have a circular cross-section, see figure 2.4.
To make the derivation as simple as possible, it is necessary to change the coordinate system from Cartesian coordinates to cylindrical coordinates by a coordinate

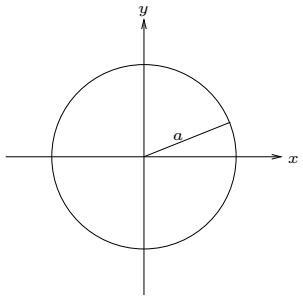

Figure 2.4: *Circular cross-section with radius a.* [1]

transformation,

$$(x, y, z) = (x, r\cos\phi, r\sin\phi), \tag{2.33}$$
$$\vec{e}_x = \vec{e}_x, \tag{2.34}$$
$$\vec{e}_r = \cos\phi\vec{e}_y + \sin\phi\vec{e}_z, \tag{2.35}$$
$$\vec{e}_\phi = -\sin\phi\vec{e}_y + \cos\phi\vec{e}_z, \tag{2.36}$$
$$\vec{\nabla}^2 = \partial_x^2 + \partial_r^2 + \tfrac{1}{r}\partial_r + \tfrac{1}{r^2}\partial\phi. \tag{2.37}$$

The symmetry reduces the velocity field to $\vec{v} = v_x(r)\vec{e}_x$. Then the Navier-Stokes equation becomes a second order differential equation,

$$[\delta_r^2 + \frac{1}{r}\delta_r]u_x(r) = -\frac{\Delta p}{\eta L}, \tag{2.38}$$

The solution to this equation is the solution to the homogeneous differential equation plus a solution to the inhomogeneous equation. The solution to the homogeneous equation has the form $v_x(r,\phi) = A + B\ln r$. One solution to the inhomogeneous equation is $v_x(r) = -\frac{\Delta p}{4\eta L}r^2$. When the boundary conditions is used, the velocity for the channel is

$$u_x(r,\phi) = \frac{\Delta p}{4\eta L}(a^2 - r^2). \tag{2.39}$$

To determine the flow rate, Q, through the system, the velocity is integrated in the equation for the flow rate, which now becomes

$$Q = \int_0^{2\pi} d\phi \int_0^a \frac{\Delta p}{4\eta L}(a^2 - r^2) = \frac{\pi}{8}\frac{a^4}{\eta L}\Delta p dr. \tag{2.40}$$

2.6.1.2 Equilateral triangular cross-section

Before performing the experiments, narrow channels are cut ins PMMA plates to fabricate the devices. These have a Gaussian profile, but for such cross section profiles, an analytical expression for the flow velocity cannot be derived. Therefore the profile can be assumed to have an equilateral triangular cross-section. The equilateral cross-section shown in figur 2.5.
The equilateral triangular cross section is defined for the domain Ω. The boundaries in the y and z directions of the cross section can be defined as a union of the three half-planes, $\frac{\sqrt{3}}{2}a \geq z$, $z \geq \sqrt{3}y$ and $z \geq -\sqrt{3}y$, where a is the length of one side of the cross-section.
The Navier-Stokes equation for in the equilateral cross-section is

$$\vec{\nabla}^2 u(y,z) = -\frac{\delta p}{\eta L}. \tag{2.41}$$

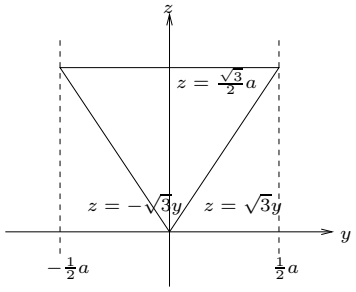

Figure 2.5: *Equilateral triangular cross-section with side length a.* [1]

A trial solution for the velocity field is formed by multiplying the expressions for the three line at the boundaries,

$$\begin{aligned} & u_x(y,z) = \frac{u_0}{a^3}\left(\frac{\sqrt{3}}{2}a - z\right)\left(z - \sqrt{3}y\right)\left(z + \sqrt{3}y\right) \\ \Updownarrow \\ & u_x(y,z) = \frac{u_0}{a^3}\left(\frac{\sqrt{3}}{2}a - z\right)\left(z^2 - 3y^2\right). \end{aligned} \tag{2.42}$$

The obtained solution satisfies the no-slip boundary condition at the boundary, $\delta\Omega$. When the Laplacian, $\vec{\nabla}^2$, acts on the trial solution, the resulting Navier-Stokes equation becomes

$$\begin{aligned} & [\partial_y^2 + \partial_z^2]u_x(y,z) = \frac{u_0}{a^3}\left(\frac{\sqrt{3}}{2}a\partial_z^2 z^2 - \frac{3}{2}\sqrt{3}a\partial_y^2 y^2 - \partial_z^2 z^3 + 3y^2\partial_z^2 z + \partial_y^2 3y^2 z\right) \\ \Updownarrow \\ & [\partial_y^2 + \partial_z^2]u_x(y,z) = -2\sqrt{3}\frac{u_0}{a^3}. \end{aligned} \tag{2.43}$$

The solution to the Navier-Stokes equation, u_0, is then determined,

$$\begin{aligned} & -2a\sqrt{3}\frac{u_0}{a^3} = -\frac{\Delta p}{L\eta} \\ \Updownarrow \\ & u_0 = \frac{1}{2\sqrt{3}}\frac{\Delta p}{\eta L}a^2. \end{aligned} \tag{2.44}$$

Now, the flow rate, Q, is calculated by integrating over y and z,

$$Q = 2\int_0^{\frac{\sqrt{3}}{2}a} dz \int_0^{\frac{1}{\sqrt{3}}z} dy u_x(y,z) = \frac{\sqrt{3}}{320}\frac{a^4}{\eta L}\Delta p. \tag{2.45}$$

2.6.1.3 Rectangular cross-section

When the laser cuts the channels for the micro fluidic cooling systems, the channels becomes relatively wide, and their cross-section can be assumed to be rectangular. There is no analytical solution to the Poiseuille flow for a rectangular cross-section. Therefore, the best analytical solution it is possible to derive is given by a Fourier sum.
The boundary condition for a Poiseuille flow in a rectangular cross-section is

$$\left[\partial_y^2 + \partial_z^2\right] v_x(y,z) = -\tfrac{\Delta p}{\eta L} \quad \text{for} \quad -\tfrac{1}{2}w < y < \frac{1}{2}w,\ 0 < z < h, \tag{2.46}$$

$$v_x(y,z) = 0 \quad \text{for } y = \pm\tfrac{1}{2}w,\ z = 0,\ z = h. \tag{2.47}$$

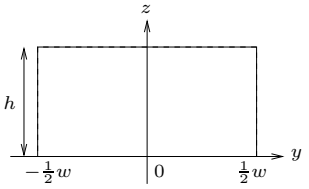

Figure 2.6: *Rectangular cross-section with height h and width w.* [1]

The velocity field for a Poiseuille flow in a rectangular channel is

$$v_x(y,z) = \frac{4h^2\Delta p}{\pi^3\eta L}\sum_{n,\text{odd}}^{\infty}\frac{1}{n^3}\left[1-\frac{\cosh\left(n\pi\frac{y}{h}\right)}{\cosh\left(n\pi\frac{w}{2h}\right)}\right]\sin\left(n\pi\frac{z}{h}\right). \tag{2.48}$$

The flow rate for a rectangular channel can be fund by solving the integral in equation 2.32. Then it can be obtained that obtain

$$Q = \frac{8h^3w\Delta p}{\pi^4\eta L}\sum_{n,\text{odd}}^{\infty}\left[\frac{1}{n^4}-\frac{2h}{\pi w}\frac{1}{n^5}\tanh\left(n\pi\frac{w}{2h}\right)\right]. \tag{2.49}$$

2.7 Hydraulic resistance

As obtained in the previous sections, a constant pressure drop, Δp, will result in a constant flow rate, Q, This connection is is described by the Hagen-Poiseuille law that states

$$\Delta p = R_{\text{hyd}}Q, \tag{2.50}$$

where R_{hyd} is the hydraulic resistance. The hydraulic resistance for the three cross-section described above can directly be derived from the expressions of flow rates, Q. The hydraulic resistance of the three described cross-sections is written in table **??**. The hydraulic resistance for the rectangular cross-section is an approximated result.

Cross-section	R_{hyd}
Circle	$\frac{8}{\pi}\eta L\frac{1}{a^4}$
Equilateral triangular	$\frac{320}{\sqrt{3}}\eta L\frac{1}{a^4}$
Rectangle	$\frac{12\eta L}{1-0.63(h/w)}\frac{1}{h^3w}$

Table 2.1: Hydraulic resistance of different cross-sections

2.7.1 Two straight channels

When two straight channels are connected to form one long channel, the expressions for an ideal Poiseuille flow is no longer valid. However, when the non-linear term in the Navier-stokes equation is insignificant small, the flow rate can be approximated by a Poiseuille flow. The magnitude of the no-linear term in the Navier-stokes equation then corresponds to Reynold's number, Re.

2.7.1.1 Two straight channels in series

When to channels are connected in series, the Hagen-Poiseuille law is approximately valid after the channels are connected. This is equivalent to that Reynold's number,

Re, is low, and the channels are long. It this case the total hydraulic resistance becomes

$$R_{\text{hyd total}} = R_{\text{hyd 1}} + R_{\text{hyd 2}}, \tag{2.51}$$

where $R_{\text{hyd 1}}$ and $R_{\text{hyd 2}}$ are the hydraulic resistance of respectively the first channel and the second channel.

2.7.1.2 Two straight channels in parallel

When two channels are connected in parallel, and it is assumed that Reynold's number, Re, is small and the channels are long, the Hagen-Poiseuille law is approxiately valid. The flow in the channels are conserved, $Q_{\text{total}} = Q_1 + Q_2$, and thus the total hydraulic resistance becomes [1].

$$R_{\text{hyd total}} = \left(\frac{1}{R_{\text{hyd 1}}} + \frac{1}{R_{\text{hyd 2}}} \right)^{-1}. \tag{2.52}$$

2.8 Conduction and convection

The physical property that describes the rate at which a material is conducting heat, is the thermal conductivity, k. A high thermal conductivity results in a high conduction of heat, and a low thermal conductivity results in a low conduction of heat. [20]
There are basically three ways of heat conduction which is conduction, convection and radiation. Conduction in fluids can be described as molecular energy transport and happens, when an energy transporting molecule moving with a high velocity hits a molecule moving with a lower velocity. Then the first molecule will transfer some of its energy to the second molecule. Thereby the velocity of the slow moving molecule is accelerated and velocity of the fast moving molecule is slowed.
Heat transfer by convection happens when heat is transported by the bulk motion of a fluid, that thereby is carrying heat with it.
Heat conduction by radiation happens when electromagnetic waves are emitted by a hot object and thereby carrying energy away from the object. [21]
In a microfluidic cooling system the heat is transferred by conduction and convection, and therefore these two ways of heat conduction will be described in details below.

2.8.1 Conduction

Conduction is described by the heat equation. The heat equation can be derived from an expression of energy conservation in a small element of a system, because the heat conducted into the element, $Q_{\text{conducted in}}$, and the heat generated within the element, Q, are equal to the heat conducted out of the element, $Q_{\text{conducted out}}$, and the change in energy stored in the element, $\frac{\partial \epsilon}{\partial t}$. Thus

$$Q_{\text{conducted in}} + Q = Q_{\text{conducted out}} + \frac{\partial \epsilon}{\partial t}. \tag{2.53}$$

If the heat conduced into the element is subtracted from the heat conducted out of the element, the amount is equal to the change in energy conducted out of the system, which is also the change in the heat flux vector, $\vec{q}$. Combining this with the equation above it results in

$$\vec{\nabla} \vec{q} = Q - \frac{\partial \epsilon}{\partial t}. \tag{2.54}$$

The heat flux vector, $\vec{q}$, is given by Fouier's law, which states that

$$\vec{q} = -k \vec{\nabla} T, \tag{2.55}$$

where k is the thermal conductivity and T is the temperature. This equation describes the molecular transport of heat in an isotropic material. An isotropic material is a material that has no preferred directions, so that the heat is conducted with the same thermal conductivity, k, in all directions.
The energy stored in the element is equal to the thermal energy,

$$\frac{\partial \epsilon}{\partial t} = \rho C \frac{\partial T}{\partial t} \tag{2.56}$$

where C is the heat capacity.
If equation 2.54, equation 2.55 and equation 2.56 are combined, the heat equation becomes

$$\vec{\nabla}(-k\vec{\nabla}T) = Q - \rho C \frac{\partial T}{\partial t} : HydraulicResistanceofdifferentcross - sections.s \tag{2.57}$$

$$\Updownarrow$$

$$\rho C \frac{\partial T}{\partial t} + \vec{\nabla}(-k\vec{\nabla}T) = Q. \tag{2.58}$$

For the steady-state solution the time dependent part of the heat equation is zero, $\frac{\partial T}{\partial t} = 0$, wherefore for steady state the heat equation becomes

$$\vec{\nabla}(-k\vec{\nabla})T = Q. \tag{2.59}$$

This is the equation FEMLab is using when the calculations is carried out. [23] [24]

2.8.2 Convection

Heat transfer will occur between a solid and a fluid in motion, when there is a temperature difference between them. When the fluid is in motion, the dominating heat transportation happens by convection, which will be described further in section **??**.
If the temperature of a solid induces a fluid to move, the phenomenon is know as natural convection. Natural convection is a strong function of the temperature difference.
If the solid is cooled by a fluid in motion, it is know as forced convection. [23]
When convection is considered in the heat equation, an amount of energy has to be subtracted from the heat equation, because it is transported away by the fluid and does not heat the system. The amount of energy is equal to

$$\Delta\varepsilon_{\text{transported}} = \rho C \vec{u}\vec{\nabla}T. \tag{2.60}$$

Including this expression in the heat equation results in

$$\rho C \frac{\partial T}{\partial t} + \vec{\nabla}(-k\vec{\nabla}T) = Q - \rho C \vec{u}\vec{\nabla}T. \tag{2.61}$$

$\Delta\varepsilon_{\text{tramsported}}$ is subtracted from Q because this amount of energy does not heat the system.
It is assumed that the fluid is incompressible, $\vec{\nabla} \cdot \vec{u} = 0$.
For a steady state system the time dependent part of the equation is zero, and therefore the time independent heat equation with the convection term becomes

$$\rho C \vec{u}\vec{\nabla}T + \vec{\nabla}(-k\vec{\nabla}T) = Q. \tag{2.62}$$

2.8.3 Boundary conditions

Based on equation 2.62 the boundary conditions for the microfluidic system can be calculated.

At the outer boundary the system is thermically isolated from the surroundings, so that the boundary condition becomes

$$\vec{n} \cdot \left(-k\vec{\nabla}T + \rho c\vec{u}T \right) = 0, \tag{2.63}$$

where $\vec{n}$ is a normal vector perpendicular to the boundary.
At the inlet, the water flowing into the micro fluidic cooling system with a constant temperature. Thus the boundary condition is

$$T = T_0, \tag{2.64}$$

where T_0 is a constant temperature.
At the outlet the boundary condition becomes

$$n \cdot \left(-k\vec{\nabla}T \right) = 0. \tag{2.65}$$

When the last boundary condition is used there is no conduction perpendicular to the boundary. Thus, there is only convection on the other side of the boundary.

2.9 The Péclet number

The Péclet number, Pe, is a quantity used when describing the micro fluidic cooling systems and can be used in calculations involving convective heat transfer. It is a dimensionless number that gives the ratio between convection and conduction, see section 2.8.
The Péclet number is defined as

$$Pe = \frac{u_0 \rho C L}{k}, \tag{2.66}$$

where ρ is the density of the fluid flowing in a channel, C is the heat capacity, k is the thermal conductivity, u_0 is the mean velocity refering to a characteristic velocity scale and L states a characteristic length scale, for instance the height of the channels.
If Pe is small, $Pe \ll 1$, conduction is important, because the velocity of the fluid is very small. If, on the other hand, Pe er big, $Pe \gg 10$, then convection becomes important.
For a derivation of the Péclet number, see appendix 12.

Chapter 3

Numerical simulations involving FEMLab

The examples of poiseuille flows and convection-diffusion described previous are very important in fluid mechanich. However, it is only possible to solve partial differential equations like Navier-Stoke's equation and the heat equation analytical in special and relatively simple cases with highly symmetry. The micro fluidic cooling systems studied in this project are fairly complex micro fluidic problems. Therefore it is necessary to perform numerical simulations to get solutions to the complicated partiel differential equations, that appear in the calculations.
In this project the equations are solved to optimize the systems using the numerical solver program FEMLab, witch is working by using MatLab, that transforms the problems into matrix problems. FEMLab performs a high-level programming language implementation of nonlinear topology optimization based on the MatLab programming language, and it is able to solve fairly complex microfluidic problems involving for instance the Navier-Stokes equation and the heat equation relatively uncomplicated. FEMLab is using a finite element method, FEM, which is very good for fluidic systems with a low Reynolds number, not exhibiting turbulence. [1]

3.1 The finime element method, FEM

The finite element method, FEM, approximates a problem involving partial differential equations with a problem having a finite number of unknown parameters by introduction of finite elements describing the possible form of the approximate solution. Thereby FEMLab performs a discretization of the original problem.
The starting point for the FEM method is a mesh, splitting up the geometry of the problem into small triangular units of the same shape. When performing the final element method, equation will only be solved in the mesh points, called the mesh vertices, which are the corners of the triagular units, and the equation will be approximated between the points. Therefore, the greater the number of mesh points defined, the greater the accuracy of the calculations will be. [15]
The finite element method, FEM, will not be described here, because it is not necessary to understand in order to run the FEMLab and MatLab programming code. The fundamental MatLab scripts used to perform the topology optimization of the micro fluidic cooling systems were written before the project began. These have most of all been used as a tool, and only a few changes have been made within them. In contrast, the design of the cooling systems and the physical constants were stated by use if the graphical user interface in FEMLab.

3.2 The MMA topology optimization method

The goal of the topology optimizations is to distribute a certain amount of a solid inside a design domain, Ω, such that the structures of the optimized micro fluidic cooling system becomes optimal with respect to the temperature of the cooling system. The temperature has to be as low as possible for a well-defined pressure difference or velocity over the inlet and outlet of the cooling systems and for a given set of geometrical and behavioral constraints.
To reach the goal a method called "Method of Moving Asymptotes", MMA, is performed while running the problem defined in FEMLab and called from the MatLab codes. The method is designed for problems containing a large number and degrees-of-freedom, and thus it is well suited for problems involving topology optimization. An illustration of the MMA method is shown i figure 3.1.

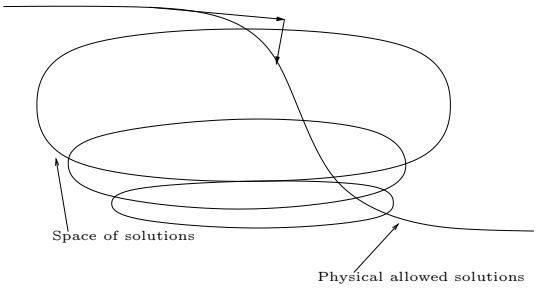

Figure 3.1: *Illustration of the MMA optimization method.* [6]

During an optimization, at first the program is giving a guess on the solution to the problem, $\gamma^{(k)}$, that consider the physically conditions being valid for the system. The guess will of course not become the best solution to the problem. Thus an optimization has to be performed.
For the guess, the slope of the line representing the physical allowed solutions may be found, to which the tangent is followed until the domain of the physical allowed solutions is exceeded. By moving back to the line again, a second and even better guess, $\gamma^{(k+1)}$, can then be obtained and so on. The procedure is repeated until a global minimum is reached, because then the optimization is complete. Every time a guess is performed, the program makes an iteration and non-linear partial differential equations have to be solved.
To be sure of that the minimum found is a global and not only a local minimum, the line representing the allowed solutions has to be smoothen out at the beginning of the optimization, and so it can only be the minimum of the smoothen out curve and thereby it is a global minimum, the only local extremum on the curve, that will be reached in the end. Restoring the curve to its original form, and following it backward, the result may be refined to make sure that it actually is correct. [12] [6]

3.3 The design variable field, γ

During the topology optimizations a material distribution has to be performed. The basis principle of the method is to replace the original discrete design problem with a continuos one where the material inside the micro fluidic cooling systems is allowed to vary continuously between solid and void, that is open channels.
The desing area, Ω, of a micro fluidic cooling system ofot which the optimization has to be performed is drawn in the graphic user interface in FEMLab. Ideally, channels for the waterflow through the system ought to be cut in a solid. But only water is

considered in the system. Therefore, in the beginning, the area of the cooling system can be assumed to be filled with a sponge, because that kind of material either consists of solid or empty holes, in which water is able to flow. The sponge can be assumed as being a porous idealized material of spatial varying permeability in the design domain, Ω, where solid walls correspond to the limits of very low permeability, and open channels correspond to the limit of very high permeability. Thus, during the optimization, it is the amount of moving water and the amount of stationary water that will change. For the micro fluidic cooling systems is corresponding to the relationship between channels and walls. To define this relationship a design variable field, γ, that defines where the water is moving and where it is stationary. γ can also be assumed to control the local permeability of the medium. For γ at respectively the wall and open channels holds

Walls:	$\gamma = 0$
Open channels:	$\gamma = 1$

When the topology optimization is completed, there will be either walls or open channels at each of the points defined for the design area of the micro fluidic cooling systems, and γ will only take the values $\gamma = 0$ or $\gamma = 1$, respectively. Anyway, smeared-out gray-scales will appear at the boundaries of the topology optimized structures, it what areas there will be neither empty channels nor walls, which is not in agreement with the conditions established for the optimizations. Afterall, the smeared-out gray-scales appear because MatLab and FEMLab are performing numerical optimizations, and thus the result will never be exact.
It was described above that only water is considered to appear the system. Therefore the so-called walls of the system actually is stationary water, so that the results of the optimizations are not physically correct, because the walls in fact consist of a solid having other material parameters than the water. Anyway, the assumption with stationary water is a reasonable approximation to reality, and it makes the optimizations relatively simple. [6] [12]

3.4 The Darcy force

Darcy's law states that when water is flowing through a micro fluidic cooling system, that can be described as a sponge as described in section 3.3, it is influenced by a frictional force, the so-called Darcy force, $\vec{f}_{\text{Darcy}}$, which is given by

$$\vec{f}_{\text{Darcy}} = -\alpha\vec{u}, \tag{3.1}$$

where $\vec{u}$ is the velocity of the water, and α is the inverse of the local permeability of the system at a certain point. α is dependent on the relationship between the walls and the open channels in the micro fluidic cooling systems. Equation 3.1 is only approximately valid for a porous media, but because only solids wall and open channel are assumed to be represented for the final structure, the equation can be used. Therefore, the equation can be used in the calculations.
For a distinct point of the cooling system, α can be written as a function of the design variable field, γ, by convex interpolation,

$$\alpha\gamma = \alpha_{\min} + (\alpha_{\max} - \alpha_{\min})\frac{q(1-\gamma)}{q+\gamma} \quad \text{for} \quad \gamma \in [0;1], \tag{3.2}$$

where q is a real and positive design variable function due to tune the shape of γ. q is important for the structures of the micro fluidic cooling systems when these are topology optimized. If the variale functin q is increased in the MatLab code some of the problems with smeared-out gray-scale structures may disappear.
To write up the equation for $\alpha\gamma$, it was assumed that $\alpha = \alpha_{\min}$, when the colling system is not containing any solid (or stationary water), and $\alpha = \alpha_{\max}$, when the

system is completely filled with a solid. For water flowing in a two dimensional channel it is assumed that $\alpha_{\min} = 0$. On the other hand, when the system is completely filled with a solid, water is unable to flow through it and so $\alpha_{\max} = \infty$. However, the FEMLab and MatLab program is unabble when performing numerical calculation involving the number infinity. Thus $\alpha_{\max}$ is have to be a very high number, because the Darcy number, Da, is established to be $Da = 1 \cdot 10^{-5}$ in the program.
Darcy's number, Da, is a dimensionless number that states the relationship between viscous and porous friction forces. Darcy's number is proportioale to the Darcy force.

$$Da = \frac{\eta}{\alpha_{max} l^2} \tag{3.3}$$

$$\Updownarrow$$

$$\alpha_{max} = \frac{\eta}{Da \cdot l^2}, \tag{3.4}$$

where l is a characteristic length scale of the system and u is a caratheristic velocity. Darcy's number has an influence on the structures of the optimized cooling systems. [12] [6]

3.5 The objective function, ϕ, and specific geometry

The FEMLab and MatLab program is optimizing a objective function, $\phi(\vec{u}, \gamma)$, which, generally, in FEMLab is defined as

$$\phi(\vec{u}, \gamma) = \int_{\Omega} A(\vec{u}, \gamma) d\vec{r} + \int_{\partial\Omega} B(\vec{u}, \gamma) d\vec{s} + \sum_{\partial^2\Omega} C(\vec{u}, \gamma). \tag{3.5}$$

For the objective function the first term corresponds to the design area, Ω, of the defined micro fluidic cooling system, the second term corresponds to the boundaries of the geometri, $\partial\Omega$, and the third term corresponds to defined points, $\partial^2\Omega$, within the geometry. [12] [6]
During the optimizations a value for A is the only one term that is defined, because the optimizations have to be performed on the whole area of the micro fluidic cooling system. $B = 0$ and $C = 0$, and so

$$\phi(\vec{u}, \gamma) = \int_{\Omega} A(\vec{u}, \gamma) d\vec{r}. \tag{3.6}$$

From the objective function the average temperature, T, of the optimized micro fluidic cooling systems can be derived when dividing by the area, A_{cooler}, of it,

$$T = \frac{\phi(\vec{u}, \gamma)}{A_{\text{cooler}}}. \tag{3.7}$$

During the optimization, ϕ is always miminized, so that $A = T$. In this way the temperature, T, of the design region, Ω, is minimized.

Chapter 4

Set-up for topology optimization problems using FEMLab

The topology optimization problems are solved using a numerical solver programs FEMLab and MatLab. Starting FEMLab from MatLab makes is possible to define and perform calculations on complicated topology optimization problems.
The geometry of the problems and the physical parameters for the problems are defined in the FEMLab graphical user interface, GUI, and associated MatLab programmes are used to solve the topology optimization problems.

4.0.1 The Navier-Stokes application mode, geometry and mesh

When starting FEMLab, "Fluid Dynamic" is chosen for a two dimensional problem. Then it is chosen that is it an "Incompressible Navier-Stokes" equation that has to be solve for "Steady-State Analyses", because the water flowing in the channels is assumed to be steady-state as described in section 2.1. Now it is possible to solve problems involving liquids or gases in motion.
The geometry of the problem is defined in two dimensions in the FEMLab GUI. The geometry is separated into different parts to have the central design region defined besides the inlet and outlet for the system. When performing the simulations, all physical parameters have to be defined in SI-units, and thus the lengths defined for the structure is in meter.
The choose of mesh is important for the stability and the accuracy of the numerical obtained results. The mesh for the difference parts of a structure is defined in "Subdomains" under "Mesh Parameters" in the menu "Mesh". In the design region of the micro fluidic cooling systems a fine mesh is defined, while for the inlet and outlet a coarser mesh is drawn.
The "Incompressible Navier-Stokes" application mode solves the Navier-Stokes problem for the pressure for the velocity vector components appearing in the equation.
Navier-Stokes equation, not including the electrical force density, and the continuity equation for an incompressible, steady-state fluid are

$$\vec{F} = \rho\frac{\partial\vec{u}}{\partial t} - \eta\vec{\nabla}^2\vec{u} + \rho(\vec{u})\cdot\vec{\nabla})\vec{u} + \vec{\nabla}p \tag{4.1}$$

$$\vec{\nabla}\vec{u} = 0, \tag{4.2}$$

where $\vec{F}$ is the total force or volume force, p is the pressure, $\vec{u}$ is the velocity of the liquid flowing in the system, η is the viscosity of it and ρ is the density of it.
FEMLab uses a generalized version of the Navier-Stokes equation in terms of transport

properties and velocity gradients. Starting with the momentum balance in terms of stresses and inserting an expression for the viscous stress tensor, $\tau_{\text{visc}} = \eta(\vec{\nabla}\vec{u} + (\vec{\nabla}\vec{u})^T)$, the equation becomes

$$\vec{F} = \rho\frac{\partial\vec{u}}{\partial t} - \vec{\nabla}(\eta(\vec{\nabla}\vec{u} + (\vec{\nabla}\vec{u})^\dagger) + \rho(\vec{u})\cdot\vec{\nabla})\vec{u} + \vec{\nabla}\vec{p} \tag{4.3}$$

$$\vec{\nabla}\vec{u} = 0. \tag{4.4}$$

An expression for the viscous stress tensor, $\eta(\vec{\nabla}\vec{u} + (\vec{\nabla}\vec{u})^T)$, witch is the second part of the total stress tensor, $\tau = -p\vec{I_{ij}} + \eta(\vec{\nabla}(\vec{u}) + (\vec{\nabla}v)^T)$, see section 2.5, is inserted in the equation to obtain the form of the Navier-Stokes equation used in the FEMLab "Subdomain Settings",

$$\rho(\vec{u}\cdot\vec{\nabla})\vec{u} = \vec{\nabla}\cdot(-p\cdot I_{ij} + \eta(\vec{\nabla}\vec{u} + (\vec{\nabla}\vec{u})^\dagger)) + \vec{F} \tag{4.5}$$

$$\vec{\nabla}\vec{u} = 0 \tag{4.6}$$

In the dialog box for "Subdomain Setting" under "Physics" the parameters of the liquid flowing in the system is defined. Water is used in this project, and thus the physical parameters are $\rho = 1000$ kg/m^3 and $\eta = 0.001$ mPa·s. The gravitation force and the hydrostatic pressure will cancel each other out and thus the volume force $\vec{F} = (F_x, F_y) = 0$.
In "Boundary Settings" under "Physics" the properties for the boundary conditions of the Navier-Stokes equation is determined. The boundaries for both the inlet and the outlet has the property "Normal flow/Pressure", because the water is flowing straight out of the channel, so that the components of the velocity perpendicular to the water flow is zero.
To drive the water through the system, for the inlet and the outlet the pressure is defined to be $p_0 = dp$ and $p_0 = 0$, respectivily.
It is also possible to set a velocity of the water flowing into the system. Then for the inlet a boundary condition "Inflow/Outflow velocity" is chosen in "Boundary Settings", while for the outlet "Pressure" with $p_0 = 0$ is still chosen. The water is flowing in the x direction, u, and the velocity profile for the inlet is a parabolic function defined as

$$u = s(1-s)6u, \tag{4.7}$$

where s is a function defined by FEMLab, that changes between 0 and 1 within the simulations. The velocity in the y direction, v, is zero. Thus $v = 0$.
For the boundaries surrounding the system, the boundary condition is "No Slip", because the liquid is always stationary at the boundaries. Thus $\vec{u} = 0$.
For the boundaries within the structure it does not make sense to have boundary conditions. Therefore these are defined to be "Neutral" as if there were no boundaries. [19]

4.0.2 The conduction and convection application mode

The conduction and convection application mode in FEMLab included heat transfer by conduction and heat transfer by convection. Is is added to the problem by choosing "Convection and Conduction" in the application mode "Heat Transfer".
In FEMLab the nonconservative formulation for the heat equation is used,

$$\rho c\frac{\partial T}{\partial t} + \vec{\nabla}\cdot(-k\vec{\nabla}T) = Q - \rho c\vec{u}\cdot\vec{\nabla}T, \tag{4.8}$$

where c is the heat capacitance, T is the temperature, k is the thermal conductivity and Q is the heat added to the system. The fluid is assumed to be incompressible and steady-state. Thus $\frac{\partial T}{\partial t} = 0$. Then the equation becomes

$$\vec{\nabla}\cdot(-k\vec{\nabla}T) = Q - \rho c\vec{u}\cdot\vec{\nabla}T. \tag{4.9}$$

In "Subdomain Settings" the physical parameters $\rho = 1000\,\mathrm{kg/m^3}$, $c = 4180\,\mathrm{J/(kg{\cdot}K)}$ and $k = 0.56\ \mathrm{W/(m{\cdot}K)s}$ for the water flowing in the system is defined for the whole structure. A constant for the heat flow through the design structure, which size is given in MatLab, is defined as $Q = Q$. For the rest of the system $Q = 0$. The velocities in respectivily the x and the y directions is defined as $u = u$ and $v = v$.
For the "Boundary Conditions", the condition "Temperature" is chosen for the inlet. The initial condition is defined to be a constant temperature, T. For the outlet the boundary condition "Convective Flux" is chosen, because only convective flux is allowed to exit the domain,

$$\vec{n} \cdot (k\vec{\nabla}T) = 0, \tag{4.10}$$

where $\vec{n}$ is a normal vector perpendicular to the boundary.
The boundaries surrounding the structure is defined to be "Thermal Isolation", and the boundaries within the structure are "Neutral", not having any influence on the problem. [18]

4.0.3 The PDE application mode

All fields have now been added to the system except the design field, γ.
The application mode "PDE, General Form" is used to define the γ-field for the problem. When the field is added, the dependent variable defined to be γ, and the element "Lagrange - linear" is chosen. The partial differential equation, PDE, application form is used when solving PDEs that can be nonlinear like the Navier-Stokes equation and the heat equation.
In "Subdomain Settings", the equation for the PDE for the structure is defined,

$$\vec{\nabla} \cdot \vec{\Gamma} = F \tag{4.11}$$

where the coefficient Γ is a flux vector and F is a force term. The γ-field is is updated outside by use of MatLab. Therefore it is not necessary to associate a set of equations for the field, and thus the coefficients $\vec{\Gamma} = 0$ and $F = 0$.
Under "Init", an initial condition for the γ field is defined to be $\gamma(t_0) = \gamma_0$.
In "Boundary Settings" equations for the boundary conditions is defined as,

$$-\vec{n} \cdot \vec{\Gamma} = \vec{g} + \left(\frac{\delta R}{\delta v}\right)^T \mu \quad \text{and} \quad \mathrm{R} = 0 \tag{4.12}$$

The boundary conditions for the γ-field are not changed. Therefore FEMLab defines the coefficient R and g to become $R = -\gamma$ and $g = 0$. Then all dynamics is removed from the γ-field.
At last the objective function, ϕ,see section 3.5, is added to the system. The expressions for A, B and C in the objective function are defined in the respectively "Scalar Expressions", "Boundary Expressions" and "Point Expressions" under "Expressions" in the "Options" menu. The optimization is only performed for the design field, Ω, at which the temperature has be minimized. Thus $A = T$, $B = 0$ and $C = 0$. [16]

4.0.4 Creating a set-up file and running the program

When the geometry of the problem is defined in the FEMLab GUI, it is saved as a MatLab "Geometry" file. The Navier-Stokes problem, the heat equation and the values for the objective function are all included in the "Geometry" file, because these are defined in the FEMLab GUI. However, the Matlab file contains more information than needed, and thus this extra information has to be deleted from the set-up file before it is possible to run the program. [17]
Other MatLab scripts are connected to the set-up file to solve the problem. When running a "Main" scrip, it will call and run all the other MatLab scripts, including the "Set_up" file. In the $Main$ all physical constant used is included in the problem

and defined as FEMLab constants, and the pressure difference over the system or a initial velocity for the inlet is defined.
In the MatLab script "GammaOn" the Darcy force is added to the Navier-Stokes problem, and the design field, γ is included. By use of the scripts "Solve" and "mmasub" the whole problem is solve and the resulting design field, γ, the change in γ for each interaction, the velocity field and finally the temperature field is showed on the screen by use of the scrip "Plot_Res".

Chapter 5

Computer simulations

5.0.5 Simulations

In this section the FEMLab simulations are described. The FEMLab simulations are carried out in order to determine the optimal temperature over the final micro fluidic cooling systems for a given pressure difference over the inlet and outlet.
In the simulations, a pressure difference is defined over the inlet and outlet of the device, but a velocity profile could also have been defined. However, this is not done because a velocity profile would result in thinner channels within the design structure, which would be very difficult to cut with the laser. Fabrication of the micro fluidic cooling systems is described in section 6.1.

5.0.6 Determination of a global minimum

The FEMLab simulations are performed as described in section 4.
For the first system, at which simulations were performed, the geometry is shown in figure 6.2 [1].

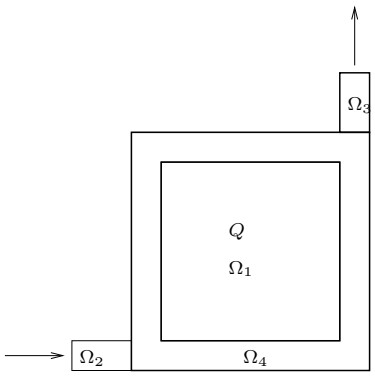

Figure 5.1: *The design of the first micro fluidic cooling system.*

For the geometry, the optimization were performed within the regions Ω_1 and Ω_4. The region Ω_2 represents the inlet and the region Ω_3 represents the outlet. A constant heat, defined by Q, is supplied to the design region Ω_1. The size of the design region Ω_1 is 1 cm $\times$ 1 cm, while the size of the design region Ω_4 is 1.4 cm $\times$ 1.4 cm. The size of the inlet and outlet is 0.2 cm $\times$ 0.5 cm.
The simulations were carried out in order to determine whether a temperature found

[1] The MatLab scripts, in this rapport referred to as the program, necessary to perform the simulations, can be found on the CD-ROM in the folder "Program T01".

for an optimized structure was a minimum temperature or not. To do so, the temperature measured from the optimization was compared to the temperature of another optimized structure, for which the pressure difference over the inlet and outlet was not the same. Thus further simulations were carried out for the same geometry, but for other pressures differences between 0.033 Pa and 2 Pa over the inlet and outlet. [2] The material parameter, $\gamma 0$, is set equal to 0.95. Thereby there has to be at least 5% material within the design structure for which the optimixations are performed. The program can choose how much material the structure contains, when performing the optimizations.
The optimized structure of the optimal systems is shown in figure 5.2.

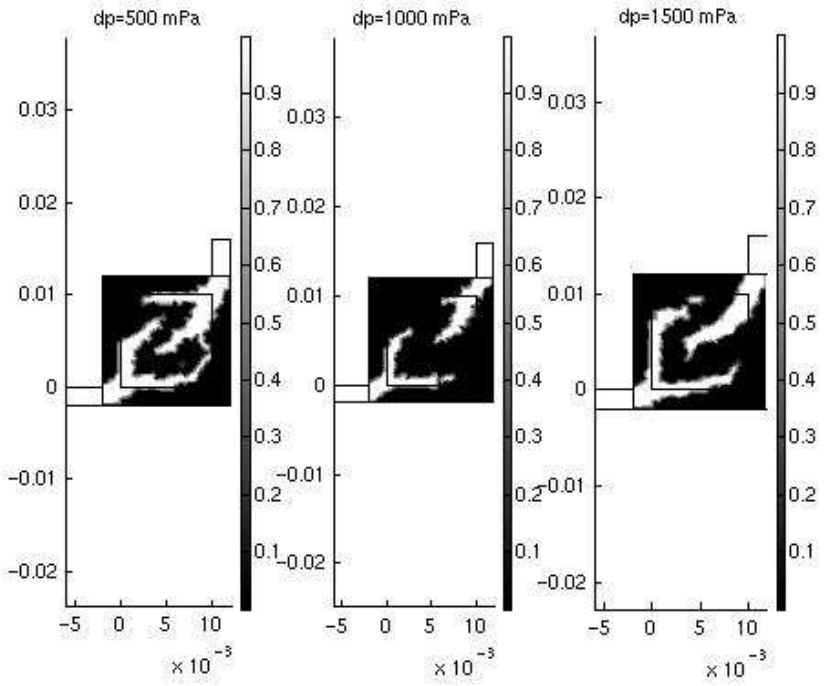

Figure 5.2: *Optimzed stucture for the micro fluidic cooling system shown in figure 6.2 optimized for different pressure differences.*

After an optimal stucture for a micro fluidic cooling system is determined, the pressure difference over the inlet and outlet is changed, and a new average temperature is calculated for the new pressure, [3]. The obtained temperature is plotted as function of the pressure, see figure 5.3 [4].
As noted from figure 5.3, the system that is optimized for a given pressure is not optimal, because none of the curves has a minimum.
The simulations was carried out for many different pressure differences and each time the obtained result was the same, it was not possible to get an optimized structure. Therefore, it was revealed that the parameters in the program used by the MMAsub routine to calculate the geometry of the optimal stucture was not correct. The reason for this was, that The MMAsub routine needs four variables to carry out an optimization. The first variable is $f = \frac{\Phi}{\Phi_0}$, where Φ is the objective function and Φ_0 is a

[2] The MatLab program for which the geometry is defined is showed in the appendix on the CD-ROM in the folder "Program T01", and the MatLab script for the Main program for different pressures is shown in the in appendix on the CD-ROM in the folder "Program T01".

[3] The MatLab scripts, in which the variation of the pressure and the average temperature is calculated, is shown in the appendix on the CD-ROM in the folder "Plot programs"

[4] The MatLab script plotting the temperature as a function of the pressure can be found on the CD-ROM in the folder "Plot programs".

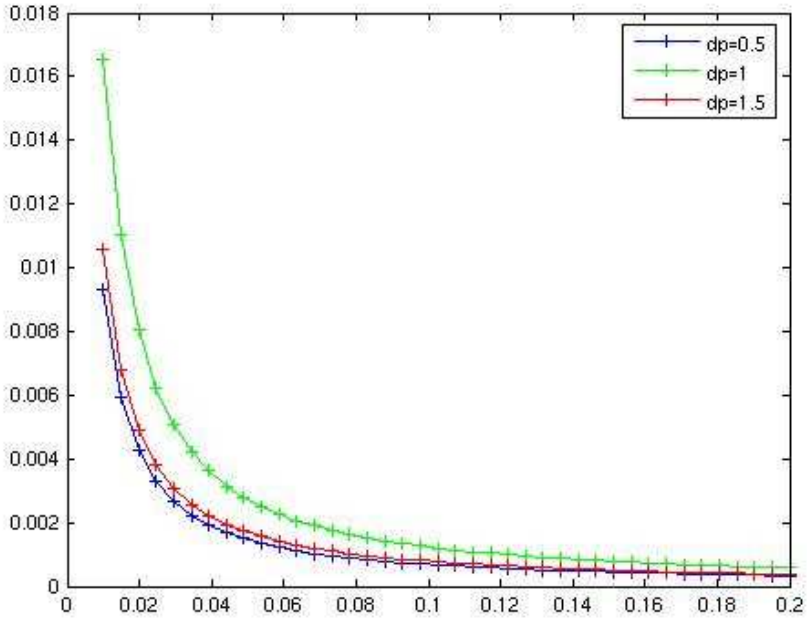

Figure 5.3: *The temperature plotted as a function of the pressure for the optimized micro fluidic cooling system. The legends specify which system the different curves belongs to.*

constant. The second variable, the MMAsub routine needs, is $g = \int |A| \cdot dA - \gamma_0 \leq 0$, where $\int |A| \cdot dA$ is the volume of the material that the stucture contains and γ_0 is the maximum volume of material that the stucture are allowed to contain. g ensures that the material limit is maintained. g always have to be equal or less than zero, so that the volume of the material, the design field contains, does not exceed the condition on γ_0. Therefore, the MMAsub routine needs to have the derivative of g and f with respect to γ. The derivative of f with respect to γ is calculated in the MatLab code. The derivative of g with respect to γ is correspomding to the volume of each mesh point. This value is set to one inthe program.
The assumption that was wrong during the simulations, was that g was set equal zero, because the optimal stucture might be one that contains less material then the allowed volume. Therefore g was changed to $g = \int |A| \cdot dA - \gamma_0$ and the $\frac{dg}{d\gamma}$ was changed to be equal to γ for the i'te element. Then the same stucture was simulated with the new conditions.
In the simulations the channels became very wide compared to the channels optioned in the simulations before the changes were made. Furthermore it was noted that the stucture is completely filled with water.
From the simulations it was noted that the structure was emptied for material and the amount of material within the structure was the limit for $\gamma 0$. Therefore, it was concluded that micro fluidic cooling system is most optimal when water can fill all the structure, when it is flowing through it. The reason for this is, that when water is flowing through all the stucture, the heat is transported by convection, whereas when the heat is transport through the material, it happens by conduction. Convection is a more efficient way of heat transportation compared to conduction, as thus the most optimal micro fluidic cooling system is obtained when it is completely filled with flowing water.

5.0.7 Changes of the design variable field, γ

Even though the program is calculating the structure of the most optimal micro fluidic cooling system, the stucture is might be difficult to fabricate this structure, because it will collapse. Therefore γ_0 is then fixed at 0.6. Thereby the program have to have at least 40% of the stucture filled with material. The geometry of the new micro fluidic cooling system in shown in figure 5.4 [5]. The region around the heated area is removed or otherwise the program will fill all the material into the area between the heated area and the edge of the cooling system, design field Ω_4.

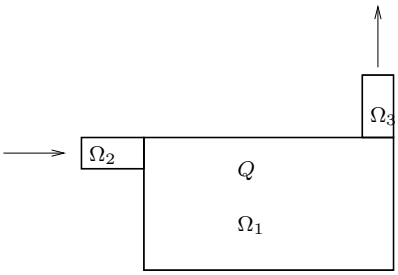

Figure 5.4: *The new design of the micro fluidic cooling system.*

Heat is constant applied to the design region Ω_1. The heat is described, Q. The design region Ω_1 is 1 cm $\times$ 2 cm. The regions Ω_2 and Ω_3 are respectively inlet and outlet, which size is 0.1 cm $\times$ 0.2 cm.
The pressure difference over inlet and outlet is varied from $\Delta p = 0.033\,\text{Pa}$ to $\Delta p = 2\,\text{Pa}$. The optimized structures is shown in figure 5.5.

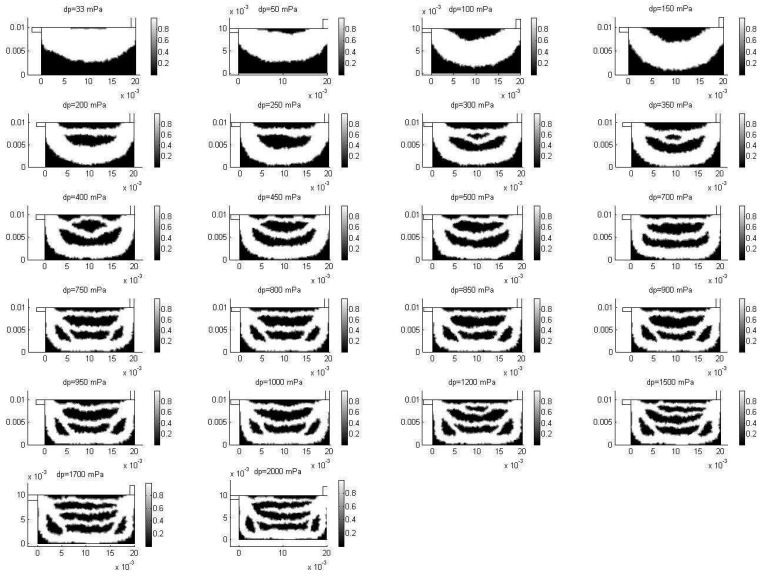

Figure 5.5: *The stucture of the micro fluidic cooling system optimized at different pressure differences.*

[5] The MatMab script that defines the geometry is shown in the appendix on the CD-ROM in the folder "Program T03"

As it can be noted from figure 5.5, there is only one channel from $\Delta p = 0.033\,\text{Pa}$ to $\Delta p = 0.15\,\text{Pa}$. This channel is very wide in the system optimized at $\Delta p = 0.033\,\text{Pa}$ and only the upper half of the system is cooled. In contrast, the cooling distribution of the channel in the system optimized at $\Delta p = 0.15\,\text{Pa}$ is more even. As it noted from the figure, there is a evolution of the structures from $\Delta p = 0.3\,\text{Pa}$ to $0.7\,\text{Pa}$ where a channel splits up into two channels. The same evolution is seen between $\Delta p = 1.2\,\text{Pa}$ and $\Delta p = 1.7\,\text{Pa}$.
For stucture optimized to $\Delta p = 2\,\text{pa}$ there is a channel that terminates in the material. This error occurs because a very small volume of water actually are able to pass through the material, but it is unphysical and thus these solution cannot be used. From the figure it is noted that the stucture becomes more complex when the pressure is increased. If the pressure is increased above 2 Pa, the structures would contain an increasing number of channels that terminates in the material.
The temperature as a function of the pressure is determinated for the optimized structures [6]. The results is shown in figure 5.6. From the figure 5.7 it is noted, that the optimized stucture not in all cases resolve in the lowest average temperature.

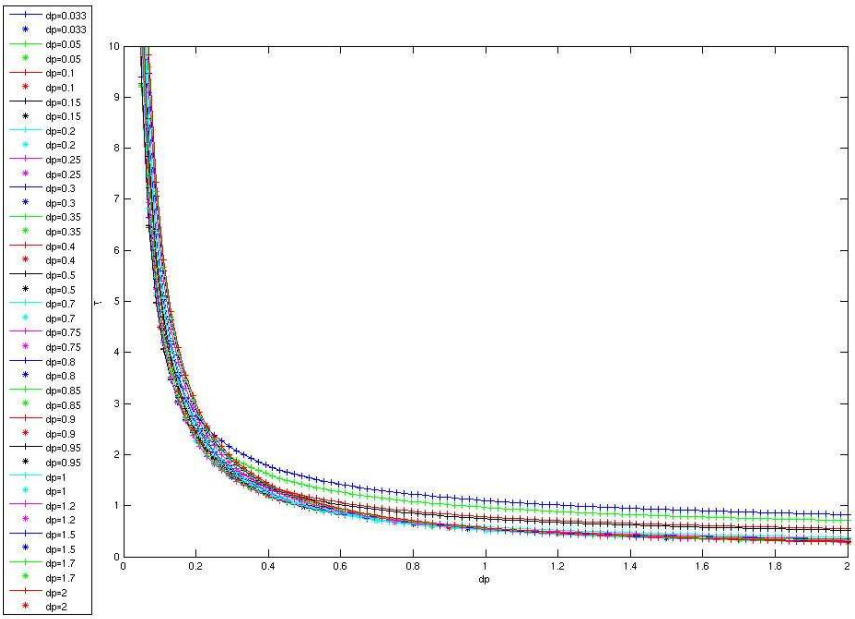

Figure 5.6: *Temperature plotted as a function of pressure for the optimal stucture of the micro fluidic cooling system optimized for different pressure differences. The legends specify which system the different curves belongs to.*

5.0.8 The MMAsub routine

The error in the average temperature could be caused by the the MMAsub routine, because when the MMAsub routine is runned, it needs a constant, c, that determines the allowed distance to the boundaries of the solutions defined by γ_0. If the minimum is very close to a restricted area of the solution, the MMAsub routine will not allow the program to continue to the minimum. Therefore, the optimal stucture will not be situated in a minimum.
After performing the coundary condition mentioned above, the constant c was changed, so that is becomes possible for the program to find a solution closer to the boundary. The default value for the constant c stated in the MatLab profgramme is $c = 1000$.

[6] The MatLab script can be found on the CD-ROM in the folder "Plot program"

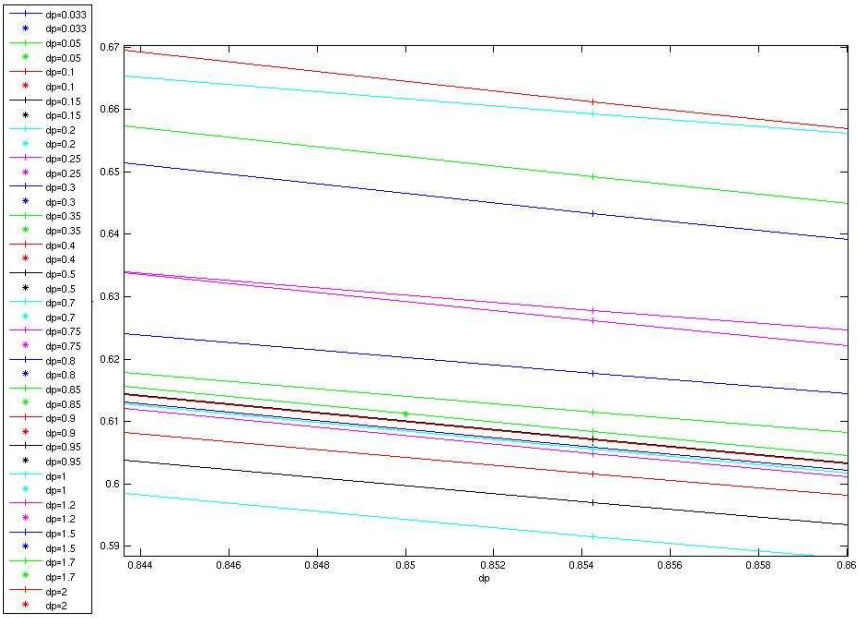

Figure 5.7: *The optimal stucture for the micro fluidic cooling system optimized at different pressure differences, the * denotes the average temperature of the optimal system.*

To find the minimum value for c, where the solution still obeys the condition for γ_0. The program is ruined for different values of c, and the constant γ_0 is determined. Then γ_0 is plotted as a function of c, see figure 5.8.
When the final value of γ_0 exceeds its upper limit, the value of c becomes to small and thus it has to be increased. The interval where γ_0 ecceed its upper value is between 70 and 76. Therefore this area has to be investigated further. A plot of γ_0 as a function of c for the interval $70 - 76$ is shown in figure 5.9.
From the figure it is noted that the value of γ_0 is unstable from 70 to 76. Therefore the constant c is changed to 76 to be sure of that the γ_0 condition always is obeyed.
To determine whether the change in the value of c has any influence on the optimization of the system or not, the simulation are performed for pressure differences between $\Delta p = 0.5$Pa and $\Delta p = 0.7$Pa, because in this interval, the obtained solutions were not the optimal solutions as they had to be. afterwards, the pressure is changed to determine the temperature for the systems.
As noted from figure 5.10, the change in the c value does not have any influence on the fact that the systems are not optimal at the pressure difference, they are optimized for. The pressure difference is very small and there is almost no change in the structure of the design area. Therefore, the error might be caused because the program has found a global minimum for the structure at the pressure range. The optimization is solved numerically, and thus there is only a finite number of mesh points in the simulation, and the solution can only be calculated as precise as the convergence criterion determines.

5.0.9 Increase of the pressure difference

The pressure difference over the micro fluidic cooling systems is still to small to be measured because the pressure difference cannot exceed $\Delta p = 1.7$Pa. Above this pressure, the channels start to terminate into the material, and thus the solutions becomes unphysical. To increase the pressure difference over the micro fluidic cooling system, a very long inlet is determined in FEMLab. The new structure is shown in

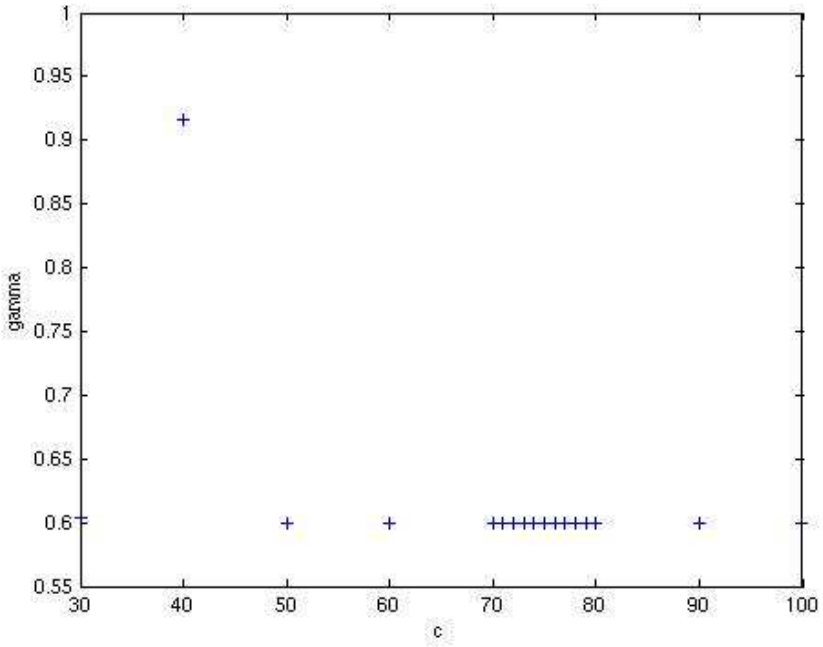

Figure 5.8: γ_0 *plotted as function of* c

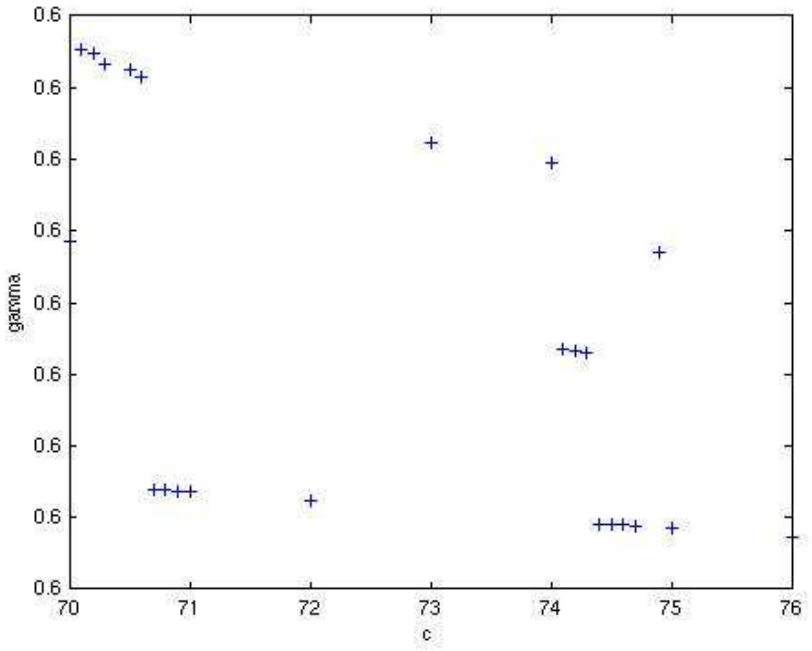

Figure 5.9: γ_0 *plotted as a function of* c *in the interval* 70-76

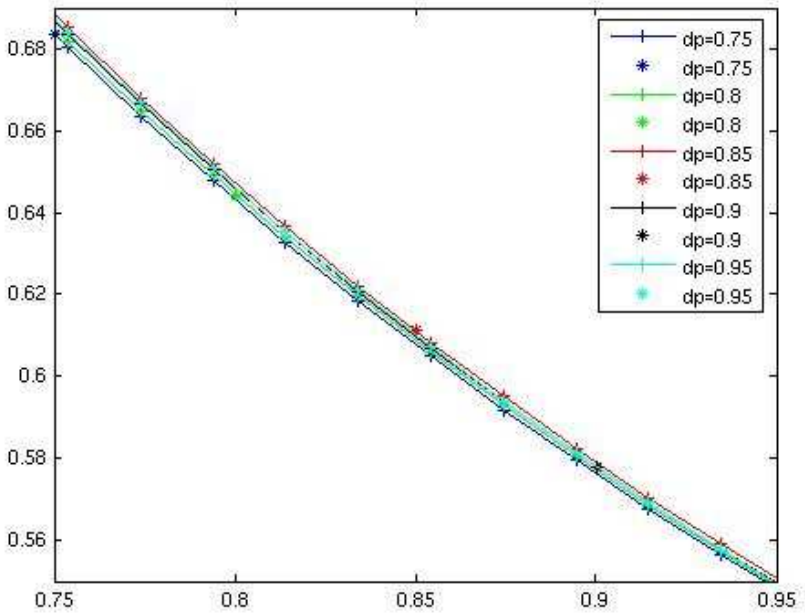

Figure 5.10: *Temperature plotted as a function of the pressure difference over the optimized cooling system. The program is runnet with* $c = 76$

figure 5.11.
The wide of the inlet and outlet is changed to $\Delta p = 0.2$cm, which makes it easier to draw the helical line i FEMLab. The simulations are runnet for different pressure differences over the system and it is discovered that the pressure difference cannot exceed $\Delta p = 2$ Pa, because systems with a higher pressure difference has channels that terminates into the material, as illustrated on figure 5.12 .
This structure is fabricated i a PMMA plate as described in section 6.1.

5.0.10 The final system

The pressure difference over the devices has to be even higher, and thus the systems described below could not be used for practical experiments. Therefore it was decided to define the inlet and outlet as long helical line. This was not simulated in FEMLab, but defined with use of the laser program. It was possible ti calculate the pressure difference over the micro fluidic cooling systems if the hydraulic resistant for the inlet and outlet was determinated. The only part of the system that is simulated in FEMLab, is the design region. A the inlet and outlet, boundary conditions are defined in the same way as earlier. The new structure is shown in figure 5.13. The temperature of the water at the inlet is fixed to be $T = 25°$C, corresponding to the temperature of the water used in the experiments, that was the same as the temperature in the lab where the experiments were performed.
The width of the inlet and the outlet is set to $w = 0.5$mm. The simulated were performed for pressure differences between $\Delta p = 0.5$Pa and $\Delta p = 4$Pa in steps of $\Delta p = 0.5$Pa. The obtained result is noted in figure 5.14.
As noted from the figure, the systems optimized for higher pressure differences than $\Delta p = 2.5$Pa have channels that terminates into the material and thus these are unphysical.
The pressure of the optimized systems is varied and the new temperatures are calculated. The average temperature over the design region as a function of the pressure

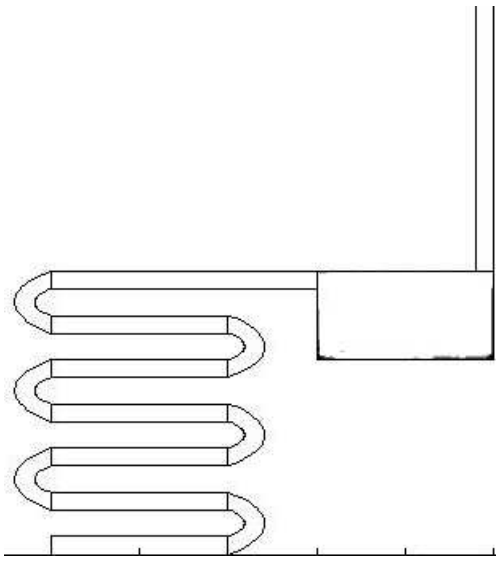

Figure 5.11: *The geometry for the micro fluidic stucture with a long inlet, draw in FEMLab as a helical line.*

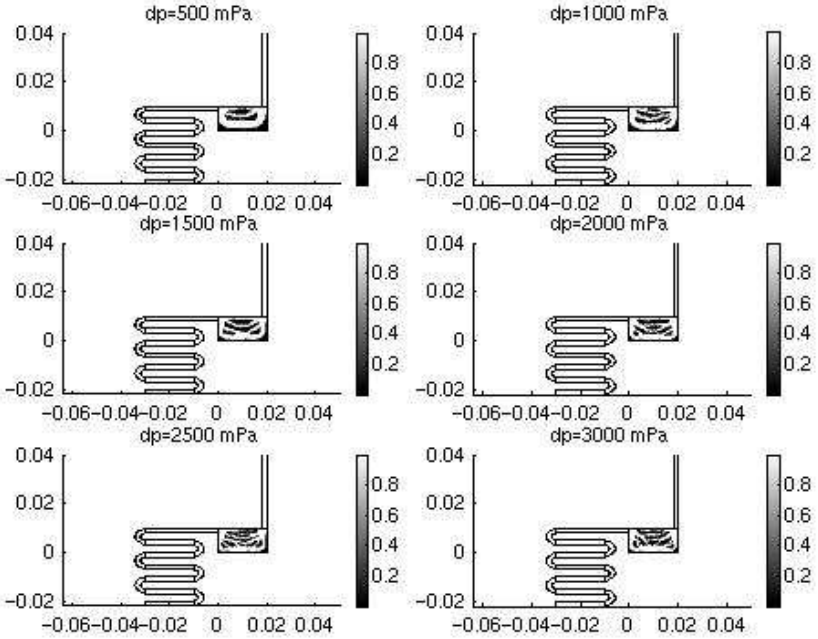

Figure 5.12: *The structure of a optimized micro fluidic cooling systems, optimized at different pressures.*

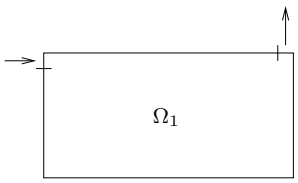

Figure 5.13: *Geometry of the final micro fluidic cooling systems.*

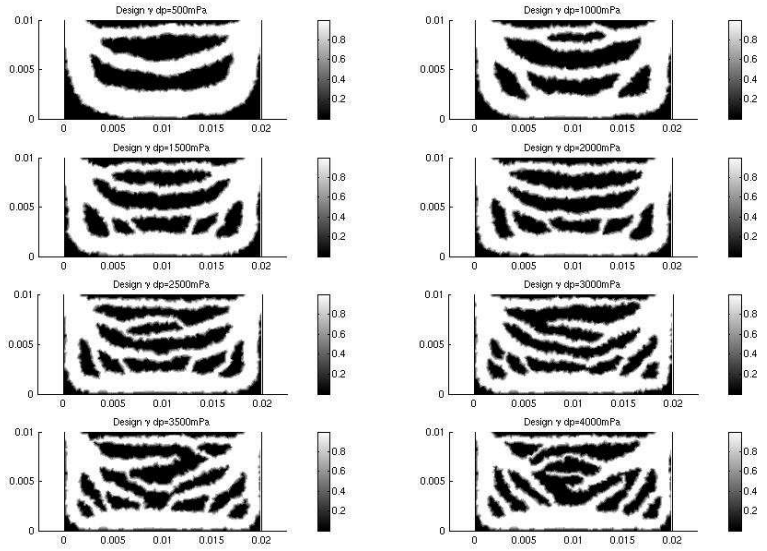

Figure 5.14: *Structure of the final optimized micro fluidic cooling systems, optimized for different pressures.*

is plotted, see figure 5.15. From the figure it is noted that the optimized structures is not the optimal structure at the optimal pressure.
The temperature field and the velocity field are plotted for the design area, see figure 5.16.

5.1 Conclusion

The first stucture optimized reveals an error in the program which was corrected. Then γ_0 was fixed at 0.95, which the result that the hole structure was emptied of material. This empty structures would be difficult to fabricate i practice because it might collapse, and the result is not interesting for the simulations. Therefore, γ_0 was fixed at 0.6 and the geometry was changed. The pressure difference was increased over the inlet and outlet because a higher pressure difference was easier to measure when performing the experiments.
When the pressure difference over the inlet and outlet was increased, channels that terminating in the material appeared, and thus the solution became unphysical and the micro fluidic cooling systems would not work in practice, because water could not be pressed through these.
When the pressure difference for the optimized structures is varied and the corresponding temperatures are calculated, it is revealed that the systems are not optimal at the optimal pressures. This might be caused by the MMAsub routine. Therefore the constant c is changed, and the optimal value for the c is found to be 76, because at this value the limit for γ_0 is obeyed. However, the change of the constant c does not have any influence on the average temperature of the optimized system.
To obtain a higher pressure difference over the micro fluidic cooling system, a helical line is formed, while the width of the inlet and the outlet is increased to $w = 2\,\mathrm{mm}$. This optimized system were fabricated in practice, but it was not used, because the hydraulic resistance over it was found to be too low.
For the final design for which optimizations were performed, the width of the inlet was only $w = 0.5\ mm$, and channels for the inlet and the outlet were not included

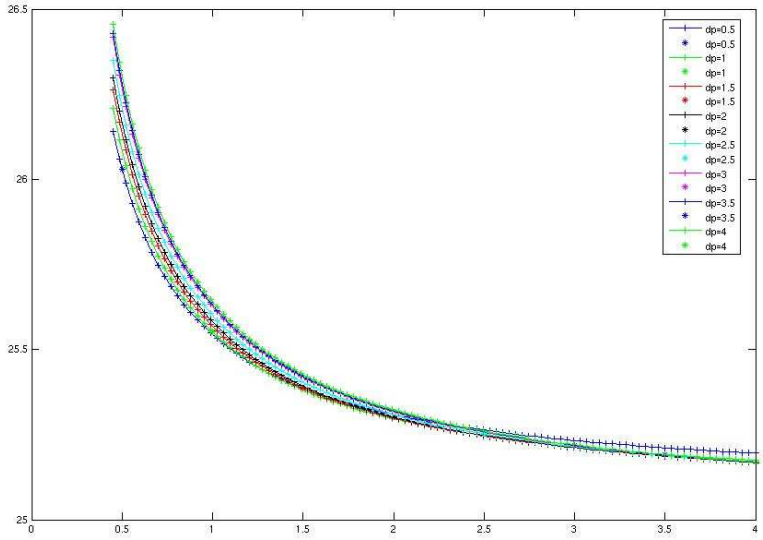

Figure 5.15: *The structure of the optimized micro fluidic cooling system, optimized at different pressures.*

in the simulations. The final structure was optimized for pressure differences up to $\Delta p = 2.5$ Pa, which was the highest pressure obtained for any of the optimized geometry's, before the channels started to terminate within the material. It would therefore be reasonable to assume that if the inlet and the outlet were made even thinner it would be possible to obtain geometries at higher pressure differences over the inlet and outlet, before channels begin to terminate within the material.
The two structures that was fabricated in practice, are chosen to be the systems optimized for $\Delta p = 0.5$ pa and $\Delta p = 2.5$ Pa, because the structures of these micro fluidic cooling systems did not have channels that terminated into the material.

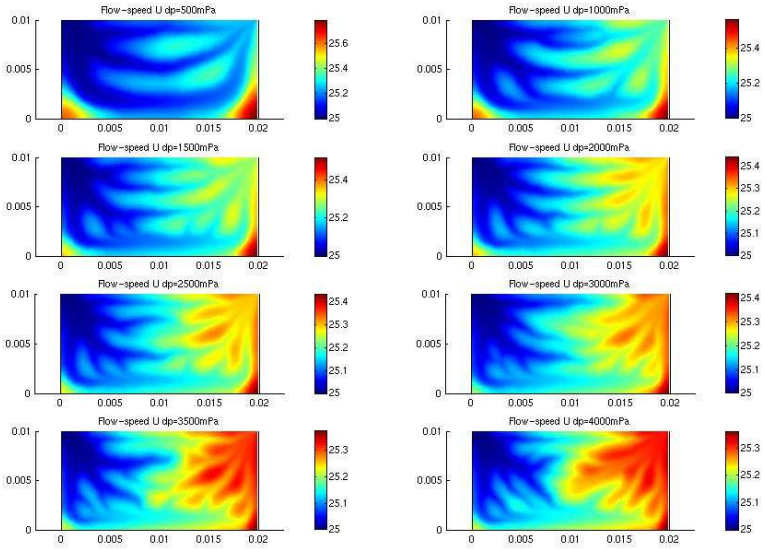

(a) *Temperature fields for the optimized micro fluidic cooling systems, optimized for different pressures.*

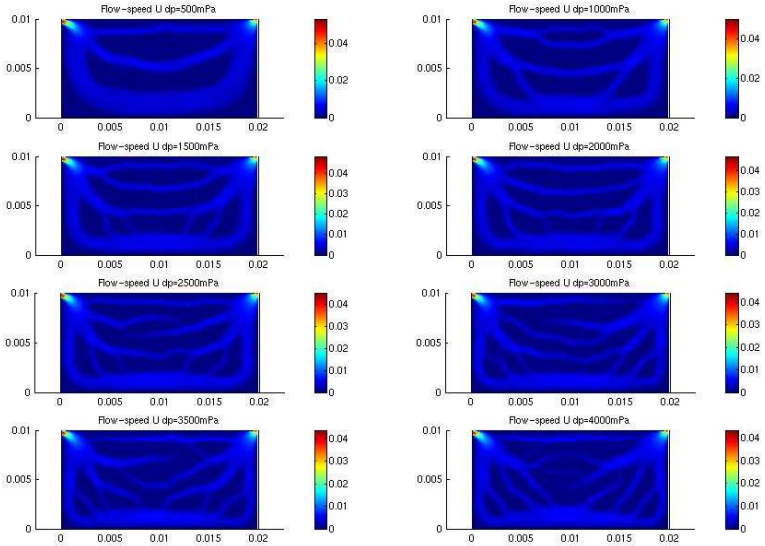

(b) *Velocity fields for the optimized micro fluidic structure, optimized for different pressures.*

Figure 5.16: *Velocity and temperature field for the final structure.*

Chapter 6

Fabrication of micro fluidic cooling systems

6.1 Fabrication of micro structures with a CO_2 laser

For fabrication and further experiments performed with the topology optimized cooling systems, the structure of these were fabricated in poly methylmethacrylate polymer (PMMA) using a CO_2 laser system. This fabrication method has many advantageous because it is very fast and simple and flexible for the purpose. The CO_2 laser set-up is shown in figure 6.1

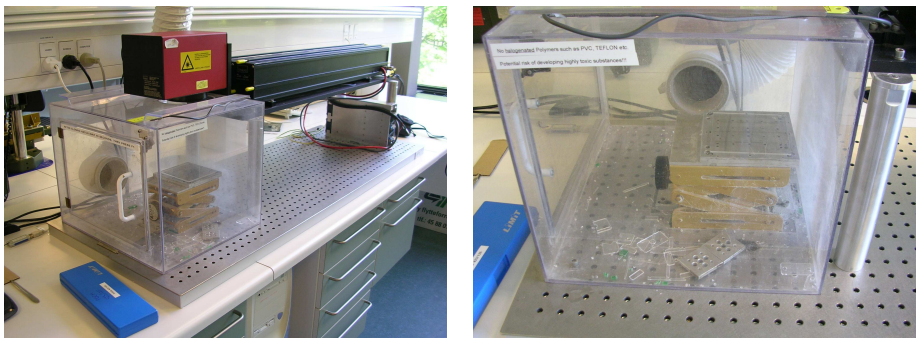

(a) *The CO_2 laser.*

(b) *A piece of PMMA placed under the laser head ready for fabrication of micro fluidic structures.*

Figure 6.1: *CO_2 laser set-up used for fabrication of the micro fluidic structures. The laser is connected to a computer.*

The CO_2 laser is an infrared laser representing a material removing fabrication method. It evaporates substrate material directly by applying heat with the laser beam. The infrared laser used is a carbon dioxide laser, which emits radiation at a wavelength of $\lambda = 10.6\ \mu$m.
The material used for the micro fluidic structures is PMMA polymer, which has a high absorbance of about 0.92 in the infrared region. PMMA also combines a low heat capacity with a low heat conductance. Therefore, any absorbed heat will result in a rapidly rising temperature being able to melt some of the polymer.
The laser system is controlled by a two dimensional computer CAD-program which controls a mirror-equipped head deflecting and focussing the laser beam. Using the computer it is among other factors possible to set the power of the laser beam, the velocity of it, the number of passes it makes over the same channel, the resolution

and the scan direction. The CAD-program can move the laser to any position within a square working field of 110 mm × 110 mm.
However, the width, depth and profile of the fabricated channels are not only depending on the properties mentioned until now, but also, among other things, on the optical properties of the laser system, the layout processing sequence, the nature of the laser ablation and thermodynamically properties of the polymer. The optical properties of the laser system determine the incident laser power, the spot size, the depth of the field and the divergence of the laser beam, while the thermodynamically properties of the polymer determine how it reacts to the beam.
The evaporation mechanism of the polymer and the absorbance of it are temperature dependent. The polymer is conducting heat away from the melting zone in an uneven manner, especially at the corners in the bottom of the channels; the conducting heat loss is always higher in these areas, which results in a decreased ablation here. Because of this the dimensions of the channels will change during the fabrication and therefore can become very difficult to measure. From observed channel profiles measures with an optical microscope they can be assumed to have a Gaussian profile
The conductive heat and capative heat loss terms causes a certain amount of heat that is not available to evaporate from the PMMA and therefore disperses into the adjacent material. The size of the affected area depends on the relative amount of the heat loss terms and the time available for dispersing heat into the surrounding material. It is observed that the channel width depends on the cutting sequence, and the channel depth depends on the length of the channel. Therefore, if a channel is cut with more than one pass, the cooling time between the passes becomes relevant. The available cooling time depends on the channel length, which means that shorter channels will be deeper at the same laser settings.
Deflecting of the laser beam on surface produces the channels, when it hits the surface under a changing angle while the beam moves. The consequence is that an absolutely symmetric channel profile only can be produced if it is centred in the middle of the channel direction below the head of the laser beam.
The higher the velocity of the laser beam, the higher the relative heat loss into the surroundings of the structures will become, meaning that fine precise structures have to be fabricated with lower velocities than straight channels. Observations have shown that the channel depth in linearly proportional to the number of passes at a fixed velocity. The channel size also depends on the spot size of the laser beam, which is time-dependent, since the resulting Gaussian profile does that a slow moving laser beam results in broader channels than a fast moving beam.
When PMMA is heated up, it remains in the solid glass state until it reaches glass temperature at about 115°C, while at higher temperatures it becomes easily rubbery and mouldable. If even more energy is added to the system, at temperatures between 350°C and 380°C, thermal decomposition of PMMA begins, which does that the polymer chains spontaneous break during a process called propagation, leading to development of monomers (MMA), which are volatile, but also carbon dioxide and other gasses evolve during the thermal decomposition of PMMA in the presence of air.
While cutting a channel the heat introduced into the polymer material also results in bulges or splashes running parallel to the channels because some of the polymer melts and is driven out of the channels. This may influence the quality of the bonding process, risking to clog the channels. Therefore, after fabricating of the micro fluidic structures, it can be necessary to polish the cut plane to avoid artefacts from the cutting process that can distort the channel profiles. [3]

6.2 Fabrication of devices

For fabrication of the devices, it is very important that the structures of the fabricated micro fluidic cooling systems are in agreement with the topology-optimized structures

calculated with FEMLab and MatLab to get accurate measurements. Anyway, it is never possible to avoid all sources of error, primary because of uncertainties when using the laser as described in section 6.1.
The structures of the micro fluidic cooling systems are defined by the γ-field saved as a FEMLab file when running the optimization program. This file contains both the structure of the inlet and outlet and the micro fluidic cooling system, because they were all included in the optimizations. The FEMLab-file describing the γ-field is converted into a Bitmap-file because the laser program, WinMark, can only read Bitmap-files.
Unfortunately, the resolution of the Bitmap-file is not good enough to prevent dented points at the edges of the channels. Therefore an exact copy of the inlet and outlet channels was drawn using the program CorelDRAW. Using the program Corel PhotoPaint, the black and white colours of the γ-field for the optimized micro fluidic cooling systems were inverted. All grey-scale colours were removed by setting the contract of brightness to 100%, thereby trying to prevent mistakes at the edges. At last the two drawings were put together and exported as a PNG-file with a resolution of 300 times 300 pixels, witch is the best advantage possible.
After some tests it was decided by use of an electronic Vernier calliper gauge that the channels has to be cut first horizontal and then vertical, so that the laser program had to run in two sections. The best parameters giving channels that are 1 mm deep for each of the two sections are,

	Micro fluidic cooling system, inlet and outlet
Mark passes	3
Velocity	800 mm/s
Power	20 %
Resolution	1000

The rest of the parameters are as the default settings given by the WinMark laser program.
To remove the device from the PMMA plate, after cutting the channels, a rectangle was drawn around it and the device was cut using the laser. The size of the rectangle is so that the inlet and outlet go beyond it to prevent edges caused by the laser. The channels have to be in the middle of the devices, between the top and the bottom of it. Therefore, because the channels are 1 mm deep, they were cut in a 2 mm thick PMMA plate, and for each device a lit was cut in a 1 mm thick PMMA plate, having the same size as the bottom with the channels cut.
Afterwards the devices were bounded by pressing the top and bottom together by used of a clamp. Two metal blocks ensured that the force was even distributed over the device, and the blocks were protected from the melting PMMA by use of a glass layer during the bonding process. The devices were inserted in an oven and heated up to 109°C for about 60 minutes. Devices in the oven during the bonding process are shown in figure 6.3. After the bonding process metal fittings were fastened at the inlet and outlet with epoxy glue and so the devices were ready for further experiments. One of the final devices is shown in figure 6.2.

Unfortunately, afterwards it was concluded that the inlet and outlet channel were too broad and even not long enough to give a well-defined pressure difference that could be measured with use of the pressure sensors, and so experiments were never performed on these cooling systems. Therefore new devices had to be fabricated.

6.2.1 Fabrication of new devices

The width of the inlet and outlet of the devices had to be smaller, and the size of it was established to be 0.5 mm. Thus new micro fluidic cooling system had to be optimized

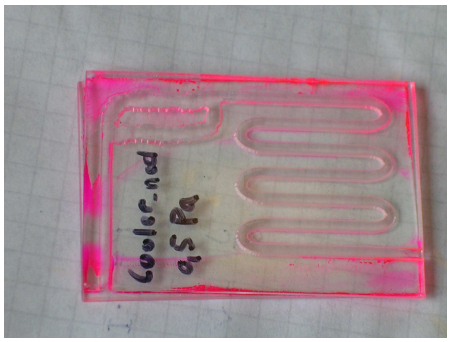

Figure 6.2: *One of the first fabricated devices.*

Figure 6.3: *Devices in the oven during the bonding process.*

before the fabrication could take place. The optimizations were only performed for the cooling system to prevent mistakes caused by the shape of the inlet and outlet during the experiments.
Because the width of inlet and outlet had to be only 0.5 mm and to prevent dents in corners of the structures, the inlet and the outlet were now defined in a new manner. They were drawn as vectors in the WinMark laser program, and a wobble thickness, defining the width of the channels, and a wobble step size, defining how smooth the channels had to be, were determined. Using the wobble function, the laser cutting of the channels was the performed so that the laser head moves back and forward when cutting the channels. The smaller step size, the more smooth channels, and thus the step-size had to be very small to make the channels as smooth as possible to give a uniform flow through them.
One consequence of the wobble function was that the shape of the channels for the inlet and outlet were cut in pieces, one by one. Therefore the order, in which these pieces were cut, was very important to prevent splashes where the laser begins cutting a channel or other relating effects. Furthermore, the shape of the channels was not well defined anymore. But as long as the channels were fabricated in the same way and with the same parameters for all devices, it did not matter, because only the

resistance over the inlet and outlet was important, the reason being that these were not included in the FEMLab optimizations. For determination of the resistance of the inlet and outlet channel, a device was fabricate without any micro fluidic cooling system, but with the same length of the channels as for the devices containing the micro fluidic cooling systems. This device and the one of the devices including a micro fluidic cooling system are shown in figure 6.4. The parameters used when cutting the

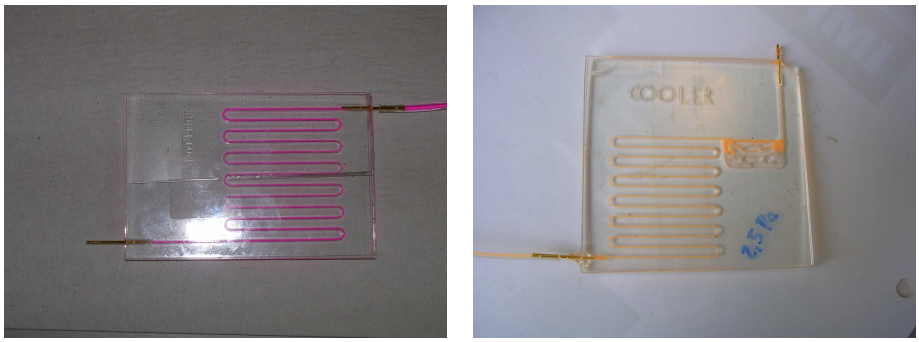

(a) *Device fabricated for measurement of the resistance of the inlet and outlet.*

(b) *Device with a micro fluidic cooling system including inlet and outlet. The pressure difference over the micro fluidic cooling system has to be 2.5 Pa. .*

Figure 6.4: *The inlet and outlet for the micro fluidic cooling systems. These devices were unfortunately too big to be bounded well enough.*

micro fluidic cooling system with the laser were the same as for the first fabricated systems. At the inlet and outlet at the boundaries of the devices the channels were made a little broader and deeper making it possible to glue a metal inlet and outlet to the devices. The parameters used when cutting the inlet and outlet are shown in the table below. The cooling systems were still cut in a 2 mm PMMA plate and the lids were still cut in a 1 mm PMMA plate.

	Inlet and outlet	Inlet and outlet at boundaries
Mark passes	2	2
Velocity	800 mm/s	800 mm/s
Power	30 %	45 %
Resolution	300	300
Wobble	On	On
Wobble thickness	0.50 mm	1.30 mm
Wobble step size	0.05 mm	0.05 mm

The size of the new devices was about 6 cm × 6 cm and so new metal blocks were fabricated for the bonding process to distribute the force equally over the devices. Unfortunately it did not succeed to make more than a few good devices because almost all of them were not bonded well enough, and thus they were leaking water.

6.2.2 Fabrication of the final devices

A solution to the bonding problem might be to make the devices smaller for a better distribution of the power during the bonding process. Therefore a new inlet and outlet were defined in the WinMark laser program in the same manner as for the previous devices, but with less distance between the inlet and outlet channels. The new devices were cut using the same laser parameters as previous, and both devices with and without micro fluidic cooling systems were fabricated. Furthermore a device containing a simple test structure, a one 1 mm deep, broad, twisted channel, instead of a cooling system was defined as a vector in WinMark an fabricated for examination

of the temperature dependence of the pressure. The parameters for this channel are shown in the table below. Devices containing the new inlet and outlet and the test structure is shown in figure 6.5, and a screen shot from WinMark determining a device with one of the final topology optimized cooling structures is shown i figure 6.6.

	Test structure
Mark passes	2
Velocity	500 mm/s
Power	40 %
Resolution	300
Wobble	On
Wobble thickness	2.00 mm
Wobble step size	0.05 mm

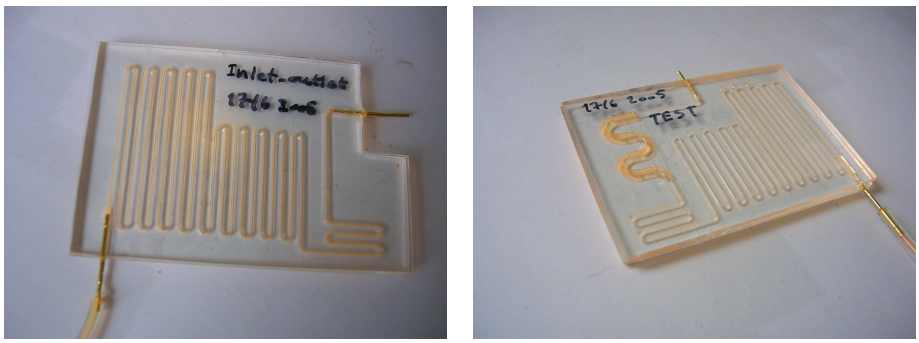

(a) *Device fabricated for measurement of the resistance over the inlet and outlet.*

(b) *Device with a simple test structure made for examination of the temperature dependence of the pressure difference.*

Figure 6.5: *Devicess for test of respectively the resistance of the inlet and outlet and the temperature dependence of the pressure difference over the inlet and outlet.*

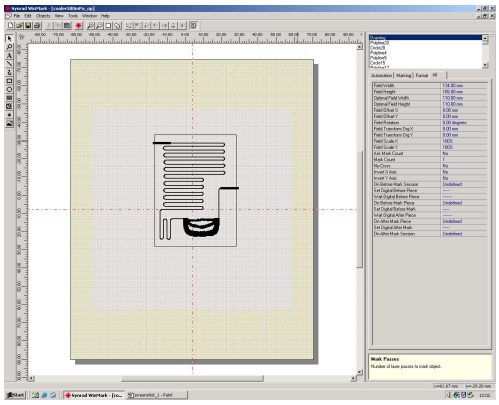

Figure 6.6: *Screen shot from WinMark determining a device with one of the final topology optimized cooling systems.*

After fabrication and bonding of the new devices, unfortunately, the bonding problems did continue. Several solutions were tried to prevent this problem. For instance, the force of the clamp, the time and the temperature during the bonding process were raised, but the result was that the channels melted together, so water couldnot come through them - or they were still leaking water.
The most probable reason for the bondings problems was that it was caused by the

PMMA, because the two PMMA plates at respectively the top and bottom of the devices were made of two different kinds of PMMA, or the surface of top plate was coated with something that did not bind very well to the bottom plate while these were bonded together.
It was tried to remove the possible surface coating with ethanol, but this was not a god idea, because it resulted in cracks within the PMMA caused by stress within it. Thus the solution to this problem was to use the same kind of PMMA for the top and the bottom, even though it had the consequence that the micro fluidic structure would not be in the middle of the devices. Therefore, now 1.5 mm thick PMMA plates were used for the top, and the micro fluidic cooling systems, inlet and outlet were cut in 2 mm thick PMMA plates for the bottom. Then it was succeeded to fabricate some devices that could be used for experiments.

6.2.3 Conclusion

Fabrication of devices with micro fluidic cooling systems is not always an easy process because a lot of factors enters in the fabrication process.
It is not easy to find the most optimale bonding force, time and temperature, where bonding always will succeed - if there are any. And uncertainties during the laser cutting will always cause some uncertainties that cannot be prevented. Therefore it might be difficult to reproduce devices, but it was tried as good as possible.
It is not optimal that the cooling systems fabricated at last were not in the middle of the devices because of the thickness of the PMMA plates, which was 1.5 mm and 2 mm, because it by no means was possible to used the 1 mm PMMA plates because it would not bound to the other PMMA plates. A solution to this problem might be to remove 1 mm of the 2 mm PMMA plates and then use it. But this was not found to be necessary because the uncertainties for further measurements of the temperature would not have been prevented anyway.
When bonding is performed on PMMA plates in the clean room at DANCHIP, DTU, the plates are first heated up to 80°C for some amount of time. During his process all stress will disappear from the PMMA, and it ten becomes possible to clean the PMMA plates and thereby remove all dirt from the surfaces using ethanol instead of water. Furthermore the plates would have become totally flat, preventing it from bending because of the heat arising during the cutting of channels with the laser. Thus if this process were performed to the devices in this project, the bonding process might have been easier.
Another idea might have been to try to make the size of the devices even smaller, thereby a more equal distribution of the force during the bonding process would have been possible. The size of the devices was minimized when fabricating the last devices, but because, at last, some of these were successfully bonded, it was not found necessary to make the devices even smaller.

Chapter 7

Experimental set-up

To heat up the micro fluidic cooling systems while running the experiments, a heating element is placed under the structure of it. Cobber plates on the top of cooling systems and below it, between the heating element and the cooling system, are placed for a uniform distribution of the heat. The size of the micro fluidic cooling systems is 1 cm $\times$ 2 cm, and so the size of the heating element and the cobber sheets are the same. The size of the whole device is, of cause, bigger than the micro fluidic cooling system itself, but heat only have to be applied to the cooling system, not on the inlet and outlet channels.
The "sandwich" consisting of the micro fluidic cooling system, the heating element and the cobber plates is placed on a holder and fixed by use of a clips. Between the layers "cooling" plasma is applied to glue the parts together and to give a better distribution of the heat through these. The "sandwich" is shown in figure 7.1.

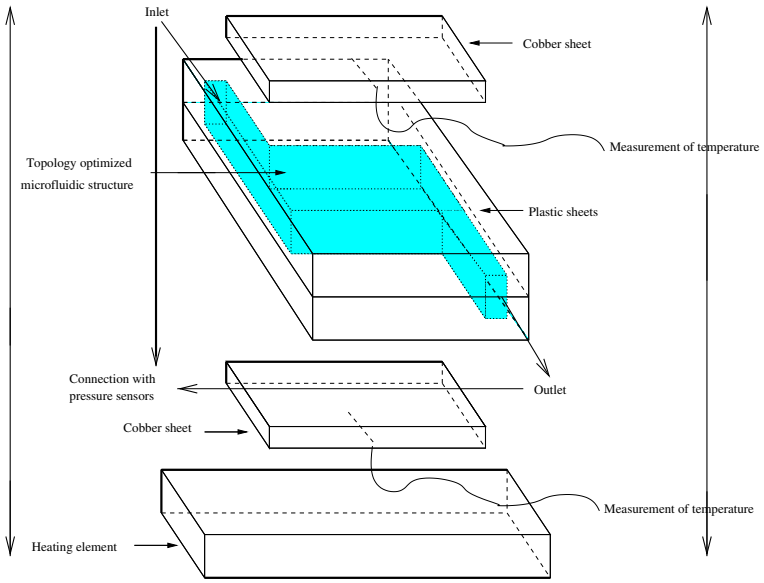

Figure 7.1: *"Sandwich" consisting of a micro fluidic cooling systems, a heating element and cobber sheets.*

To measure the temperature of the cobber sheets, small holes are drilled in which temperature sensors or so-called thermistors are mounted.
A plastic bag containing small, isolating styrene balls covers the "sandwich" to prevent heat flow from it. Thereby the heat of the cobber plate on the top of the cooling system will heat up faster and so the temperature of it will become higher than with-

out the isolating.
Water is sent through a tube connection to the system with a constant velocity or flow rate by use of a glass squirt mounted on a squirt pump. When starting performing experiments a plastic squirt was used, but it was determined that it was not well suited for the purpose, because plastic is very soft compared to glass, resulting in comparatively long relaxation times for the pressure over the system. The tube, the water is send through, is made of Teflon, that is a relatively hard material, to prevent extensions of it during the experiments. However, connections between for instance the tube and the device are made of small pieces of silicone tube. When the water has been send all the way through the system it drips out into a bowl placed at the end of the tube.
Just before and after the device the tubes are connected to pressure sensors for measurement of the pressure difference over the device. When measuring the pressure it is very important that the height of pressure sensor is the same. Therefore the connections to the sensors are taped to the same metal box.
The pressure tensor connected to the system at the outlet of the devices will measure the atmospheric pressure, or almost atmospheric pressure, because no system after the outlet can cause a change in the pressure. Anyway, it is necessary yo have a pressure sensor at the outlet, because there will be small variation in the pressure, and these have an important influence on the experiments, because small pressuredifferences have to be measured.
The pressure sensors and the temperature sensors are connected to an electronic board, which gets a constant power from a power supply. The heating element is connected to another power supply. Furthermore the electronic board is connected to a computer with LabView installed. The LabView program measures the voltage output of the pressure sensors and the temperature sensor, which afterward have to be translated into respectively pressure and temperature by use of data sheets for the components.
A schematic drawing of the set-up is shown in figure 7.2, and a picture of it is shown in figure 7.3.

7.1 Measurements of pressure and temperature

7.1.1 The pressure sensors

Two electrical pressure sensors are used to measure the pressure over the micro fluidic cooling systems, at respectively the inlet and the outlet of the system.
A pressure sensor is a little electronic device that is split up into two parts separated by a thin electrical conducting membrane. The pressure sensors are connected to the cooling system with a T-fitting and a tube just before the inlet and just after the outlet.
The tube has to be completely filled with water, because otherwise the measurement of the pressure will not be exact, because air in the tube will be compressed when influenced by a pressure.
When water is sent through the cooling system, the membrane is influenced and so the electrical resistance of the pressure tensor is changed. Each pressure sensor will then give an output voltage, which can be converted into a pressure. [7]

7.1.2 Measurement of pressure

The output of the pressure sensors measured with the LabView program is a voltage and not directly a pressure. Therefore, to determine the pressure, it is necessary to

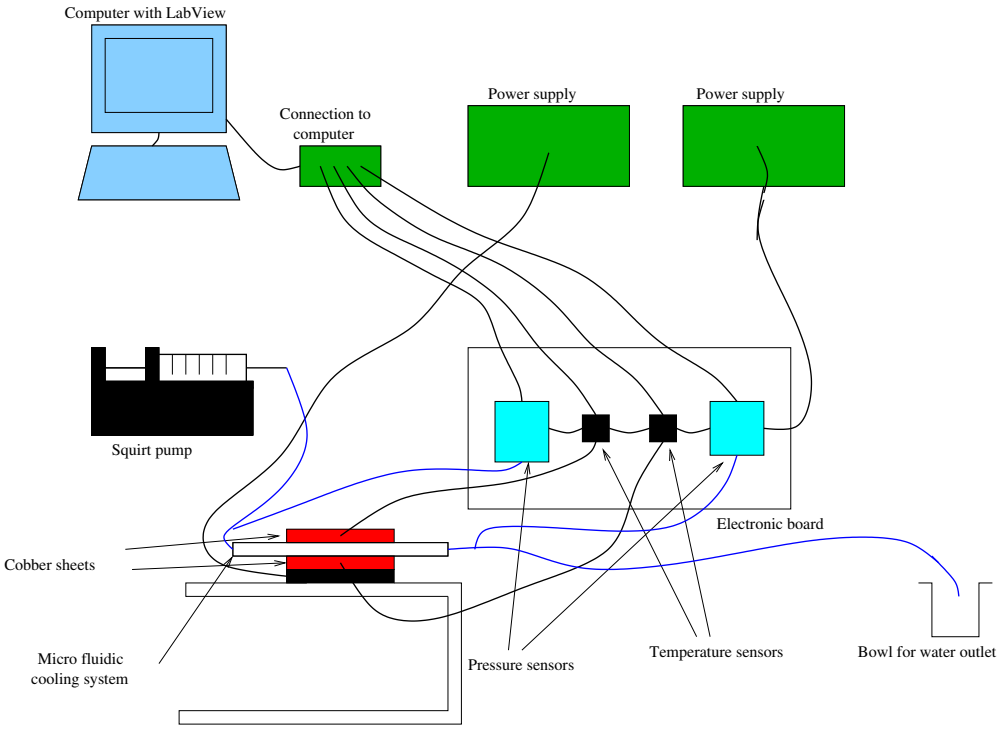

Figure 7.2: *Schematic drawing of the experimental set-up. A plastics bag containing small, isolating styrene balls covers the "sandwich", but this it not shown on the drawing.*

Figure 7.3: *Set-up for the experiments. The plastics bag containing small, isolating styrene balls covering the "sandwich" is not shown on the picture.*

find a connection between pressure, p, and voltage, V.
From the data sheets, see appendix 14, for the pressure sensors, see appendiks, two data points are given for the full measurement range,

Pressure	Voltage
-50 mm Hg = -6666.1 Pa	0.5 V
50 mm Hg = 6666.1 Pa	4.5 V

From these data points an expression for the general connection between the voltage measured by use of LabView and the pressure is found by calculating the slope, a, of a line through the points. Thus

$$\Delta p = \frac{6666.1 - (-6666.1)}{4.5 - 0.5}\Delta V = 3333.1\Delta V \tag{7.1}$$

The pressure sensors used in this project are very sensitive. They are not able to measure a higher output voltage than 4.5 V. Therefore the flow rate, Q, determining the velocity of the water flowing through the system may not be greater than this condition is always satisfied or else the pressure sensors will be overloaded and the measurements useless.

7.1.3 The temperature sensors

The temperature of the copper plates on the top and the bottom of the micro fluidic cooling systems are measured by use of two temperature sensors. These are temperature-sensitive electronic components called thermistor or negative temperature coefficient, NTC. For NTC thermistors the resistance decreases as the temperature rises. Thermistors are very useful for temperature measurements because they have a very small size. They are very sensitive and response very fast to changes in resistance. A standard tolerance of the resistance is available for a thermistor to define the precision of the termistor at some reference point. The thermistor used in this project has a very little tolerance of +/- 0.2°C at 25°C according to their data sheets.
The thermal and electrical properties of a thermistor are a function of the geometry of it, of what kind of oxides it is made of and what kind material responsible for the connection to the rest of the experimental set-up. The thermistors used in this project are so-called bead type thermistors because of the round shape of their bodies. They are very small, so that they can inserted into a small hole drilled in each of the copper plates. They have platinum alloy leadwires which are directly sintered in their bodies made of metal oxides mixed with a suitable binder to control the spacing between the wires and glued into a polyimide tube with epoxy. [13] [14]

7.1.4 Measurement of temperature

The output of the temperature sensors or thermistors measured with LabView is a voltage and not directly a temperature. Therefore, to determine the temperature it is necessary to find a connection between temperature and voltage.
Each thermistor is connected to the rest of the experimental set-up in an electrical circuit as shown in figure 7.4.
For the electrical circuit the connection between the resistance and the voltage is

$$V_{\text{out}} = \frac{R_{\text{bottom}}}{R_{\text{bottom}} + R_{\text{thermistor}}} \cdot V_{\text{in}}. \tag{7.2}$$

$V_{\text{in}} = 5$ V is determined on the power supply and it is kept constant during the experiments. R_{bottom} is the resistance of a resistor in series connection with the thermistor.

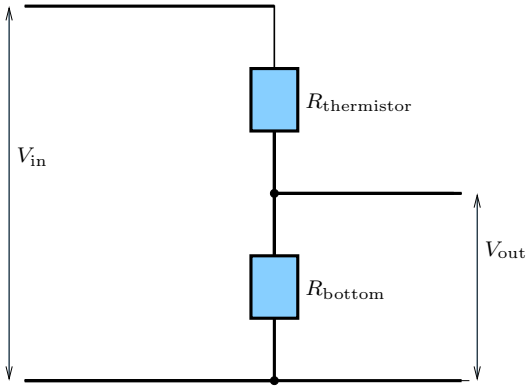

Figure 7.4: *Schematic drawing of the set-up with each of the thermistors.*

The resistance of this is measured by use of an ohmmeter to be $R_{\text{bottom}} = 2491\Omega$. From the data sheets, see appendix 14, for the thermistors, see appendiks, the connection between temperature T, and measured resistance, $R_{\text{thermistor}}$, is given for some particular values of the resistance. By inserting this data points in the expression 7.2, it is possible to determine a connection between the output voltage, V_{out}, and the temperature, T, for each value of $R_{\text{thermistor}}$.
Plotting and curve through the determined points and calculating a function for the best line through them gives an expression for he general connection between the output voltage measured with LabView and the temperature,

$$T = 23.234V_{\text{out}} + 2.6075 \tag{7.3}$$

The expression for connection between output voltage and temperature is shown in figure 7.5.

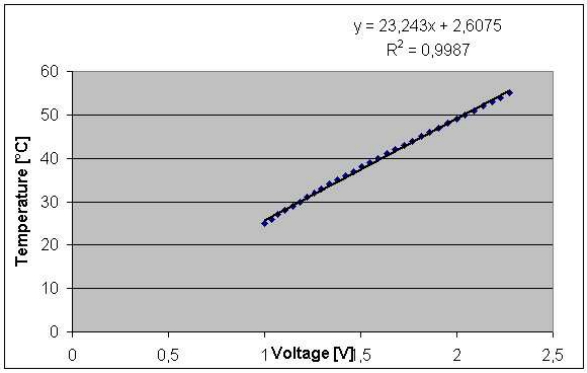

Figure 7.5: *Connection between output voltage and temperature.*

Chapter 8

Experiments

8.1 Relaxation time of the system

8.1.1 Purpose

When performing the first experiments in this project, water was sent through the system by use of the syringe pump with a plastic syringe mounted. Unfortunately it was observed, that it took a disproportionate amount of time for the system to relax and the pressure to become the same for the two pressure sensors after the pump was stopped.
The reason for this phenomenon is that plastic is a relatively soft material The resistance of it is very high, and it will be pressed together and react as a spring when exposed to a force of for instance the syringe pump.
If the relaxation time for the system is very long, it will be difficult to perform experiments, and it will be necessary to wait a relatively long time between measurements. Furthermore, a long relaxation time will result in unwanted uncertainties.
Therefore the plastic syringe was replaced with a glass syringe. Glass is a relatively hard material, but it will still take a while for the system to relax. Therefore, to obtain welther the relaxation time has a major influence on the experiments or not, this has to be examined.

8.1.2 Method of approach

Instead of a device containing a micro fluidic cooling system, a Teflon tube is mounted on the system between the two pressure sensors measuring the pressure over the inlet and the outlet, respectively. The length of the tube is $L = 24.2$ cm, and the radius of it is $a = 0.4$ mm.
A glass syringe is filled with water and mounted on the syringe pump, and the pump is started with a flow rate being $Q = 3$ ml/min $= 5.01 \cdot 10^{-8}$ m^3/s. When the pressure at the inlet seems to be constant, the pump is stopped, and thus the system will relax. The pressure measure at the inlet and the outlet is continuous written to a file and saed by used of LabView.

8.1.3 Data processing

The measurement points gives a voltage which has to be converted into a pressure. This is done as explained in section 7.1.2. 50 measurement points are obtained each second. Therefore it takes 1/50 second between two measurement points and thus a time scale is defined.
Now, the pressure measured at respectively the inlet and the outlet of the is plotted as a function of the time as shown in figure 8.1.

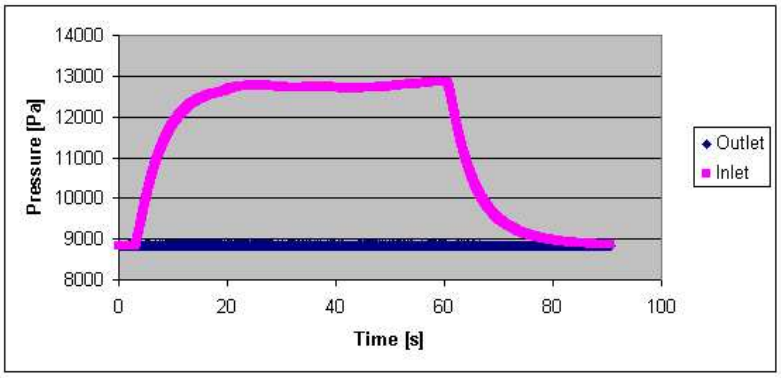

Figure 8.1: *Measurement of relaxation time for a system with a tube inserted between the two pressure sensors. A glass syringe is mounted on the syringe pump sending water through the system.*

The graph shows that when water is send through the system, the pressure over inlet of the tube rises very fast until a constant value is reached after about 20 seconds. It is seen that the syringe pump is stopped after about 60 seconds, because the pressure then falls rapidly. Then, finally, it is seen that the relaxation time of the system is about 30 second, because after this amount of time, the pressure sensor will measure atmospheric pressure again.
The pressure over the outlet is almost the same during the experiment as it has to be because it is the atmospheric pressure that is measured.
The obtained data for the experiment can be found on the CD-ROM in the folder "Relaxation time".

8.1.4 Conclusion

Repeating experiments performed with the same tube, and later experiments performed with a device containing a test system, inlet and outlet, see section 8.5, all showed the same tendency. In each case the relaxation time for the system was almost the same.
The conclusion for this experiment might then be, that if a glass syringe is mounted on the syringe pump instead of a plastic syringe, the relaxation time for the system is so low, that it does not have any influence on the measurement of the pressure, if only measurements are performed so that the system will relax for a short while, before the next measurement is performed.

8.2 Heat conduction through a PMMA plate

8.2.1 Purpose

At one stage it was tried to heat up a device containing a micro fluidic cooling system with stationary water to obtain whether the two copper plates in a "sandwich" containing the micro fluidic cooling system, the heating element and the copper plates would obtain the same temperature or not.
The power of the heating element were turned on, so that the temperature of the bottom copper plate was about 50 °C, and the measurements were started. Unfortunately, after the system had been left to it own for almost a day, the temperature of the upper copper plate was only raised about $5^{\circ C}$ compared to room temperature, which was the consequence of, that the heat would be conducted away from the system to the surrounding air, although air actually is a relatively good isolator because the thermal conductivity of it is very low.
Therefore it was concluded that it was necessary to have some kind of isolating to cover the system. Thus a plastic bag were filled with small styrene balls and placed on the system so that the isolating layer were about 10 cm.
To estimate the effect of the isolating layer in a more experimental way than previous, measurements were now performed with a piece of PMMA between the two copper plates, both for an isolated and for an unisolated system. Furthermore, the results of the experiments were compared to a FEMLab simulation of the heat flow through a "sandwich" structure containing a PMMA plate between two copper plates.

8.2.2 Method of approach

A piece of a PMMA plate was placed between the two copper plates, above the heating elements. The size of the PMMA plate was 4 cm × 4 cm, and the thickness of it was 2 mm. For the first measurement, the system was not isolated, while for the second measurement a plastic bag containing small styrene balls was used to isolate the system from the surroundings, so that the thickness of the isolating layer was about 10 cm.
The power was turned on the heating element, and it it was heated up. The temperature of the two copper plates was measured for about an hour. One measurement point was obtained each second. The power to the heating element was the same for both experiments.
The obtained data for the experiments can be found on the CD-ROM in the folder "PMMA".

8.2.2.1 FEMLab simulations

Afterwards, simulations of the heat conduction was performed by use of FEMLab using a Transient Analyze under the "Heat Transfer by Conduction" application mode. The simulations were performed for a system containing a PMMA plate placed between two copper plates, having the same dimensions as in the experiment, fir wich the surface of the bottom plate was heated up. The simulations were performed for both an isolated system and for an unisolated system surrounded by 10 cm air. In both cases the heat conduction was obtained at different times to obtain how the temperature through system would behave as function of time and thickness of the "sandwich". The simulation time was stated to be an hour.
The physical constants for PMMA, copper and air used in the simulation are,

	PMMA	Copper	Air
Thermal conductivity, k	0.21 W/(m·K)	400 W/(m·K)	0.0271 W/(m·K)
Heat capacity, c	1190 J/(kg·K)	8700 J/(kg·K)	1005 J/(kg·K)
Density, ρ	1470 kg/m^3	385 kg/m^3	1.127 kg/m^3

The surface temperature of the bottom copper plate was defined to be 35°C, because FEMLab defines the zero-point reference temperature to be 0°C. Thus if the the room temperature is assumed to be 25°C, the temperature of the copper plate becomes 60°C − 25°C = 35°C, which is assumed to be a reasonable value compared to the temperature, that will be measured for an sisolated system below.

8.2.3 Data processing

The output voltage from the temperature sensor are converted into a temparature as explaned in section 7.1.4. The temperature sensors connected to the two copper plates measure a voltage and not directly a temperature. Therefore the measured voltage are converted into a temperaturse as described in section 7.1.4.
For both the isolated and the unisolated system, the temperature of the upper and the bottom copper plate is plotted as function of the time, at which the system is heated up, see figure 8.2(a) and figure 8.3(a), respectively. Furthermore, the temperature difference between the two copper plates, $T_{\text{top}} - T_{\text{bottom}}$, was determined and plotted as function of the time, see figure 8.2(b) and figure 8.3(b), respectively
From figure 8.2(a) it is noted, that for the unisolated system the temperature of the

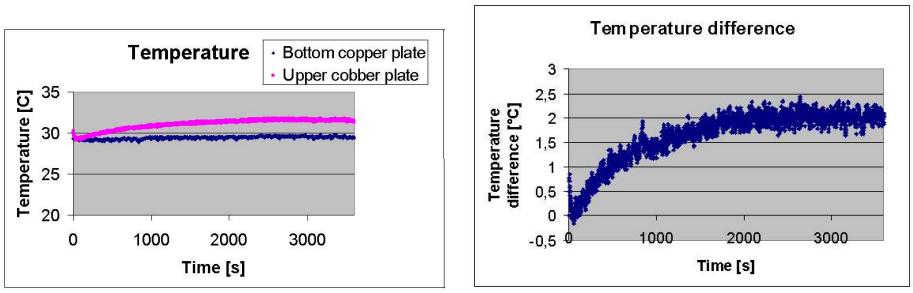

(a) *Temperature of respectively the top and the bottom copper plate as function of time.*

(b) *Temperature difference as function of time.*

Figure 8.2: *Temperature as function of time for the uinsolated system.*

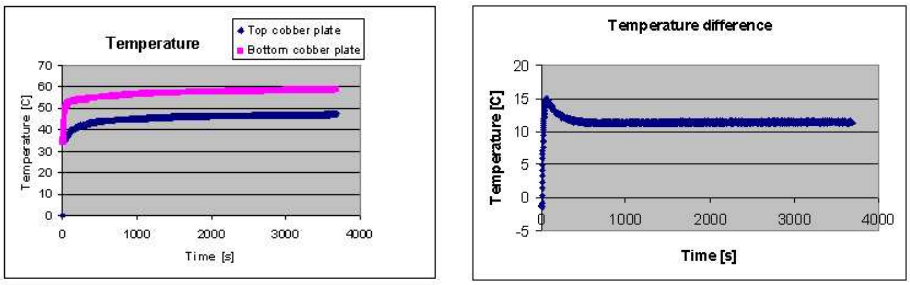

(a) *Temperature of respectively the top and the bottom copper plate as function of time.*

(b) *Temperature difference as function of time.*

Figure 8.3: *Temperature as function of time for the system isolated by a layer of styrene balls inside a plastic bag.*

upper copper plate was almost constant during the experiment. The temperature of the bottom copper plate rises very slowly and it will take a long time before the temperature of it reachess a constant value. After performing the experiment for more

than an hour, the temperature of the bottom copper plate was only about 32°C which is only about 2°C more than the temperature of the bottom copper plate.
From figure 8.3(a) it is noted, that the temperature of both the bottom and the upper copper plate rises exponential during the whole experiment. After performing the measurements for an hour, the temperature of the bottom copper plate was about 48°C, while the temperature of the upper copper plate was about 60°C. The measured temperatures of the two copper plates therefore were much higher compared to the uisolated system.
The plot of the temperature difference for the top and the bottom copper plate for the unisolated system, see figure 8.2(b), shows that the temperature difference increases and becomes constants, as the system is heated up. However, after a while it reached a constant, but very low value being about 2°C. The plot of the temperature difference for the isolated system, on the other hand, see figure 8.3(b), shows that the temperature difference indicate a tendency of being an exponential decreasing curve, because the temperature of both the top and the bottom copper plate increase exponentially.

8.2.3.1 Data processing of FEMLab simulations

For the FEMLab simulations, the profile of the heat flow through the "sandwich" structure for the isolated system is shown in figure 8.4. From the figure it is noted that the temperature of the two copper plates is almost the same after a hour. This is not in accordance withs the results obtained for the experimal set-up, where the temperature difference between the two cobber plates is significant and constant after a while. Futhermore it is noted that the temperature is lowest at the edges of the PMMA plate, because it takes a while before the heat is conducted into these areas, while these are not directly heated.

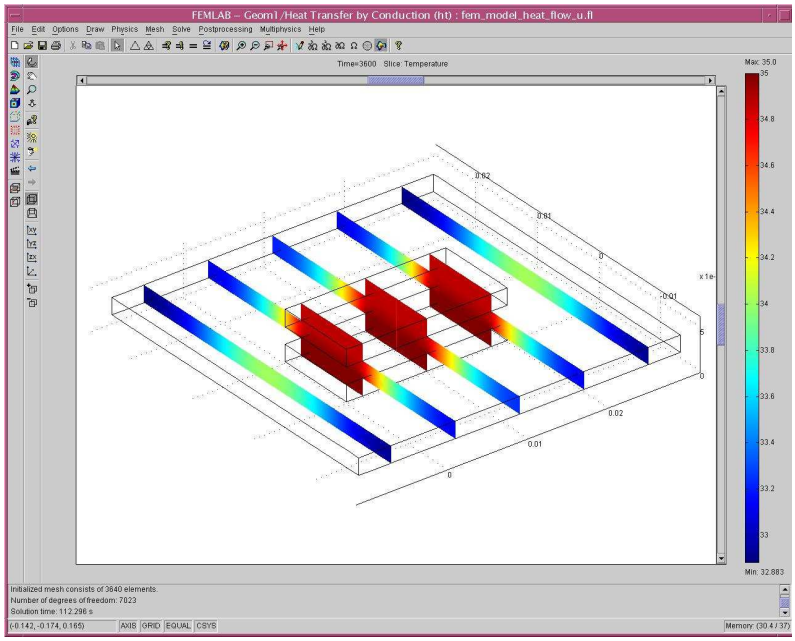

Figure 8.4: *Profile of the heat flow through the "sandwich" structure at different times simulated by use of FEMLab.*

Profiles of the heat flow through the middle of the "sandwich" structures, shown by the red line in figure 8.4, plotted as function of the thickness for the unisolated

system and for the isolated system, see figure 8.5(a) and figure 8.5(b), respectivily. The heat profiles are shown for times between 100 s and 3600 s, with 100 s between each calculated profile.

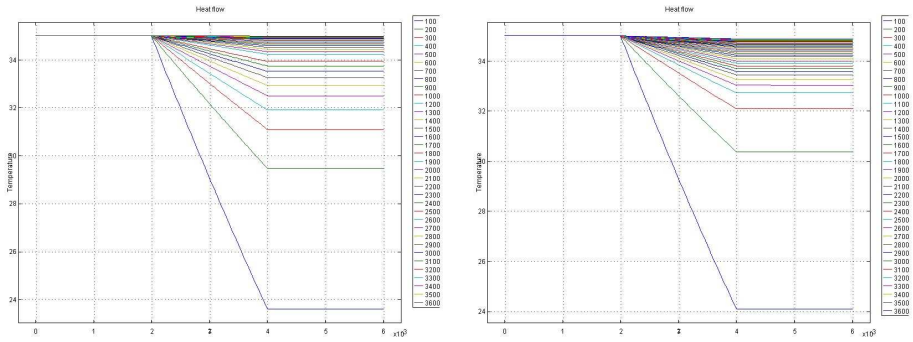

(a) *Temperature as function of thickness for an unisolated system.*

(b) *Temperature as function of time for an isolated system.*

Figure 8.5: *Temperature as function of thickness for a "sandwich" structure containing a PMMA plate between two copper plates, where the bottom plate is heated up. The heat conduction is shown at various times.*

From the figures it is notes that there is a difference in the conduction for the isolated and the unisolated system. At short times, it has an effect that the system is isolated, but as the time tends to an hour or more, the heat conduction through the isolated and unisolated system is almost the same. The heat conduction through the copper plates as function of the time is noted to be an almost straight line, because the thermal conductivity of copper is very high compared to the thermal conductivity of PMMA, and thus the line showing the heat conductance as function of time for PMMA is a decreasing line.

8.2.4 Conclusion

The results of the experiments obtained for an unisolated system and for a isolated system is very different. For the unisolated system almost all heat is conducted into the sorroundings, resulting in a very small temperature difference between the two copper plates after an hour. When the system is not isolated, the heating element will in principle have to heat up the whole room, until the temperature everywhere is the same.
For the isolated system, on the ohter hand, the temperature difference shows a tendence of forming an exponential decreasing curve, tending to a constant value after a short while. The isolating styrene balls therefore has a major effect on the amount of heat conducted away from the two cobber plates, and the temperature of the whole system raises more rapidly when it is isolated.
The temperature difference is obtained because it is not possible to prevent loss of energy into the sorrundings. However, for the micro fluidic cooling systems it is not the absolute temperature that is interesting, but the temperature difference of the two cobber plates. Thus, it is the temperature difference obtained for different cooling systems, that has to be obtanied, when experiments are performed with water flowing through these with a well-defined pressure over the inlet and outlet.
Finally, the conclusion of the experiments is, that when performing experiments on the micro fluidic cooling system, these have to be isolated.
The two FEMLab simluations yield almost the same result for the isolated and for the unisolated system, and they are very different from the obtained experimental results. The reason for this might be that the unisolated system simulated by FEMLab is only sorrounded by 10 cm air, and air is a comparatively good isolator. The

isolated system simulated with FEMLab is totally isolated, while this is not the case for the system in the experimental set-up. Thus a better maching of the simulations and the experiments might be obtained, if the system in the experimental set-up was better isolated. However, it is not possible to avoid thermal heat conduction into the sorrounding totally.
An other reason why the results obtained results for the simulations and the experiment differ, is that only conduction is included within the FEMLab simulations, even thougt convection might also be represented, but the influence on the results caused by convection is very difficult to predict, because it is caused by movements within the system. Thus, convection is not included in the FEMLab simulations.

8.3 Resistance of a tube

8.3.1 Purpose

Before experiments are performed with devices containing the micro fluidic cooling systems, the hydraulic resistance has to be obtained for the inlet and outlet of the devices. The measurement of this hydraulic resistance has to be very accurate, because the pressure difference over the micro fluidic cooling system is very small. Therefore the uncertainty for the measurements involving pressure has to be determined.
To prove the accuracy of the experimental results in this project and to obtain whelther it is possible to repeat experiments, it is tried to determine the hydraulic resistance for a piece of tube.
For a tube the calculated hydraulic resistance is easy to calculate theoretically. The hydraulic resistance of a tube having a circular cross-section is given by equation 2.40 in section 2.6.1.1,

$$R_{\text{hyd}} = \frac{8}{\pi}\eta L\frac{1}{a^4}, \tag{8.1}$$

where η is the density of the water flowing in the tube, L is the length of it and a is the radius of it. [1]

8.3.2 Method of approach

A piece of a Teflon tube was mounted between the two pressure sensors in the experimental set-ups.
A glass syringe was filled with water and mounted on the syringe pump, which was started with a flow rate being Q=1 ml/min = $1.67{\cdot}10^{-8}$ m^3/s. 10 measurement points were obtained each second, and measurements were obtained for about a minute, until the pressure had reached an almost constant value. Then the syringe pump was stopped. Afterwards the flow rate, Q, was raised with 1 ml/min = $1.67 \cdot 10^{-8}$ m^3/s, and measurements were obtained in the same way as before. Several series of measurements were obtained in the same way until the flow rate was Q=6 ml/min = $1.0{\cdot}10^{-7}$ m^3/s, where the limit for the voltage measured with the pressure sensor, 4.5 V, was reached.
To obtain whelther it is possible to reproduce the experiment and obtain the same pressure difference again, it was repeated once in the same way as described above.
The obtained data for the experiments can be found on the CD-ROM in the folder "Tube".

8.3.3 Data processing

The Teflon tube used for this experiment is the same as the tube used in the experiment described in section 8.1. The length of the tube is $l = 24.2$ cm, and the radius of it is $a = 0.4$ mm. The viscosity of water is $\eta = 0.001$ Pa·m/s. Inserting these values in the expression for the hydraulic resistance, equation 8.1, the theoretical calculated value of it becomes

$$R_{\text{hyd}} = \frac{8}{\pi} \cdot 0.001\text{Pa} \cdot \text{m/s} \cdot 24.2 \cdot 10^{-2}\text{m} \cdot \frac{1}{(0.4 \cdot 10^{-3}\text{m})^4} \tag{8.2}$$

$$R_{\text{hyd}} = 2.4 \cdot 10^{10}\text{Pa} \cdot \text{s/m}^3. \tag{8.3}$$

For each of the two experiments it took a while, before the voltage measured with LabView and thereby the pressure over respectively the inlet and the outlet of the tube had reached a constant value. 10 measurement points were obtained each second for about one minute, so about 600 points were measured in total. As mentioned eatlier, it took a while before the pressure had reach an constant. Thus the first 300

measurement points for each series of measurement were disregarded. For the rest of the measurement points the average of the voltage measured for respectively the inlet and the outlet of the tube was calculated, and the resulting voltage was converted into a pressure as described in section 7.1.2.
The flow rate, Q, is plotted as function of the pressure difference, Δp, over the inlet and the outlet for each series of measurements as shown in figure 8.6.

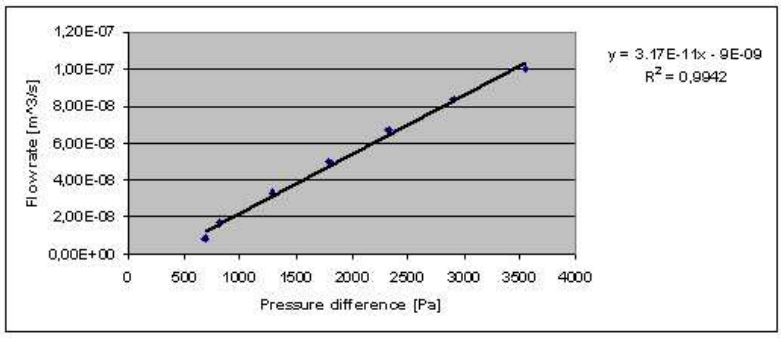

Figure 8.6: *Flow rate as function of the pressure difference over the inlet and the outlet of a Teflon tube for the first measurements with the tube. The resistance of the tube is given as the inverse slope of the best line through the measurement points.*

The hydraulic resistance of the tube can be calculated by taking the inverse of the slope of the best line through the measurement points,

$$\begin{aligned} &\Delta p = Q \cdot R_{\text{hyd}} \\ &\Updownarrow \\ &R_{\text{hyd}} = (\frac{Q}{p})^{-1}. \end{aligned} \tag{8.4}$$

Performing this calculation for result of the measurement points plotted in figure 8.6 gives

$$R_{\text{hyd 1}} = (3.17 \cdot 10^{-11}\text{m}^3/(\text{Pa} \cdot \text{s}))^{-1} = 3.15 \cdot 10^{10}\text{Pa} \cdot \text{s}/\text{m}^3. \tag{8.5}$$

The deviation from the theoretical calculated hydraulic resistance is calculated to be 31.3%.
For the repeated experiment, the similar measurement points for the flow rate, Q, as function of the pressure difference, Δp, are plotted, see figure 8.7, and the best line through these points is calculated. Calculations of the resistance of the tube now gives

$$R_{\text{hyd 2}} = (3.41 \cdot 10^{-11}\text{m}^3/(\text{Pa} \cdot \text{s}))^{-1} = 2.93 \cdot 10^{10}\text{Pa} \cdot \text{s}/\text{m}^3. \tag{8.6}$$

The deviation from the theoretical calculated hydraulic resistance is now calculated to be 22.2%.

8.3.4 Conclusion

A deviation of respectively 33.1% and 22.2% for the hydraulic resistance for experiments compared to the theoretical calculated hydraulic resistance is at first sight at lot. But it is an acceptable deviation, because a lot of uncertainty factors will have an influence on the result of the experiment, and so the hydraulic resistance obtained experimental will never become exact.
The biggest problem with regard to the deviation is that the calculated hydraulic resistance calculated for each of the series of measurements differ from each other,

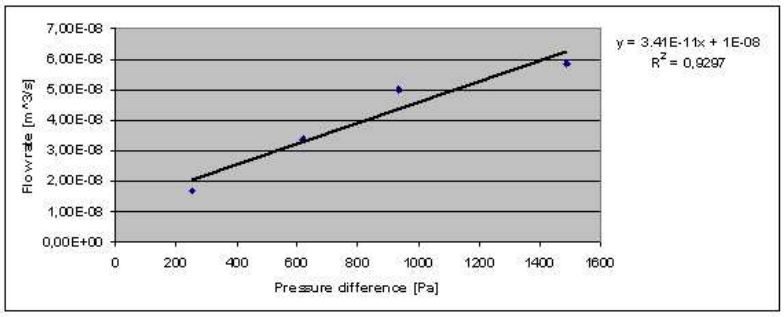

Figure 8.7: *Flow rate as function of the pressure difference over the inlet and the outlet of a Teflon tube for the sencond measurements with the tube. The resistance of the tube is given as the inverse slope of the best line through the measurement points.*

although these experiments were obtained in the same way and without any changes in the set-up. Therefore, a conclusion might be that is not possible, or it is very difficult, to repeat the experiments and get the same results.
The deviation in the experimental result from the theoretical calculation can be caused by many factors. The greatest problem might be the connection of the tube to the rest of the system, at the inlet and outlet of it, which is performed with a short piece of silicon tube. The dimensions of this tube are not included in the calculations and might, of cause, result in an error. Moreover, these small pieces of tube are made of silicone which is a fairly soft material, that perhaps might be able to a bit while water is send through them causing their radius to rise. This does also explain why the pressure calcaluted for the experiments becomes lower than the theoretical calculated pressure. The tube at which the experiments is performed, is made of Teflon, which is a fairly hard material, and thus extension of it during the experiments is not estimated to be a problem. But for the tube there will be a some unsertainty for its radius stated by the producer. Therefore there will not only be unsertainties for hydraulic resistanse obtained from the experiments, but also for the theoretical hydraulic resistance calculated for the tube.
Anyway, for the following experiments, there will not be time to repeat these a lot of times. Therefore so the conclusion might be that it is a problem, that is difficult to get the same experimental result more than once, because this will cause uncertainties of the measurements, particularly when measuring the hydraulic resistance of the inlet and outlet of the devices containing the micro fluidic cooling systems.

8.4 Resistance of the inlet and outlet

8.4.1 Purpose

Before experiments can be performed for devices containing micro fluidic cooling systems, it is necessary to determine the hydraulic resistance of the inlet and outlet. For that purpose devices containing only an inlet and an outlet were fabricated as described in section 6.1.
The relationship between the hydraulic resistance, R, the flow rate, Q, and the pressure difference, $\Delta p_{\text{inlet\_outlet}}$, over a device is stated in section 8.3.3,

$$R = \frac{\Delta p_{\text{inlet\_outlet}}}{Q} \tag{8.7}$$

8.4.2 Method of approach

The hydraulic resistance of the inlet and outlet was determined in the same way as the resistance of the Teflon tube described in section 8.3. The only difference was that now a device containing an inlet and an outlet was mounted between the two pressure sensors.
For the inlet and outlet the dimensions were smaller compaired to the radius, a, of the tube. Thus the hydraulic resistance of the inlet and outlet was bigger than the hydraulic resistance of the tube, so that the flow rate now had to be smaller.
For the flow rate it was found, that it might not be higher than $Q = 0.8$ ml/min, because for higher flow rates, the limit of the pressure sensor would be exceeded. Therefore the flow rate was raised from $Q = 0.1$ ml/min to $Q = 0.8$ ml/min in steps of $Q = 0.1$ ml/min. 10 measurement points were obtained each second and written to a file by use of LabView. The obtained data for the experiment can be found on the CD-ROM in the folder "Inlet and outlet".

8.4.3 Data processing

The hydraulic resistance of the inlet and outlet was calculated in the same way as the calculation of hydraulic resistance of the Teflon tube described in section 8.3 was performed.
For each series of measurements 10 measurement points were obtained each second. It takes a little while for the pressure difference over the system to be constant, and thus only the last 100 measurement points are used for the data processing.
The pressure difference, $\Delta p_{\text{inlet\_outlet}}$, over the system as function of the flow rate, Q, is plotted, and a tendens line is added, see figure 8.8. The hydraulic resistance of the inlet and outlet, $R_{\text{inlet\_outlet}}$, is then calculated as the inverse slope of the line,

$$R_{\text{inlet\_outlet}} = (3.49 \cdot 10^{-12})^{-1} = 2.86 \cdot 10^{11} \text{Pa} \cdot \text{s/m}^3. \tag{8.8}$$

8.4.4 Conclusion

The measurement points in figure 8.8 are almost lying on a straight line. Therefore the calculated hydraulic resistance is assumed to be useable for further measurements, even though the uncertainty might be assumed to be almost as big as the uncertainties in the hydraulic resistance determined for the Teflon tube described in section 8.3.3.
Before the experiment described above was performed, another attempt to dertermine the hydraulic resistance was performed for the same device and in the same way as described above. This experiment also gave a good connection between the pressure difference and the flow rate, because the correlation coefficient, r^2, was close to one. But the flow rate did only have to be the tenth of the flow rate stated in the experiment to give the same pressure difference compared to the experiments described above.

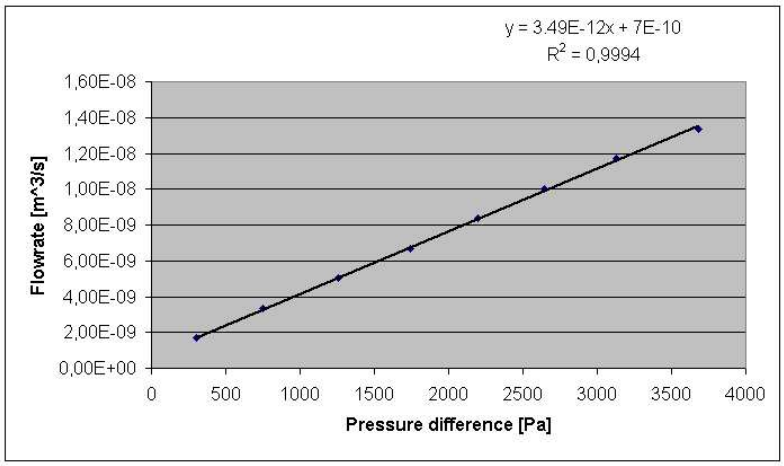

Figure 8.8: *Measurement of the pressure difference over the inlet and outlet as function of the flow rate.*

The reason for this phenomenon was found to be, that there was air in the tubes connecting the pressure sensors to the system. If there only had been air in the tubes, the time it would take for the system to reach a stable pressure would have been longer, because air can be conpressed much more than water, and thus a higher flow rate would have been required to obtain the same pressure difference over the system. However, the presence of small bubbles of water in the tubes would have been an even greater problem, because these would "bind" to the surfaces of the tubes because of surface tensions, and thus it would require a high force to pres the air in the tubes together.
Therefore all air bubbles was carefully removed from the system when performing the experiment described above, so that these would not cause an error for the calculated hydraulic resistance.

8.5 Temperature measurements of a test system

8.5.1 Purpose

The first useable devices were fabricated as described in section 6.1. It was tried to send water through the devices before experiments were performed with these. At first sight it was difficult to get water all over the micro fluidic cooling systems, because the some of the small and narrow channels within it remained empty, or air bubbles would occur in the structure, when water was sent through the system.
Therefore, when the final devices were fabricated, a device containing at simple test system instead of a micro fluidic cooling system was fabricated. The structure of the test system was one broad, twisted channel, so that the water necessarily had to fill the whole structure, when it was flowing through the system.
The water flow through the micro fluidic cooling system has to cool the upper copper plate, and the temperature has to be dependent on the flow rate, because the more water is sent through the system, the more the system will be cooled.
To obtain whelther this assumption can be applieds in practice, it is tried to measure the temperature dependence of the flow rate.

8.5.2 Method of approach

A device containing a test system is mounted in the set-up. It is sandwiched between the two copper plates, on top of the heating element, with cooling plasma between the layers. The "sandwich" structure is fixed by use of a clips, and the plastic bag filled with styrene balls is placed around it to isolate it.
A glass syringe is filled with water and mounted on the squirt pump. The water have been poured the day before the experiment is performed to make sure that is has room temperature, so that then temperature of the water will not cause any mistakes during the experiment.
The syringe pump is started, and the pressure over respectively the inlet and the outlet and the temperature of the two copper plates is measured. One measurement point is obtained each second, and the experiment has been performed for almost an hour, because 3603 measurement points are obtained totally. The flow rate, Q, and hence the pressure difference, Δp, is raised during the experiment without stopping the water flow or the measurements. The connection between the flow rate, Q, and the number of measurement points or the time is the following, s

Flow rate, Q	Measurement points
0.03 ml/min	0 to 803
0.005 ml/min	804 to 1725
0.02 ml/min	1726 to 2680
0.01 ml/min	2681 to 3603

The obtained data for the experiment can be found on the CD-ROM in the folder "Test system".

8.5.3 Data processing

The output voltage from the pressure sensors and the output voltage from the temperature sensor are converted into resceptively a pressure and a temperature as explaned in section 7.1.2 and section 7.1.4. The pressure and the temperature is plotted as function of the time, see figure 8.9.
From the figure it is very easy to see that the voltage measured with the pressure sensor at the inlet of the device changes, when the flow rate is changed, and thus the

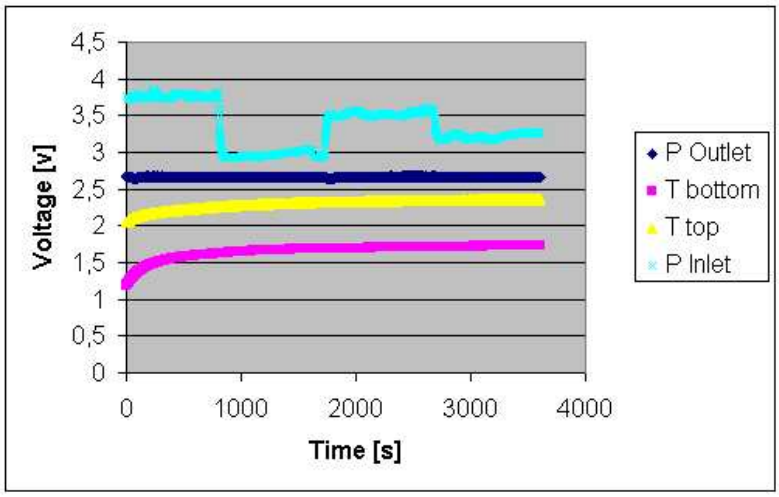

Figure 8.9: *Voltage measured by respectively the pressure sensors and the thermistors as function of time.*

pressure over the inlet changes. The change in pressure happens very fast when the flow rate is changed. Therefore, the relaxation time for the system is very short as obtained in section 8.1. The pressure over the outlet is almost constant during the experiment, because it is the atmospheric pressure that is measured.
The flow rate is first raised, then lowered and then raised again. However, the temperature does not look as if it is dependent on the flow rate, because it increases through the whole experiment, and the curve showing the temperature dependence of time forms an exponential increasing function, when the flow rate is changed.

8.5.4 Conclusion

It was not possible to measure a change in temperature as function of the flow rate. The reason for this might be that it takes a while for the whole "sandwich" structure to heat up and reach a constant temperature, and the very low flow rates at which water is sent through to system is too low to resist this raise in temperature.
The conclusion for this experiment might then be that when performing experiments for devices containing micro fluidic cooling structures, the water flow through the system has to be stopped every time the flow rate is changed and the heating element has to be turned off, because the initial conditions for the measurements has to be the same. Furthermore, measurements have to be performed for a long period of time, so that the temperature has time to reach a constant value.

8.6 Timescale measurements

8.6.1 Purpose

For the experiment performed with the PMMA plate described in section 8.2, it was obtained that the temperature difference becomes constant after a short while, when an isolated system is heated up. Therefore, in order to determinate for how long time it is necessary to perform measurements on a micro fluidic cooling system before the temperature difference between the top and the bottom copper plate reaches a constant level, this was proved for a device containing a micro fluidic cooling system. Furthermore, this experiment was performed in order to determine whether it is possible to extrapolate the obtained results. If this is possible, the time scale for the measurements can be lowered.

8.6.2 Method of approach

A device containing a micro fluidic cooling system optimized at $\Delta p_{cooler} = 0.5\,\mathrm{Pa}$, was mounted in the experimental set-up between the two pressure sensors. The micro fluidic cooling system was placed between the two copper plates, on top of the heating element, and the whole system was fixed by use of a clips. Furthermore, the plastic back filled with styrene balls was placed around the system to isolated it from the surroundings.
Water was send through the system by use of the syringe pump. The flow rate was fixed at $Q = 0.1\ \mathrm{ml/min} = 1.67 \cdot 10^{-8}\ \mathrm{m^3/s}$ during the experiment.
The experiment was carried out for an hour. During the experiment, the voltage output obtained from the two pressure sensors and the voltage output obtained from the two temperature sensors were continuous measured and written to a file. One measurement point was obtained each second. The obtained data for the experiment can be found on the CD-ROM in the folder "Timescale".

8.6.3 Data processing

The voltage output obtained from the pressure sensors and the voltage output obtained from the two temperature sensors are plotted as a function of time, see figure 8.10.

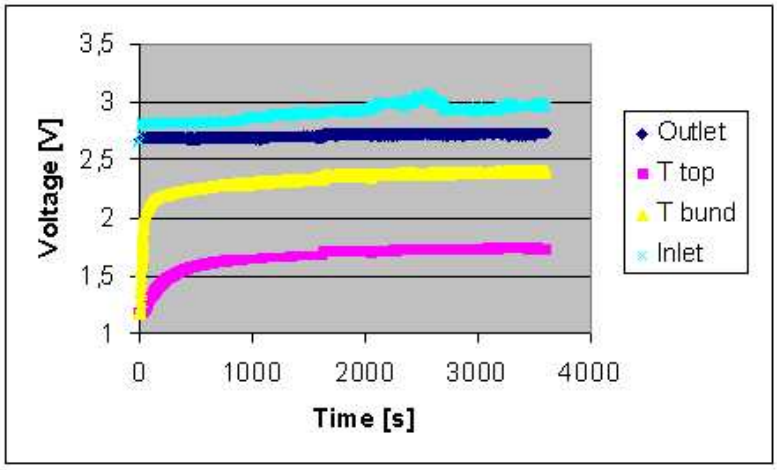

Figure 8.10: *Voltage output obtained from the pressure sensors and the temperature sensors plotted as a function of time.*

8.6.3.1 Pressure measurements

The voltage output obtained from the two pressure sensors is plotted as function of time is noted on figure 8.10 together with the temperature measurements.
The voltage output from the two pressure sensors is converted into a pressure as decried in section 7.1.2. As noted from figure 8.10, the magnitude of the pressure difference is not stable through the experiment. To get an estimate of the pressure difference, the average value of the voltage measured by the pressure sensors is calculated for measurement point 100 to measurement point 3600. Thus the average total pressure difference was calculated to be $\Delta p_{\text{total}} = 678.3\,\text{Pa}$, and the standard deviation of this average pressure difference was calculated to be ± 4.3 Pa. Calculations of standard deviations of average values is described in appendix 13.
The pressure difference over the micro fluidic cooling system, Δp_{cooler}, can now be calculated from a relation between the hydraulic resistance of the cooling system, R_{cooler}, the resistance of the inlet and outlet, $R_{\text{inlet\_outlet}}$, and the total pressure difference over the device, Δp_{total},

$$\Delta p_{\text{cooler}} = \left(\frac{R_{\text{cooler}}}{R_{\text{cooler}} + R_{\text{inlet\_outlet}}} \right) \Delta p_{\text{total}}. \tag{8.9}$$

The hydraulic resistance of the micro fluidic cooling system is calculated from the computer simulations, for which the flow rate at the inlet is calculated to be $Q = 2.6 \cdot 10^{-9}\ \text{m}^3/\text{s}$ by taking the integral of the velocity over the inlet boundary and multiplied by the height of the channel. The pressure difference over the cooling system was defined to be $\Delta p_{\text{cooler}} = 0.5$ Pa. The hydraulic resistance is then calculated from Hagen-Poiseuille's law, see section 2.6, that states

$$R = \frac{\Delta p}{Q}. \tag{8.10}$$

Now, the hydraulic resistance of the micro fluidic cooling system is calculated to be

$$R_{\text{cooler}} = \frac{= 0.5\ \text{Pa}}{2.6 \cdot 10^{-9}\ \text{m}^3/\text{s}} = 1.9 \cdot 10^8\ \text{Pa} \cdot \text{s/m}^3. \tag{8.11}$$

In section 8.4 the hydraulic resistance of inlet and outlet was calculated to be $R_{\text{inlet\_outlet}} = 2.9 \cdot 10^{11}\,\text{Pa}\cdot\,\text{s/m}^3$. The pressure difference over the micro fluidic cooling system then becomes

$$\Delta P_{\text{cooler}} = \left(\frac{1.9 \cdot 10^8 \text{Pa} \cdot \text{s/m}^3}{1.9 \cdot 10^8 \text{Pa} \cdot \text{s/m}^3 + 2.9 \cdot 10^{11} \text{Pa} \cdot \text{s/m}^3} \right) \cdot 678,3\ \text{Pa} = 0.4\ \text{Pa} \tag{8.12}$$

which is very close to the optimal pressure established for the cooling system.

8.6.3.2 Temperature measurements

The temperature output obtained from the two temperature sensors plotted as function of time is noted from figure 8.10 together with the pressure measurements.
The voltage output is converted into a temperature as described in section 7.1.4. The temperature difference of the two copper plates is then calculated and plotted as function of time, note figure 8.11.
As noted from the figure, there is a characteristic point around 100 s because beyond this point the temperature difference seems to decrease exponentially. Therefore, the measurement points beyond 100 s is fitted to an exponential function to establish whether it is possible to extrapolate the result. The curve obtained for the fitted data is shown in figure 8.12.
For the curve, the equation that the data point is fitted to is given by

$$y = a + b \exp \frac{-x}{c}, \tag{8.13}$$

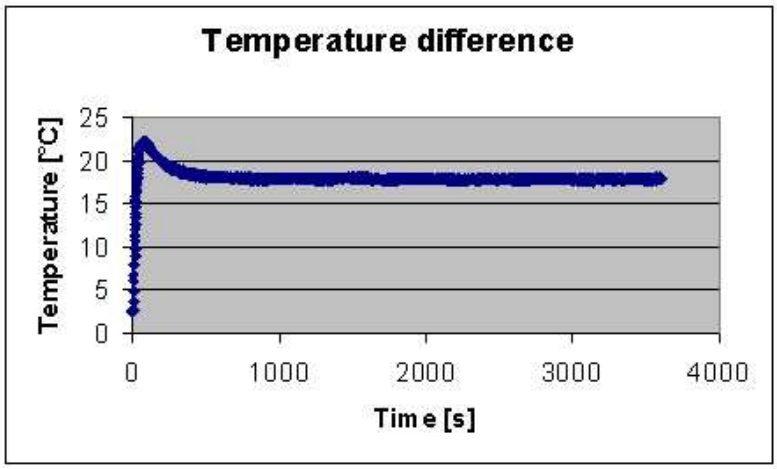

Figure 8.11: *Temperature difference plotted as a function of time.*

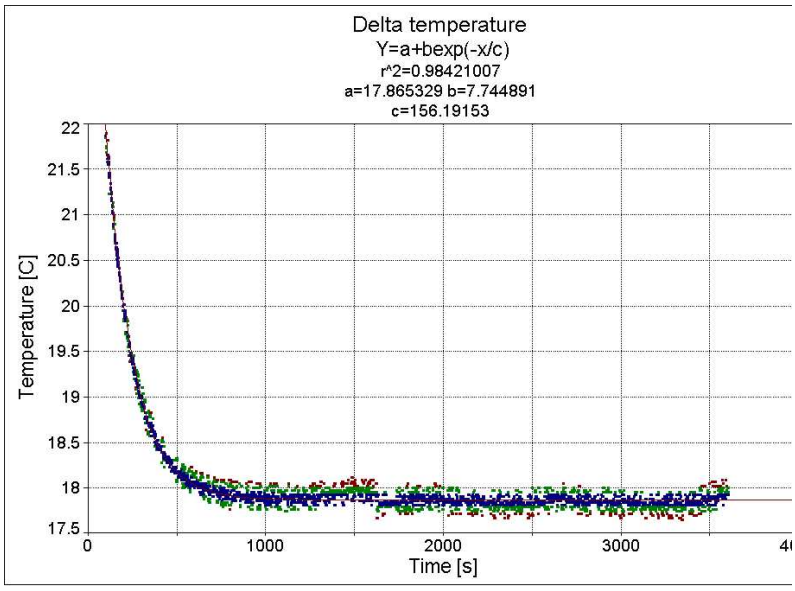

Figure 8.12: *Extrapolation of the temperature difference to an exponential function.*

because this equation gives the best correlation coefficient, r^2. The horizontal asymptote, corresponding to the temperature difference, that the system tends, is given by a, which is calculated to be $17.9°C$.
The temperature difference that the system has reached is found by calculating the average of data point 1000 to data point 3600. The temperature difference now becomes 17.9°C, with a standart deviation of the average temperature of ±2.4°C.

8.6.4 Conclusion

The results of the experiment showed that the temperature difference of the system was 17.9 ± 2.4°C. When the measurements from data point 100 to 3600 was fitted to an exponential function, the asymptote for the function was $a = 17.9$°C which is the temperature that the system will tend.
The temperature difference that the system has reached was found from the average of measurement point 1000 to measurement point 3600 to be $17.9 \pm 2.4°C$, which is almost the same as the extrapolated result.
The standart derivation of the calculated average temperature is relatively high. The reason for the relatively high standart derivation this is that the temperature difference starts to increase when the experiment is almost finished. Thus, if the average of the temperature is calculated from measurement point 1000 to measurement point 1800 instead af measurement point 3600, the average temperature difference becomes 17.9°C, with a standard derivation of ±0.8.
There is a good agreement between the measured result and the result found by extrapolation. Therefore it might be concluded that the time scale at which the measurements is carried out has to be 1000 s, because it is only necessary to obtained measurements for 1000 s before a final temperature difference of the two copper plates can be established. Furthermore it can be concluded that it is possible to extrapolate the results and obtain a precise temperature difference for the two copper plates.

8.7 Temperature measurements of the micro fluidic cooling systems

8.7.1 Purpose

As established for the experiment described in section 8.6.1, the time scale has to be $1000\,\mathrm{s} \approx 17\,\mathrm{min}$ at least.
This experiments are carried out to determinate the temperature difference of the two copper plates for two different micro fluidic cooling systems placed between the plates. For the first cooling system, the pressure difference over the inlet and outlet of it is optimized for $\Delta p_{\mathrm{cooler}} = 0.5\,\mathrm{Pa}$, and for the other cooling system, the pressure difference over the inlet and outlet of it is optimized for $\Delta p_{\mathrm{cooler}} = 2.5\,\mathrm{Pa}$.
The two micro fluidic cooling systems are chosen because they are optimized for relatively different pressures. The cooling system optimized for $\Delta p_{\mathrm{cooler}}$ =2.5 Pa are the one of all the optimized systems, where the pressure difference could be raised most, without having any unphysical channels that ends blind.
The temperature corresponding to the optimal pressures of the two systems has to be measured. For both systems, the average temperature difference is determined corresponding to the pressure differences $\Delta p_{\mathrm{cooler}} = 0.5$ Pa and $\Delta p_{\mathrm{cooler}} = 2.5$ Pa. The obtained results are compared to each other.

8.7.2 Method of approach

The pressure difference, $\Delta p_{\mathrm{cooler}}$, mentioned in the previous section, is the pressure difference over a micro fluidic cooling system. However, the pressure difference measured in this experiment, $\Delta p_{\mathrm{total}}$, is the pressure difference over the whole device, including the pressure difference over the inlet and outlet.
The pressure difference over a micro fluidic cooling system is determined from the equation 8.9,

$$\Delta p_{\mathrm{cooler}} = \left(\frac{R_{\mathrm{cooler}}}{R_{\mathrm{cooler}} + R_{\mathrm{inlet\_outlet}}} \right) \Delta p_{\mathrm{total}}. \tag{8.14}$$

To obtain the decided pressure difference over the cooling system, it is necessary to change the flow rate until the total pressure difference over the device results in the decided pressure.
The hydraulic resistance for the two cooling systems differ. Therefore, the flow rate for the two systems has to be different.
The method for the data collection is the same as described in section 8.6.2. However, before the measurements of the temperature can be performed, the pressure difference resulting in the desired pressure difference over the cooling systems is determined. The pressure difference is changed by changing the flow rate, and then the pressure difference is measured. This process is repeated until the desired pressure difference is obtained. Then the heating element is turned on.
The measurements were carried out for about 30 min, even though is has been obtained in the previous section that it is only necessary to perform the experiments for 1000 s. One measurement point was obtained each second, and the voltage from the two pressure sensors and the voltage from the two temperature sensors were continuously measured and written to a file. The obtained data for the experiment can be found on the CD-ROM in the folder "Temperature".

8.7.3 Data processing

The data processing is split up into two sections. The first section describes the experimental result obtained for the micro fluidic cooling system optimized for $\Delta_{\mathrm{cooler}} p = 0.5\,\mathrm{Pa}$ and the second section describes experimental results obtained for the system optimized for $\Delta p = 2.5\,\mathrm{Pa}$

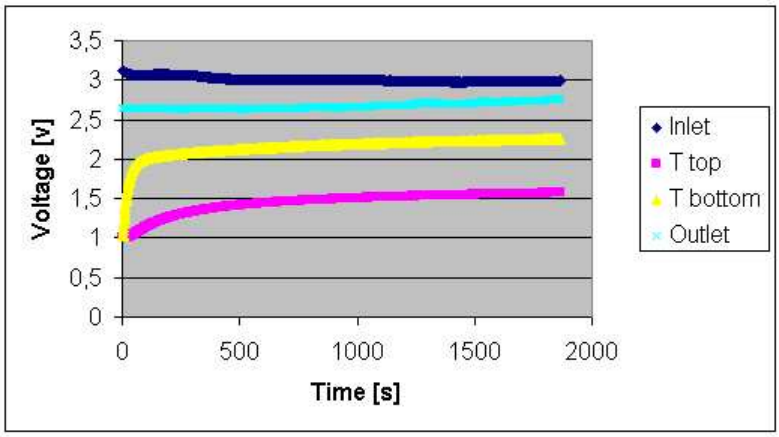

Figure 8.13: *Voltage output meassured from the pressure sensores and the temperature sensores as a function of time, for flow rate* $Q = 0.05\,ml/min$

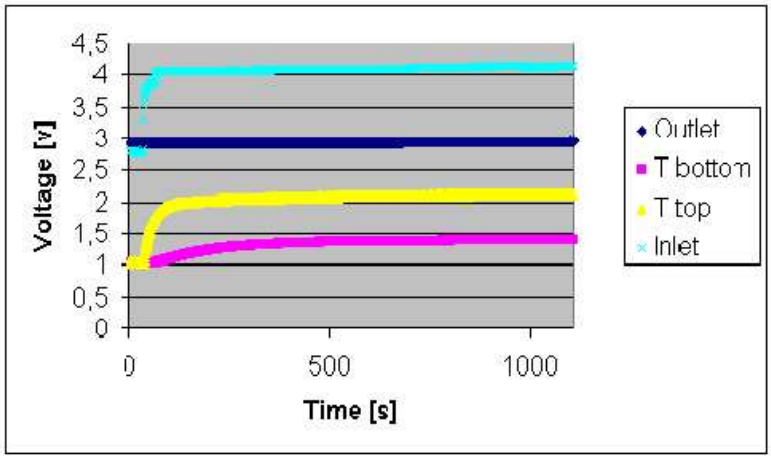

Figure 8.14: *Voltage output meassured from the pressure sensores and the temperature sensores as a function of time, for flow rate* $Q = 0.5\,ml/min$

8.7.3.1 Micro fluidic cooling system optimized for 0.5 Pa

The flow rate, Q, that results in the desired pressure difference, $\Delta p = 0.5\,\text{Pa}$, over the micro fluidic cooling system is found to be around $Q = 0.05\,\text{ml/min}$. Similar, the flow rate that results in a pressure difference of $\Delta p = 2.5\,\text{Pa}$ is found to be around $Q = 0.5\,\text{ml/min}$.
For the flow rate $Q = 0.05\,\text{ml/min}$ the measurements are carried out in 30 min. The voltage measured from two pressure sensors and the voltage measured from the temperature sensors are plotted as function of time, see figure 8.13.
For the flow rate $Q = 0.5\,\text{ml/min}$ the measurements are carried out in 17 min. The voltage measured from the two pressure sensors and the voltage measured from the temperature sensors are plotted as function of the time, see figure 8.14.

8.7.3.2 Pressure measurements

The output voltage measured by the pressure sensors is converted into a pressure as described in section 7.1.2.
The average pressure difference, Δp, over the device is calculated by determining the average value of the measurement point 100 to the last measurement point.

The average of the pressure difference, Δp, and the standard derivation of the average pressure difference, $\pm\Delta p$, for the two flow rates, Q, are calculated, and the pressure difference, Δp_{cooler}, for the cooling system are calculated from equation 8.9. The results of the calculations are noted in table 8.1.

As noted from table 8.1, the pressure difference over the micro fluidic cooling system

Q	Δp	$\pm\Delta p$	Δp_{cooler}
0.05 ml/min	1110.8 Pa	±4.7 Pa	0.7 Pa
0.5 ml/min	3864.5 Pa	±1 Pa	2.5 Pa

Table 8.1: *Pressure difference, Δp, standard derivation of the average pressure difference, $\pm\Delta p$, and the pressure difference over the cooler, Δp_{cooler}, at different flow rates, Q. The micro fluidic cooling system is optimized for Δp_{cooler}=0.5 Pa*

is almost corresponding to the desired pressure difference for both flow rates.

8.7.3.3 Temperature measurements

The output voltage measured from the two temperature sensors are converted into a temperature as described in section 7.1.4.

The temperature differences obtained for the system at the two flow rates are determined by the calculating the average from measurement point 1000 to the last data point. This is done in order to estimate the final temperature difference.

To extrapolate the average temperature, the data points from 100 to the last data point is fitted to an exponential function. The exponential function is given by

$$y = a + b \exp \frac{-x}{c}, \tag{8.15}$$

where a determines the asymptote, which corresponds to the temperature, ΔT_{exp}, that the average temperature of the system will tend. Furthermore, the temperature, ΔT, estimated from measurement point 1000 to the last measurement point and the standard derivation of the average temperature, $\pm\Delta T$, is calculated. The results of the calculations are shown in table 8.2.

A figure showing the temperature difference plotted as function of the time and a

Q	ΔT	$\pm\Delta T$	ΔT_{exp}
0.05ml/min	18.5°C	±0.002°C	18.5°C
0.5ml/min	19.6°C	±0.009°C	19.4°C

Table 8.2: *Average temperature, ΔT, standart derivation of the average temperature, $\pm\Delta T$, and the extrapolated temperature difference, ΔT_{exp}, at difference flow rates, Q. The micro fluidic cooling system is optimized for $\Delta p_{\text{cooler}} = 0.5\,Pa$*

figures for the fitted data is noted in figure 8.15.

8.7.3.4 Micro fluidic cooling system optimized for 2.5 Pa

The flow rate that gives the desired pressure difference over the micro fluidic cooling system, at $\Delta p_{cooler} = 0.5\,\text{Pa}$ is around $Q = 0.05\,\text{ml/min}$, while the flow rate that gives a pressure difference of $\Delta p_{\text{cooler}} = 2.5\,\text{pa}$ is around $0.2\,textrmml/min$.

For the flow rate $Q = 0.05\,\text{ml/min}$ the measurements are carried out for 30 min. The voltage measured from the two pressure sensors and the voltage measured from the two temperature sensors are plotted as function of time, see figure **??**.

For the flow rate $Q = 0.2\,\text{ml/min}$, the measurements are carried out for 30 min. The voltage measured from the two pressure sensors and the voltage measured from the temperature sensors are plotted as function of time, see figure 8.18(a).

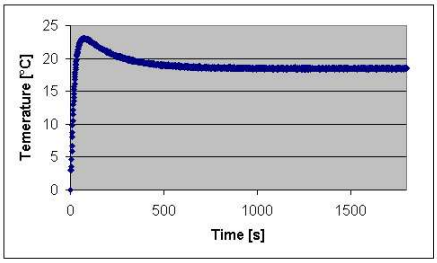

(a) *The temperature difference for a system optimized for* $\Delta p_{cooler} = 0.5\,ml/min$, *for* $Q = 0.05\,ml/min$

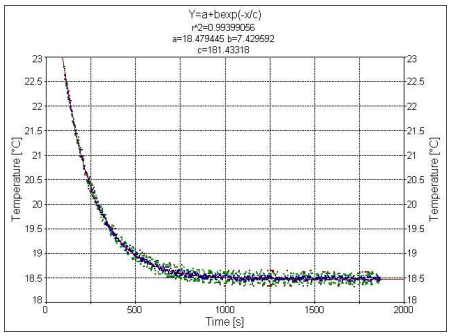

(b) *The extrapolated temperature difference for a system optimized at* Δp_{cooler} =0.5 *Pa, for* $Q = 0.05$ *ml/min*

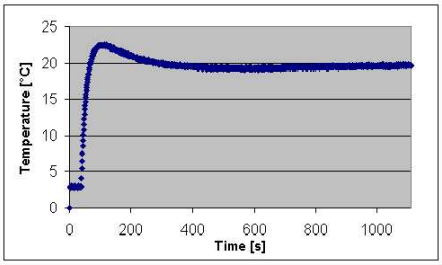

(c) *The temperature difference for a system optimized at* $\Delta p_{cooler} = 0.5\,ml/min$, *for* $Q = 0.5\,ml/min$

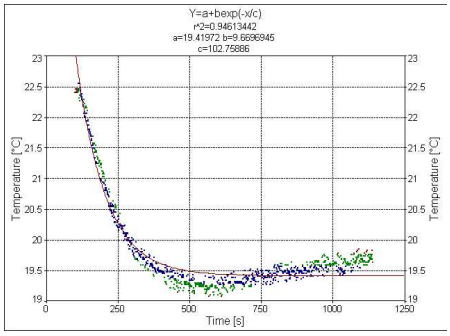

(d) *The extrapolated temperature difference for a system optimized at* Δp_{cooler} =0.5 *Pa, for* $Q = 0.5$ *ml/min*

Figure 8.15: *The average temperature for a system optimized at* $\Delta p_{cooler} = 0.5\,Pa$

8.7.3.5 Pressure measurements

The average of the pressure difference over the device, Δp, the standart derivation of the average pressure over the device, $\pm\Delta p$, and the pressure difference over the micro fluidic cooling system, Δp_{cooler}, are calculated as described in section **??**. The results of the calculations are shown in table 8.3.

As noted from table 8.3, is the calculated pressure difference obtained for both flow

Q	Δp	$\pm\Delta p$	Δp_{cooler}
0.05 ml/min	574.34 Pa	±4.9 Pa	0.5 Pa
0.2 ml/min	2756.5 Pa	±4.1 Pa	2.3 Pa

Table 8.3: *Pressure difference,* Δp, *standart derivation of the average pressure difference,* $\pm\Delta p$, *and the pressure difference over the cooler,* Δp_{cooler}, *at different flow rates,* Q. *The micro fluidic cooling system is optimized for* $\Delta p_{\text{cooler}} = 2.5\,Pa$

rates almost corresponding to the desired pressure differences.

8.7.3.6 Temperature measurements

The average temperature of the micro fluidic cooling system, ΔT, the standart derivation from the average temperature, $\pm\Delta T$, and the extrapolated temperature, ΔT_{exp}, are calculated as described in section 8.7.3.3. The results of the calculations are shown in table 8.4

A figure showing the temperature difference plotted as function of the time and a figures for the fitted data is noted in figure 8.18.

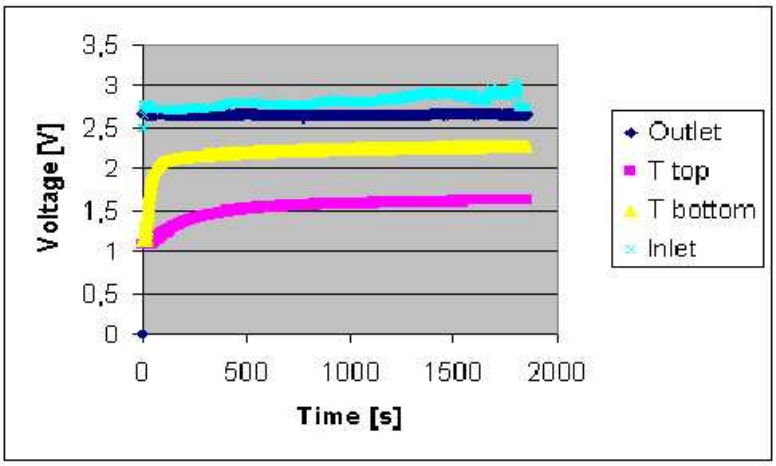

Figure 8.16: *Voltage output meassured from the pressure sensores and the temperature sensores plottet as a function of time, for flow rate* $Q = 0.05\,ml/min$

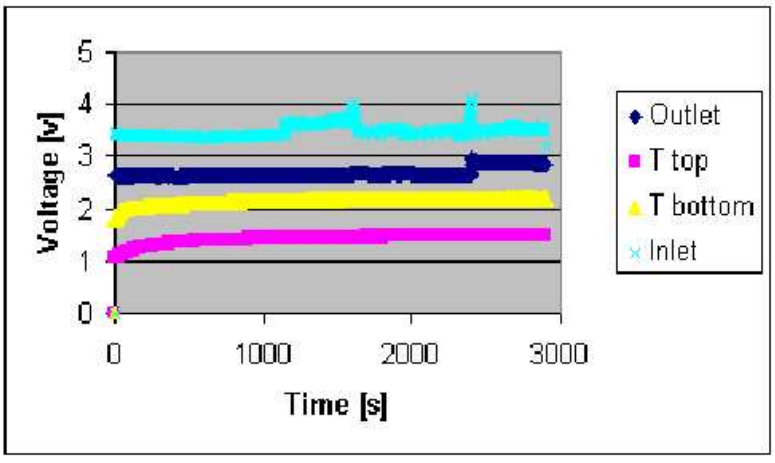

Figure 8.17: *The voltage output meassured from the pressure sensores and the temperature sensores as a function of time, for flow rate* $Q = 0.2\,ml/min$

Q	ΔT	$\pm\Delta T$	ΔT_{exp}
0.05 ml/min	17.8°C	±0.002°C	17.8°C
0.2 ml/min	19.2°C	±0.003°C	19.3°C

Table 8.4: *Temperature, ΔT, standart derivation of the temperature difference, $\pm\Delta T$, and the extrapolated temperature difference, at different flow rates, Q. The micro fluidic cooling system is optimized for $\Delta p_{\text{cooler}} = 2.5\ Pa$*

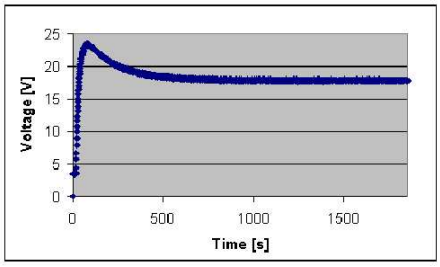

(a) *The temperature difference for a system optimezed at $\Delta p_{cooler} = 2.5\ ml/min$, for $Q = 0.05\ ml/min$*

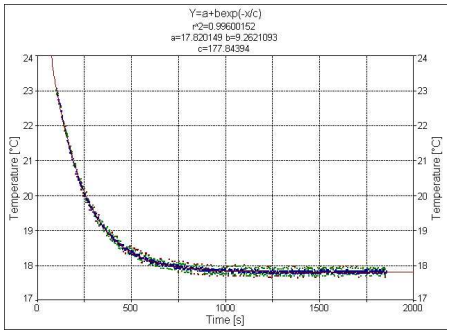

(b) *The extrapolated temperature difference for a system optimezed at $\Delta p_{cooler} = 2.5\ Pa$, for $Q = 0.05\ ml/min$*

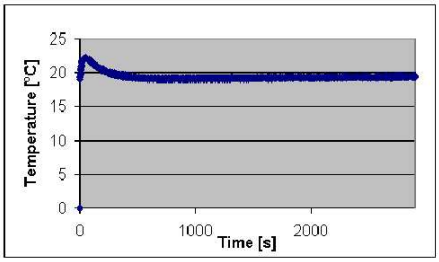

(c) *The temperature difference for a system optimezed at $\Delta p_{cooler} = 2.5\ ml/min$, for $Q = 0.5\ ml/min$*

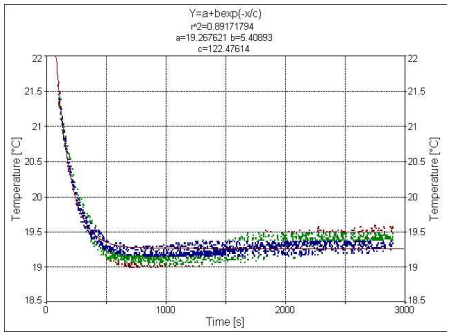

(d) *The extrapolated temperature difference for a system optimezed at $\Delta p_{cooler} = 2.5\ ml/min$, for $Q = 0.2\ ml/min$*

Figure 8.18: *The average temperature for a system optimized at $\Delta p_{cooler} = 2.5\ Pa$*

8.7.4 Conclusion

The experimental obtained temperature differences and pressure differences for the two micro fluidic cooling systems, the standart derivation of the average temperature and the extrapolated temperatures for the two systems are noted in table 8.5.

System 0.5				System 2.5			
Δp_{cooler}	ΔT	$\pm\Delta T$	ΔT_{exp}	Δp_{cooler}	ΔT	$\pm\Delta T$	ΔT_{exp}
0.7Pa	18.5°C	±0.002°C	18.5°C	0.5Pa	17.8°C	±0.002°C	17.8°C
2.5Pa	19.6°C	±0.009°C	19.4°C	2.3Pa	19.2°C	±0.003°C	19.3°C

Table 8.5: *Temperature, ΔT, standart derivation of the average temperature, $\pm\Delta T$, and the extrapolated temperature difference ΔT_{exp}, at different pressure differences over the micro fluidic cooling system, Δp_{cooler}. The two micro fluidic cooling systems are optimized for Δp_{cooler} =0.5 Pa and Δp_{cooler}=2.5 Pa, respectively.*

From table 8.5 it is noted, that the temperature is measured with very high accuracy,

because the standard deviation of the average is very low. Furthermore, it is noted that for the system optimized for $\Delta p_{\text{cooler}} = 2.5\ Pa$, the lowest temperature is obtained for both measurements performed with this device.
The measurements are carried out over a relatively long period of time compared to the measurement time found in the previous section, a which a constant temperature difference would be obtained.
Although the system is isolated by a plastic bag containing styrene balls, the surroundings will have an influence on the measured temperature of the two systems, because the syringe balls are not able to isolate the system totally from the surroundings. Furthermore, the experiments were carried out over two days, and thus the room temperature could have been different while performing the experiments for the two different cooling systems. But also the small changed might have been presented within the experimental set-up, when measurements are not performed in the same time.
The determination of the hydraulic resistance for the systems is based on the teoretical simulation. When the device are fabricated using the CO_2 laser, the structures of the micro fluidic cooling system is broaden a bit. Therefore, the hydraulic resistant for the actual system might be lower than the hydraulic resistance corresponding to the value of Δp_{cooler} used within the optimizations. Furthermore, when fabricating the devices, the dimensions of the inlet and outlet channels may differ a bit for the devices, because of uncertainties within the laser set-up.
The hydraulic resistance of the micro fluidic cooling system and of the inlet and outlet was only determined once. Therefore, it might have been determined with a great uncertainty. The uncertainty of the total pressure difference becomes relatively high so the pressure difference over the micro fluidic cooling system is neither very accurate. Is it a fact that the pressure difference over the micro fluidic cooling systems is proportional to the flow rate. Therefore the pressure difference increases as the flow rate increases, and thus the temperature difference increases.
In the previous experiment the average temperature of the micro fluidic cooling system optimized for $\Delta p_{\text{cooler}} = 0.5\,\text{Pa}$ was determined to be $\Delta T = 17.9 \pm 2.4°\text{C}$. The pressure difference over the micro fluidic cooling system then calculated to be $\Delta p_{\text{cooler}} = 0.4$ Pa. The pressure difference obtained in this experiment was $\Delta p = 0.7Pa$ and the calculated average temperature difference was $\Delta_T = 18.5$. Therefore, the temperature difference increases as the pressure difference increases, which is in agreement with the theory, because when the pressure difference is increased the flow rate is increased and more water is flowing through the cooling system. When more water is flowing through the cooling system, more heat can be conducted away from the it.
If only the temperatures obtained for the system for which the pressure different was approximately $\Delta p_{\text{cooler}} = 2.5$Pa are considered, the lowest temperature obtained for this system is lowest average temperature. Therefore it is the most optimal cooling system at $\Delta p_{\text{cooler}} = 2.5$ Pa.
The extrapolated temperatures for the average temperature of the micro fluidic cooling systems are in agreement with the average temperatures.
Unfortunately, the experiments were not repeated because of lack of time, and the therefore it is not known whether the results can be reproduced or not.

Chapter 9

Conclusion

The main purpose of the present project was to perform topology optimizations of micro fluidic cooling systems and to fabricate the systems in PMMA using a CO_2 laser.
The optimizations were carried out for several geometries. The final geometry was chosen as a rectangle and the whole design area was heated. The structure was optimized for different pressures. The results showed that the systems were optimal for low pressure differences between inlet and outlet. However, when the pressure difference was increased, the structures were no longer optimal compared to a system optimized at a different pressure. The reason for this might be that the optimization is performed numerically and therefore the optimization can only be as accurate as the number of points at which the solution is calculated.
When the pressure difference between the inlet and outlet is increased, the number of channels that terminates within the solid material is increased. This is not a physically acceptable solution to the optimization problem. However, it is found that decreasing the width of the inlet and outlet leads to an increase of the pressure difference at which the channels start to terminate in the solid.
Heat conduction experiments though a PMMA plate were carried out and the result clearly showed that the system had to be isolated from the surroundings.
Also investigated is the resistance of a tube having well-defined dimensions and the result is compared to the theoretically calculated resistance of such a tube. The result is used to estimate the precision that can be obtained for the hydraulic resistance of the inlet and outlet part of the micro fluidic system. The hydraulic resistance of the tube was measured twice, and the measurements that gave the largest coefficient of correlation resulted in a deviation from the theoretical result of 33.1 %. Therefore it was assumed that the hydraulic resistance for the inlet and outlet can be measured to an accuracy of approximately 33 %. The resistance of the inlet and outlet is used to calculate the pressure difference between the inlet and outlet of the system.
Furthermore, an experiment is carried out to establish the time needed to obtain reasonable results for the average temperature. The time scale is establish to be 1000 s, and it is shown that at this time scale the average temperature of the system can be extrapolated.
Two systems were fabricated, one system with the optimal pressure difference 2.5 Pa, and one system with the optimal pressure difference 0.5 Pa.
Measurements were carried out to establish the average temperature for each of the systems at 0.5 Pa respectively 2.5Pa.
The average temperature for the system optimized at 2.5 Pa was the lower at both pressure differences, 0.5 Pa and 2.5 Pa. Therefore the optimized system might not be the most optimal.

Chapter 10

Stress field

The density of liquids has to be defined in terms of the forces acting on them.
A fluid particle experiences surface forces like pressure and friction, that are generated by contact with other particles or the surface of a solid, and it experiences body forces like gravity and electronic forces, that are experienced throughout the particle.
The gravitation force acting on a volume elements, $d\vec{V}$, is given by

$$\vec{F}_{\text{grav}} = \rho\vec{g}d\vec{V}, \tag{10.1}$$

where ρ is the density and $\vec{g}$ is the gravitation force per unit mass, and so $\rho\vec{g}$ is the gravitation force per unit volume.
Surface forces acting on a fluid particle lead to stress. The phenomenon stress can be used, when describing how forces acting on the boundaries of a medium are transmitted throughout it.
Now, the surface of a fluid particle is assumed. The surface is in contact with other fluid particles. Thus a contact force is being generated between the particles. At some point on the surface, C, a part of it, $\delta\vec{A}$, is considered. The orientation of $\delta\vec{A}$ is given by the unit vector $\vec{n}$, that is pointing outward with respect to the particle.
The force, $\delta\vec{F}$, acting on the area $\delta\vec{A}$, have to be dissolved in two components, one normal to it, which is called the normal stress, σ_n, and one tangent to it, which is called the shear stress, τ_n. These stresses are defined as, respectively

$$\sigma_n = \lim_{\delta A_n \to 0} \frac{\delta F_n}{\delta A_n} \tag{10.2}$$

and

$$\tau_n = \lim_{\delta A_n \to 0} \frac{\delta F_t}{\delta A_n}. \tag{10.3}$$

The concepts of derivation of stress in fluids is shown in figure 10.1.

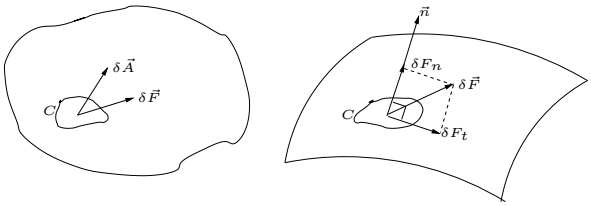

Figure 10.1: *Figure showing the concept of derivation of stress in fluids.* [9]

According to the continuum hypothesis, see section 2.2, the fluid is actually a conti nuum, and so it could have been broken up into any number of different ways of fluid

particles around the point C, and therefore obtained any different number of stresses at this point. [9]

Chapter 11

Viscosity

A steady-state flow is laminar and can be split-up into layers that flow parallel to each other, which also will mentioned in section 2.3.
The flow of a liquid will never occur without friction, even though this often is assumed, because the layers in the laminar flow "rub" against each other, while they are not moving with the same velocity. Or it could be said that if a liquid is influenced by a shear stress, it begins to yield. The magnitude of the friction is different for different liquids and can be describes by the viscosity of the liquid.

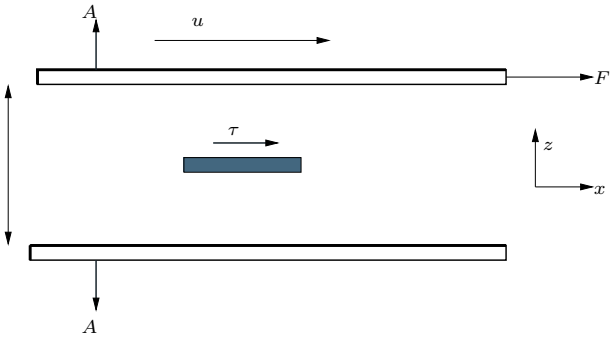

Figure 11.1: *Figure for derivation of viscosity showing two parallel plates, where on of them is moving with a constant velocity, u. A liquid is flowing between the plates with a laminar flow.*

A liquid flowing between two parallel plates is assumed, where on of the plates is moving in the x direction with a constant velocity, u, so that the plates remain parallel to each other as shown in figure 11.1. The distance between the plates is h.
The force, F, that the plate in motion has to be influenced by is proportional to its size, A, and to the velocity, u, and inverse proportional to the distance between the plates, h,

$$F = \eta \frac{u}{h} A. \tag{11.1}$$

The constant of proportionality is the viscosity, η, that for water is 0.001 mPa·s. The viscosity can be explained as being the resistance against yield for fluids.
If a thin parallel layer between the plates is considered instead of the entire space, the same tangential forces are represented, because of Newton's third law,

$$\tau_n = \eta \frac{\partial u_x}{\partial z}, \tag{11.2}$$

where τ_n is the shear stress. The directions x and z are shown in figure 11.1.
Liquids satisfying the equation 11.2 and which are independent of the shear stress are termed Newtonian fluids. [8]

Chapter 12

Derivation of the Péclet number

The Péclet number can be derived from an expression for the dimensionsless heat equation used in the FEMLab application mode and derived in section 2.8.2 for an incompressible fluid in steady-state,

$$\begin{aligned} &\rho C\vec{u}\vec{\nabla}T + \vec{\nabla}(k\vec{\nabla}T) = Q \qquad (12.1)\\ \Updownarrow\\ &\rho C\vec{u}\vec{\nabla}T - k\vec{\nabla}^2T) = Q \qquad (12.2)\end{aligned}$$

The velocity vector has both a component in the x and in the y direction, so that $\vec{u} = [v_x, v_y]$. Thus if the fluid is moving in the x direction, the velocity in the y direction is 0, $v_y = 0$. Thus

$$v_x\rho C\frac{\partial T}{\partial x} = Q + k\vec{\nabla}^2T. \qquad (12.3)$$

Now expressions in term of dimensionless number are introduced as follows

$$x = L\tilde{x} \qquad y = L\tilde{y} \qquad t = t_0\tilde{t} \qquad T = T_0\tilde{T}. \qquad (12.4)$$

If the fluid is moving in the x-direction, it is possible to make the velocity in this direction, u_x, dimensionsless by use of the chain rule,

$$v = \frac{\partial x}{\partial t} = \frac{\partial x}{\partial \tilde{x}}\frac{\partial \tilde{x}}{\partial \tilde{t}}\frac{\partial \tilde{t}}{\partial t} = \frac{L}{t_0}\frac{\partial \tilde{x}}{\partial \tilde{t}} = v_0\tilde{v}. \qquad (12.5)$$

Inserting the expression for the velocity in the expression 12.3 gives

$$u_0\tilde{u}\rho C\frac{\partial T}{\partial x} = Q + k\vec{\nabla}^2T. \qquad (12.6)$$

Rewriting the dimensionless numbers and interting gives

$$u_0\tilde{u}\rho C\frac{T_0}{L}\frac{\partial \tilde{T}}{\partial \tilde{x}} = Q + k\frac{T_0}{L^2}\vec{\nabla}^2\tilde{T} \qquad (12.7)$$

Dividing by $k\frac{T_0}{L^2}$ gives

$$\frac{u_0\rho CL}{k}\tilde{v}\frac{\partial \tilde{T}}{\partial \tilde{x}} = \frac{L^2}{kT_0}Q + \vec{\nabla}^2\tilde{T}. \qquad (12.8)$$

The Péclets number is known to be defined as

$$Pe = \frac{u_0\rho CL}{k} \qquad (12.9)$$

Then the final expression becomes [6]

$$Pe\cdot\tilde{u}\frac{\partial \tilde{T}}{\partial \tilde{x}} = \frac{L^2}{kT_0}Q + \vec{\nabla}^2\tilde{T}. \qquad (12.10)$$

Chapter 13

Calculation of standard derivations

For an amount of measurement points, the average is calculated from

$$\bar{x} = \frac{1}{N}\sum_{i=1}^{N} x_i, \tag{13.1}$$

where N is the number of measurements and x_i is the i'the measurement. The average uncertainty of the individual measurements, $x_1, x_2, x_3, ..., x_N$, is then given by the standard deviation

$$\alpha_x = \sqrt{\frac{1}{N-1}\sum(x_i - \bar{x})^2}. \tag{13.2}$$

This equation states the sample standard derivation. The significance of the standard deviation, α_x, is that approximately 68% of the measurements of x shave to lie within a distance α_x of the true value.
As long as the systematic uncertainties are negligible, the uncertainty of the average is the standard derivation of the average [25],

$$\alpha_{\bar{x}} = \frac{\alpha_x}{\sqrt{N}}, \tag{13.3}$$

which is the equation used when calculating standard derivations of experimental results obtained in this project.

Chapter 14

Data sheets for pressure sensors and temperature sensors

References

[1] Teoretical microfluics, Henrik Bruus, MIC, DTU 2004

[2] Transport Phenomena, R. Byron and others, John Wiley & Sons, 2nd edition, 2002

[3] Microstructure fabrication with a CO_2 laser system, Deflef Snakenborg with others, MIC, DTU, 2003

[4] Nano 1 - Introduction to Nanotechnology, Henrik Bruus, MIC, DTU 2004

[5] section1: Fluid Michanics and Fluid Properties, http://www.efm.leeds.ac.uk-/CIVE/CIVE1400/Section1/Fluid_mechanics.htm

[6] Topologioptimering, Katrine Andersen with others, MIC, DTU, January 2005

[7] http://mmf.ruc.dk/ jogvan/Speciale/speciale.pdf, Stine Marott Normann with others, RUC

[8] Mekanik, Gunnar Christiansen and others. Institut for Fysik, DTU, 2000

[9] Introduction to Fluid Mechanics, sixth edition, Robert W. Fox and others, John Wiley and Sons, Inc., 2004

[10] Moshe B. Fuchs, Department of Solid Mechanics, Materials and Systems, Tel Aviv University, Israel, 2002

[11] Stoftransport i planter og porøse stoffer, Lars Øgendahl, KVL, 2004

[12] a high-level programming-language implementation of topology optimization aplied to steady-state Navier-Stokes flow, Laurits Højgaard Olesen and others, MIC, DTU, 2004

[13] NTC Termistors, Bowthorpe Thermoelectronics, UK

[14] www.betatherm.com/datasheet.php?p_id=90, Micro BetaCHIP Probe (MCD)

[15] Understanding the Finite Element Method, documentation, FEMLab 3.1

[16] Using The PDE Modes, documentation, FEMLab 3.1

[17] Setup of TOPOPT S-problem using FEMLAB-GUI, Fridolin Okkels, MIC, DTU

[18] The Conduction and Convection Application Mode, documentation, FEMLab 3.1

[19] The Navier-Stokes Application Mode, documentation, FEMLab 3.1

[20] Transport Phenomea. second edition, R. Byron Bird and others, 2002

[21] http://hyperphysics.phy-astr.gsu.edu/hbase/thermo/heatra.html

[22] Physics of Continuos Matter, Exotic and Everyday Phenomena in the Microscopic World, Benny Lautrup, 2005

[23] http://www.efunda.com/formulae/heat_transfer/conduction/overview_cond.cfm

[24] Heat tranfer, Femlab Modeling Guide, FEMLab 3.1

[25] An Introducuction To Error Analyses, second edition, John R. Taylor, University Science Books, 1997